Anisotropic flow measurements by ALICE

Ilya Selyuzhenkov

(EMMI/GSI)

One day workshop on the reaction plane reconstruction and flow

GSI, March16, 2012

Outline

- Why do we measure anisotropic flow?
- Measurement techniques: correlations and non-flow
- Elliptic flow at LHC
- Flow fluctuations and higher harmonics
- Directed flow
- Fourier decomposition of the 2-particle azimuthal correlation

Traveling across the phase diagram by varying the collision energy

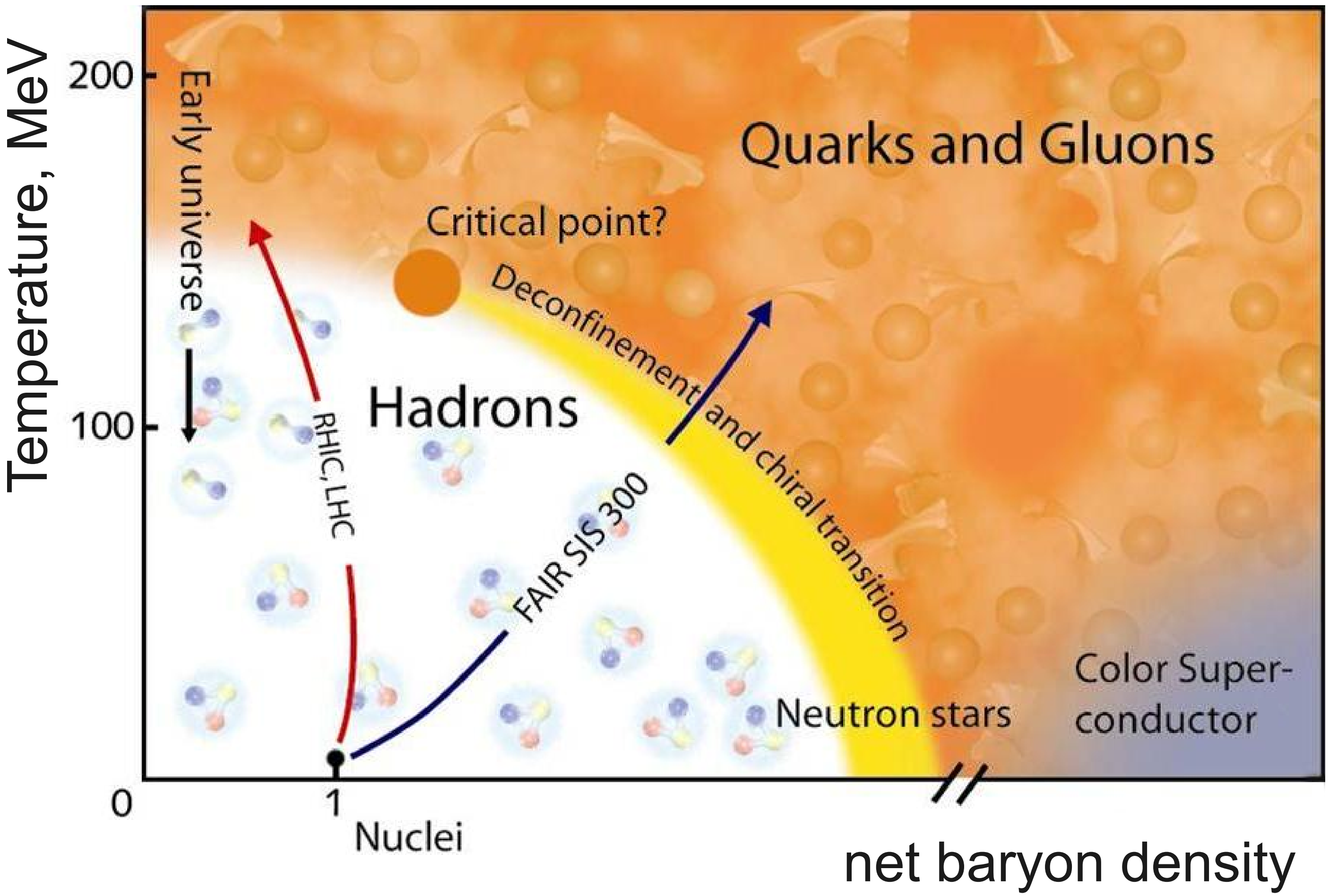

AGS/SPS (CERN)

FAIR (GSI/Germany)

NICA (Russia)

$$\sqrt{s_{NN}} \sim 1-10\,GeV$$

RHIC (BNL/USA)

$$\sqrt{s_{NN}} \sim 10-200\,GeV$$

LHC (CERN)

$$\sqrt{s_{NN}} \sim 2-5\,TeV$$

By varying the incident collision energy
(i.e. measurements at different accelerators)
we can travel across the phase diagram

Evolution of the system created in HIC

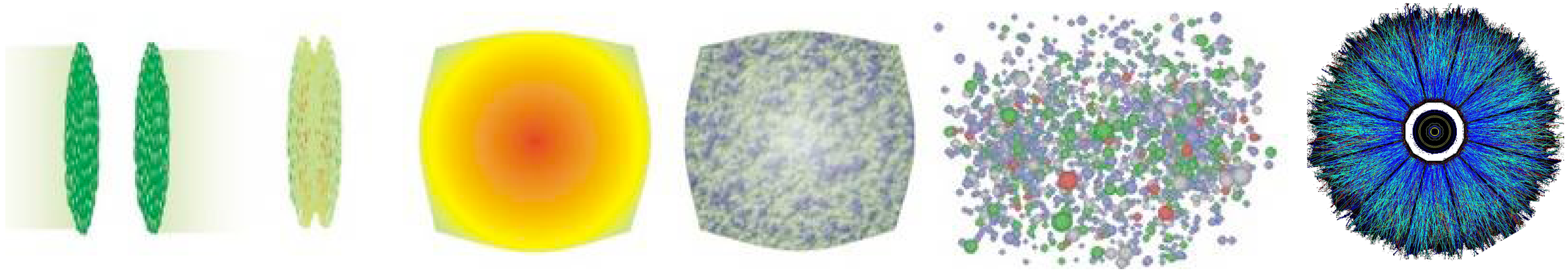

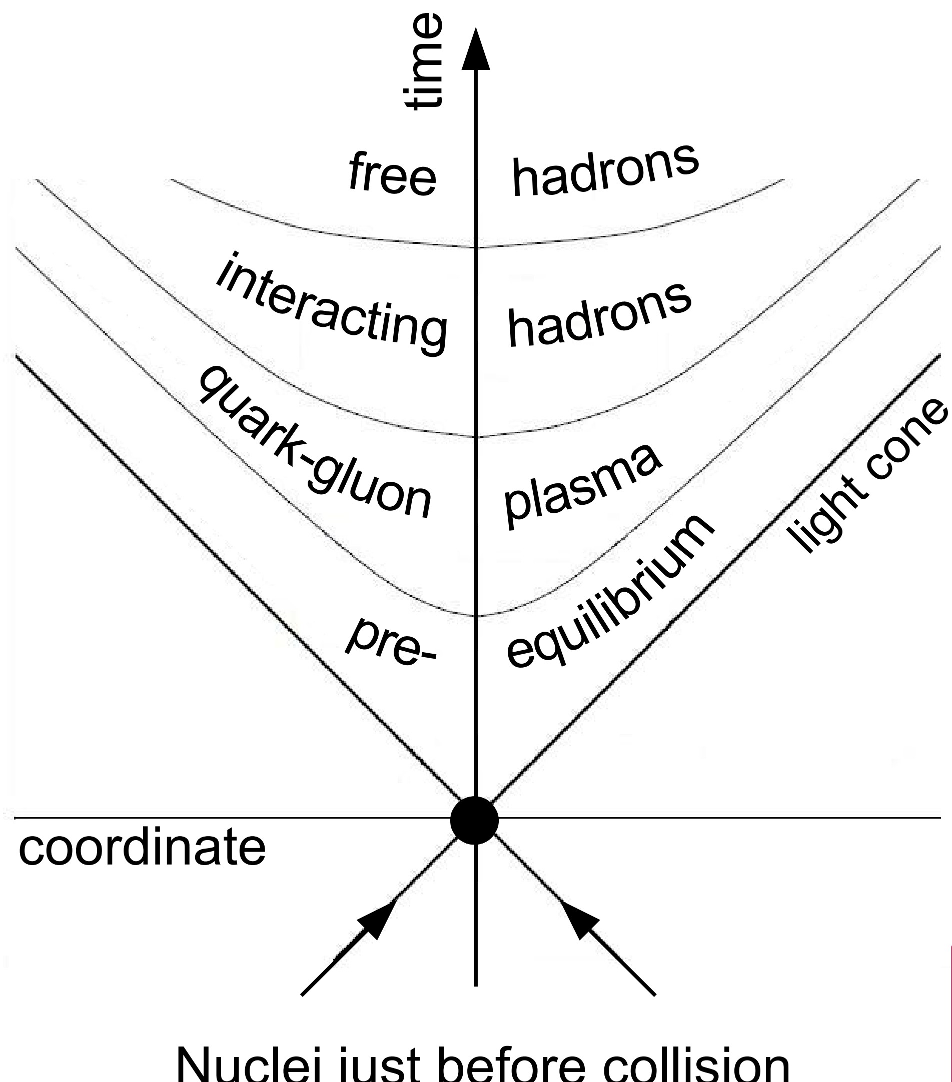

- Initial pre-equilibrium state
  hard parton scattering & jet production
  gluonic fields (Color Glass Condensate)
- Quark-gluon plasma formation
  thermalization (hydrodynamics)
- QGP expansion and decay
  phase transition of partons into hadrons
  - Hadronization
  - Rescattering & chemical freeze out
  - Kinetic freeze out (stop interacting)
- Experimentally access only hadronic state

Many observables need to be studied to establish the properties of QGP

Colliding nuclei has a finite size

Peripheral collision (large ***b***)

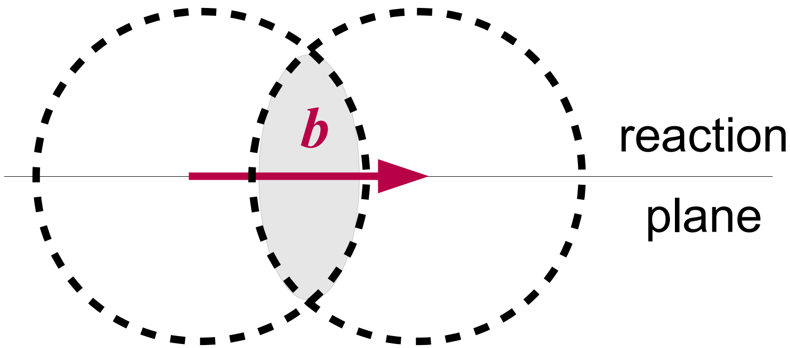

Overlap region is strongly asymmetric in the transverse plane

Central collision (small ***b***)

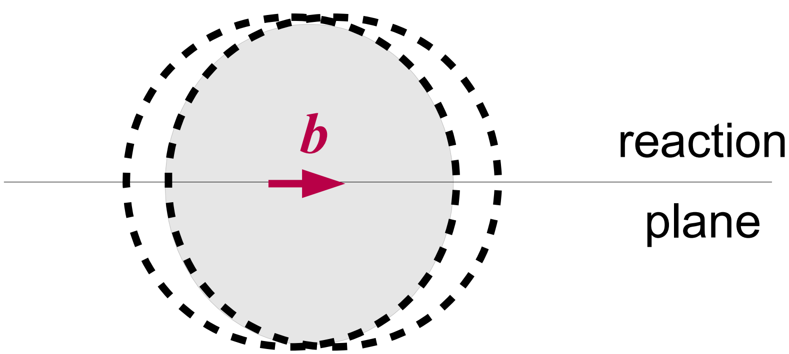

Overlap region is close to be symmetric in the transverse plane

Asymmetry of the overlap region depends on the impact parameter

b - impact parameter

Nucleon-nucleon collisions in the overlap region

Peripheral collision

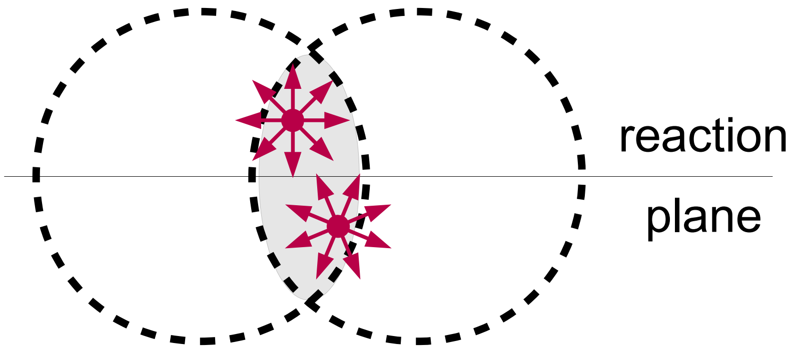

Small number of nucleon-nucleon collisions:
few particles produced

Central collision

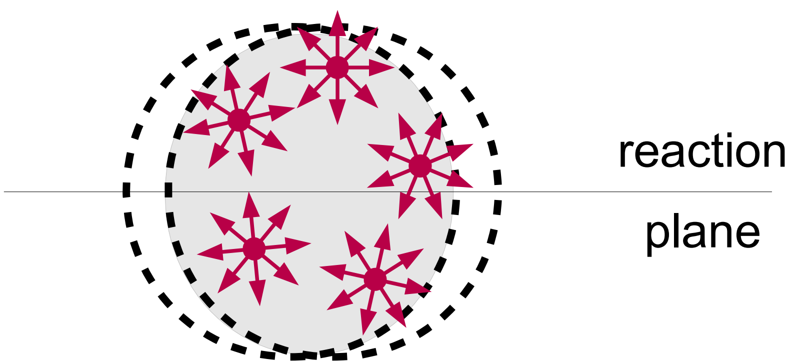

Large number of NN collisions:
abundant particle production

Number of produced particles
is correlated with the impact parameter

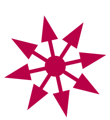
- elementary nucleon-nucleon (NN) collision

Produced particles interact with each other

Particle emitted out-of-plane

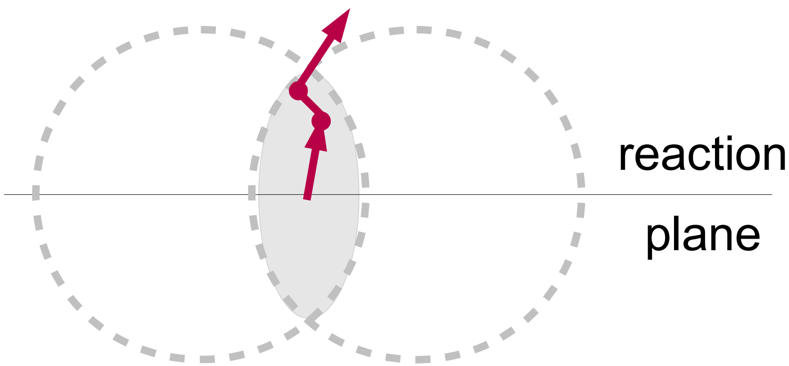

Emitted in-plane

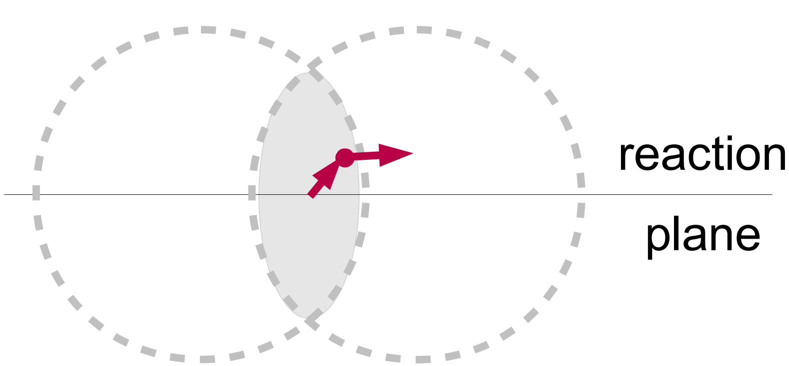

Multiple interaction with medium

Less interaction - small modification

Particle collectivity

Peripheral collision

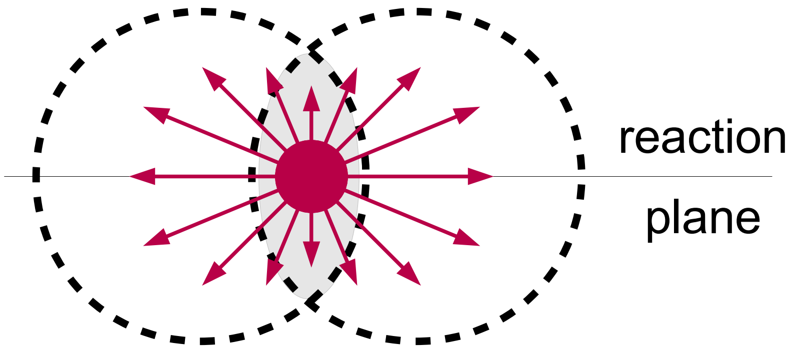

Strong coordinate space asymmetry transforms into the azimuthal asymmetry in the momentum space

Central collision

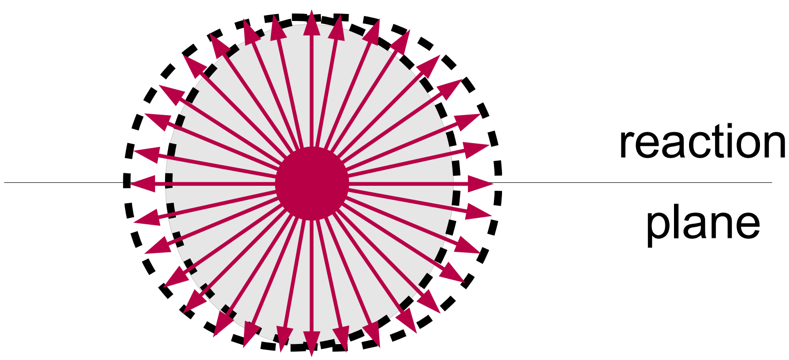

Multiple interaction with medium but small initial spacial asymmetry:
small asymmetry in the momentum space

Correlated particle production wrt. the collision plane of symmetry

Quantifying azimuthal asymmetry

Coordinate space asymmetry is ~ ellipsoidal quantified by eccentricity:

$$\epsilon_s = \frac{\langle y^2 - x^2 \rangle}{\langle y^2 + x^2 \rangle}$$

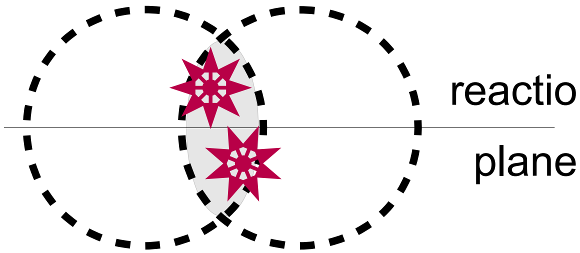

x, y - position of each elementary NN interaction

Quantifying azimuthal asymmetry

Coordinate space asymmetry is ~ ellipsoidal
quantified by eccentricity:

$$\epsilon_s = \frac{\langle y^2 - x^2 \rangle}{\langle y^2 + x^2 \rangle}$$

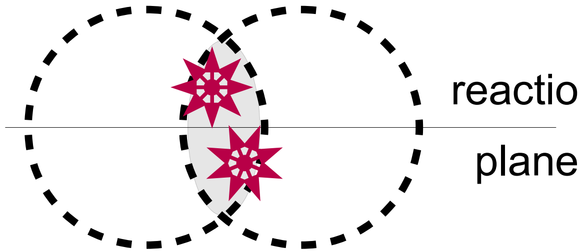

x, y - position of each elementary NN interaction

Momentum space asymmetry:

$$e_p \sim \frac{\langle p_x^2 - p_y^2 \rangle}{\langle p_y^2 + p_x^2 \rangle} \rightarrow \langle \cos(2\Delta\phi) \rangle$$

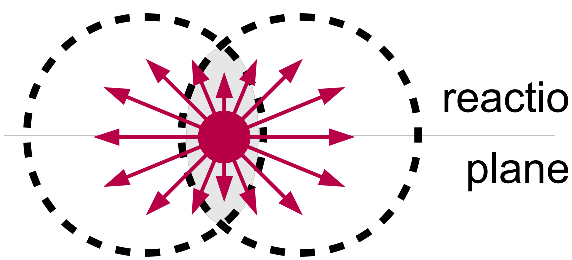

Second Fourier harmonic in momentum space

p_t - particle transverse momentum

$\Delta\phi$ - azimuthal angle relative to the reaction plane

Time evolution of the spacial and momentum asymmetries

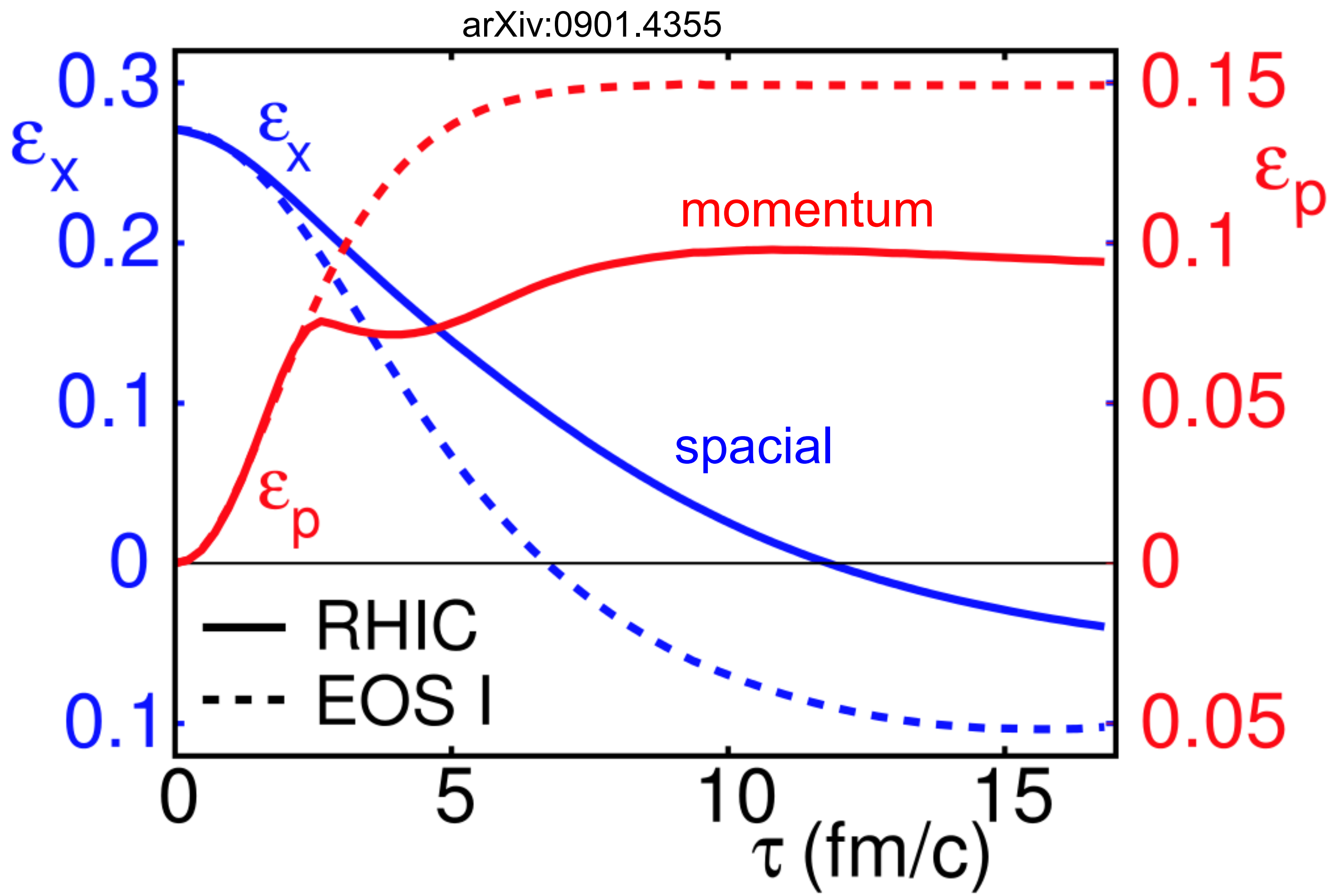

Spacial asymmetry drops very fast

Momentum asymmetry develops very early

EoS I: massless ideal gas
EoS RHIC: matching Lattice QCD

Momentum asymmetry is sensitive to:

- Early times of the system evolution
- Equation of State

Anisotropic transverse flow: Fourier harmonics

Fourier decomposition of the particle azimuthal distribution wrt. the reaction plane:

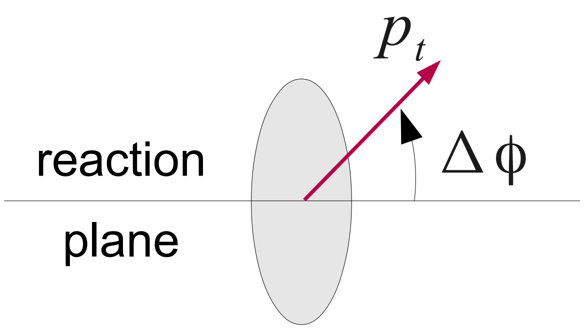

$$\frac{dN}{d(\Delta\phi)} \sim 1 + 2\sum_{n=1} v_n(p_t,\eta)\cos(n\Delta\phi)$$

No “sin” terms because of the collision symmetry

$v_n(p_t,\eta)$ – anisotropic transverse flow coefficients

v_1 - directed flow
v_2 - elliptic flow
v_3 - triangular flow

Different types of transverse flow

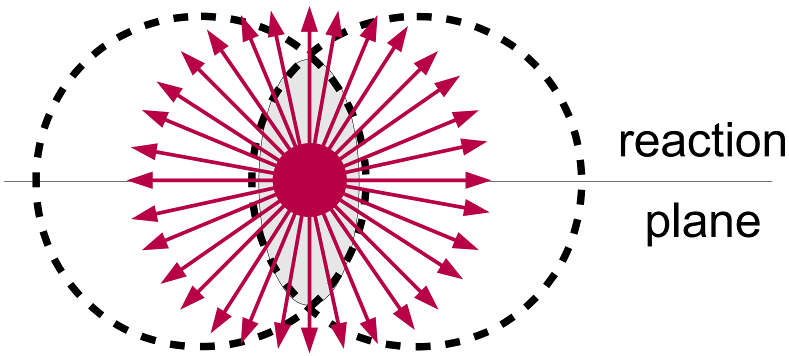

Radial flow (symmetric in azimuth)

Reflects the history of the radial expansion
Boost particle spectra to
higher transverse momenta

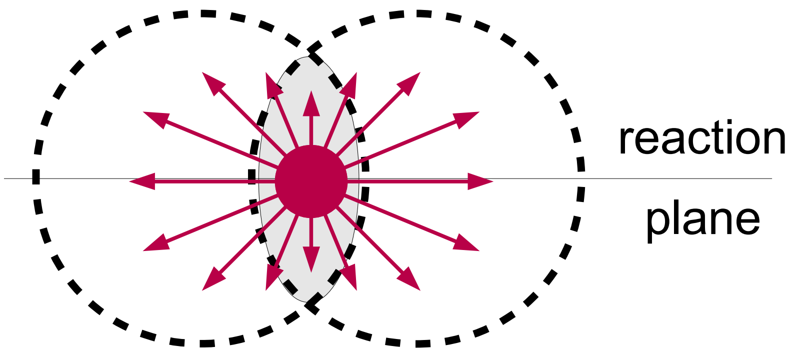

Elliptic flow: $v_2 = \langle \cos 2\Delta\phi \rangle$

Originate from ellipticity of the overlap region
Self quenching effect - develops at early time
(spacial asymmetry decrease with expansion)

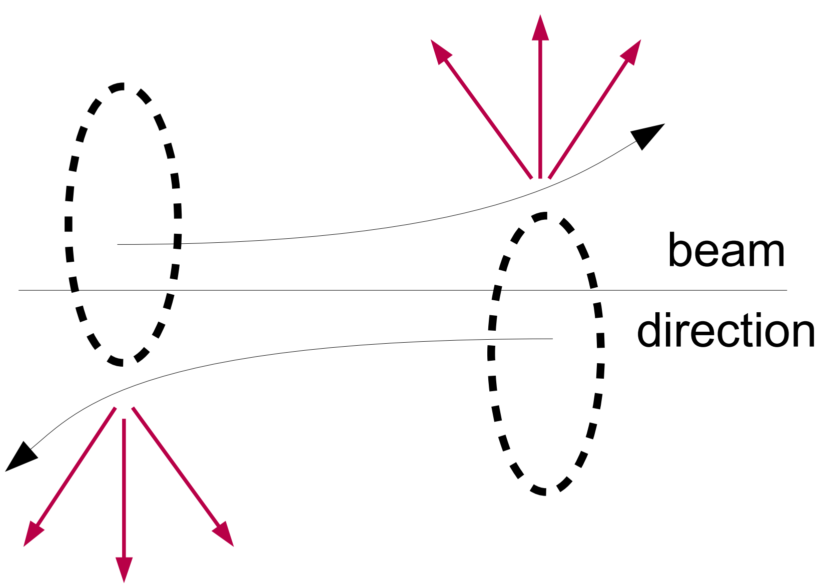

Directed flow: $v_1 = \langle \cos \Delta\phi \rangle$

Deflection of particles in the beam direction.
Develops at earliest time.
At forward (large) rapidity is sensitive to
the pre-equilibrium stage

Experimental measurements of the anisotropic flow

Modern ultra-relativistic HI colliders

Relativistic Heavy Ion Collider

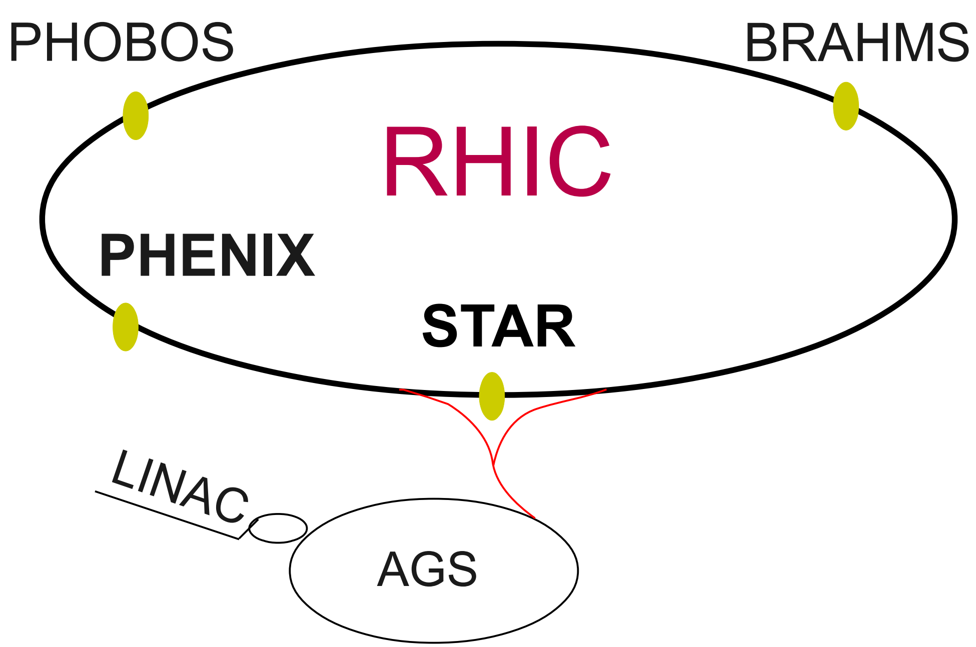

Large Hadron Collider

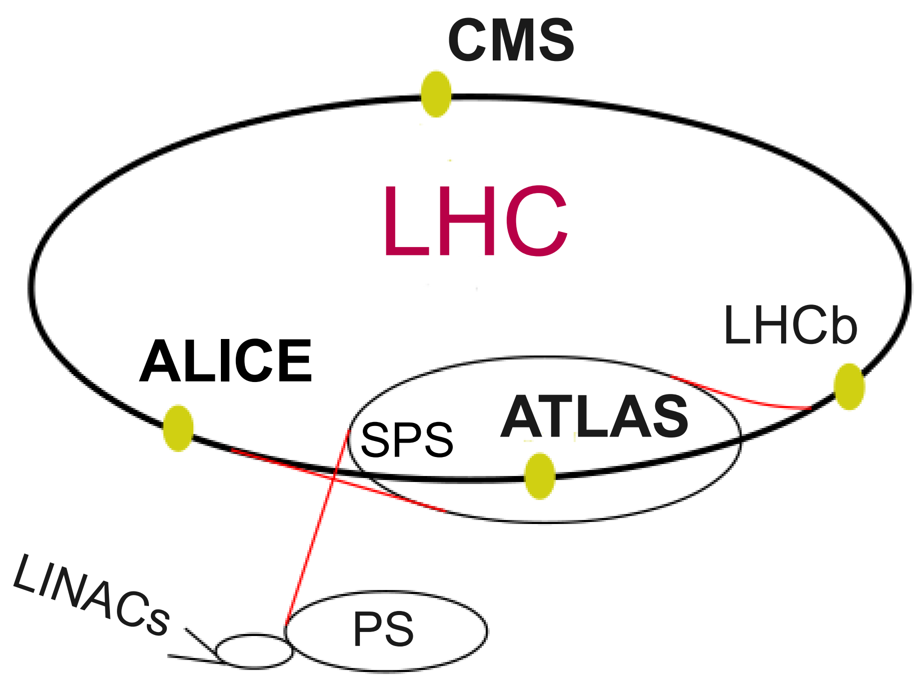

	RHIC	LHC
Location	BNL (USA)	CERN (Europe)
Circumference	3.8 km	27 km
Species	p, d, Cu, Au, U polarized protons	p, Pb
Center of mass energy per nucleon pair	in GeV 7.7-38, 62, 200 500 (pp only)	in TeV 0.9, 2.76, 7 (pp) 2.76 (Pb)

Current heavy-ion experiments at RHIC and LHC

STAR (Solenoidal Tracker At RHIC)

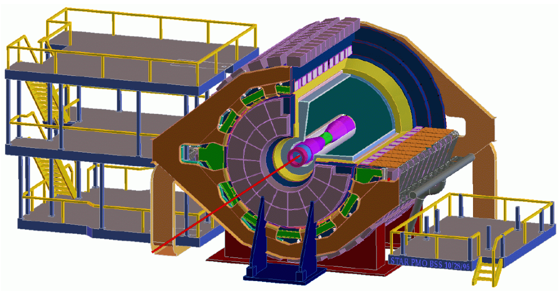

ALICE (A Large Ion Collider Experiment)

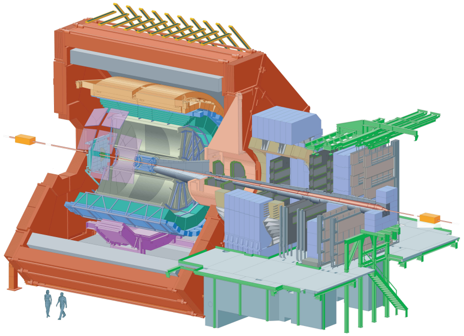

PHENIX (Pioneering High Energy Nuclear Ion Experiment)

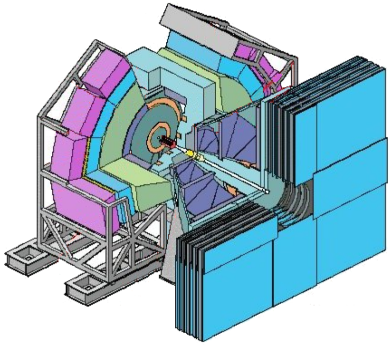

ATLAS (A Toroidal LHC Apparatus)

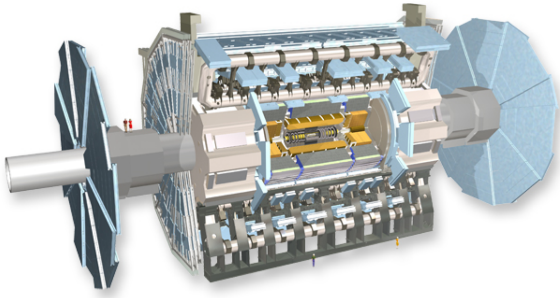

CMS (Compact Muon Solenoid)

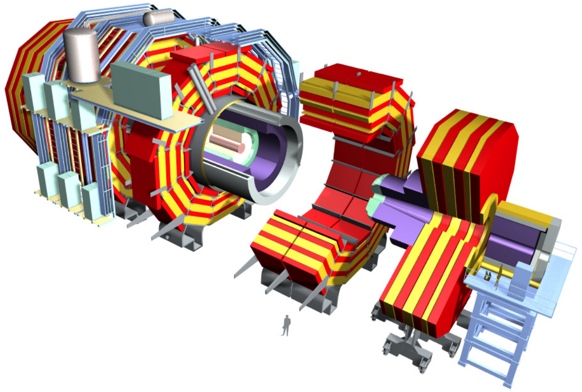

Main capabilities for heavy-ion studies:

Charge particle tracking and identification:
- full azimuth, large rapidity coverage
- wide p_t range: ~ 100 MeV/c to ~ 100 GeV/c

Calorimetry and rare probes:
- neutral particles, photons, jets, heavy flavor

The ALICE subsystems used for the flow measurements

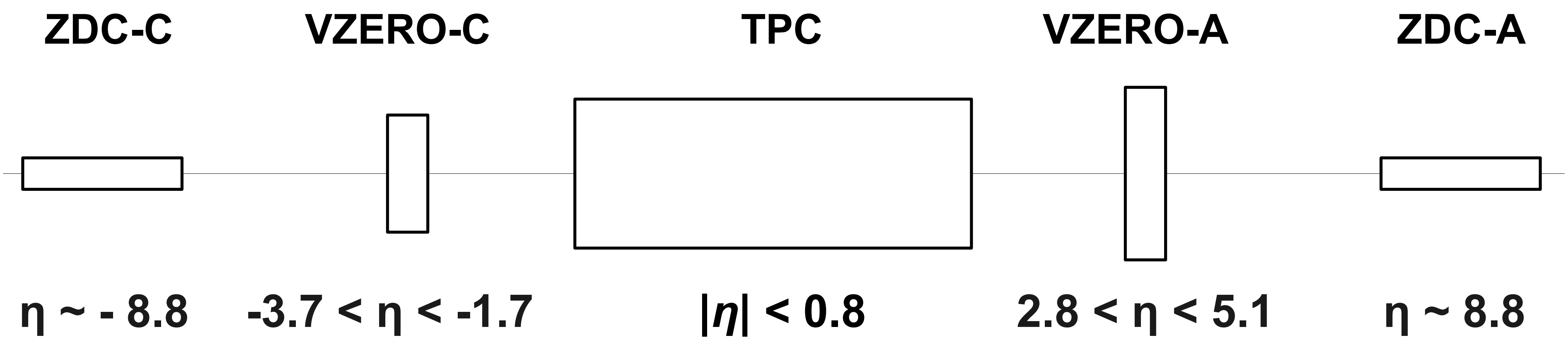

TPC:
Time Projection Chamber
charged tracks at midrapidity

VZERO:
Forward Scintillator Arrays
multiplicity counters

ZDCs:
Zero Degree Calorimeter
recoil neutrons at beam rapidity

Data from LHC running in November 2010

System	Energy, $\sqrt{s_{NN}}$	Events
Pb-Pb	2.76 TeV	13 M

Charged particle cuts for correlations:

Pseudo-rapidity: $|\eta| < 0.8$

Transverse momentum $p_t > 0.15$ GeV/c

Reaction plane:

Estimated with TPC, VZERO, and ZDCs

Anisotropic flow measurement: Using collectivity to study collectivity

Reaction plane is not known experimentally
Orientating wrt. to the laboratory frame changes event-by-event

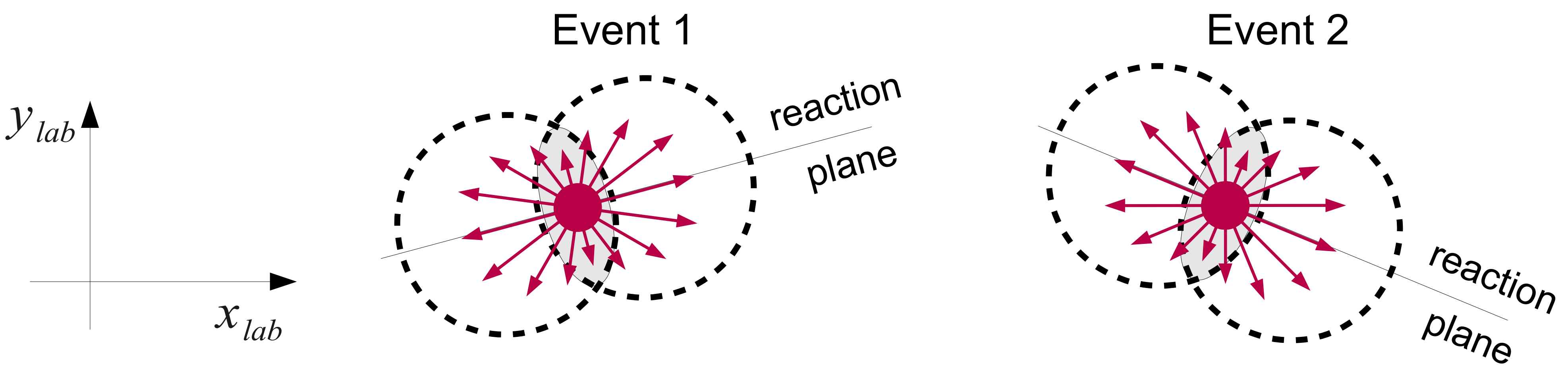

Only measuring particles distribution in the momentum space

If the momentum distribution is azimuthally asymmetric due to flow,
then this asymmetry should be correlated
with the impact parameter direction (reaction plane orientation)

Use particle azimuthal distribution in the event
to estimate the reaction plane angle – event plane vector

Event plane vector

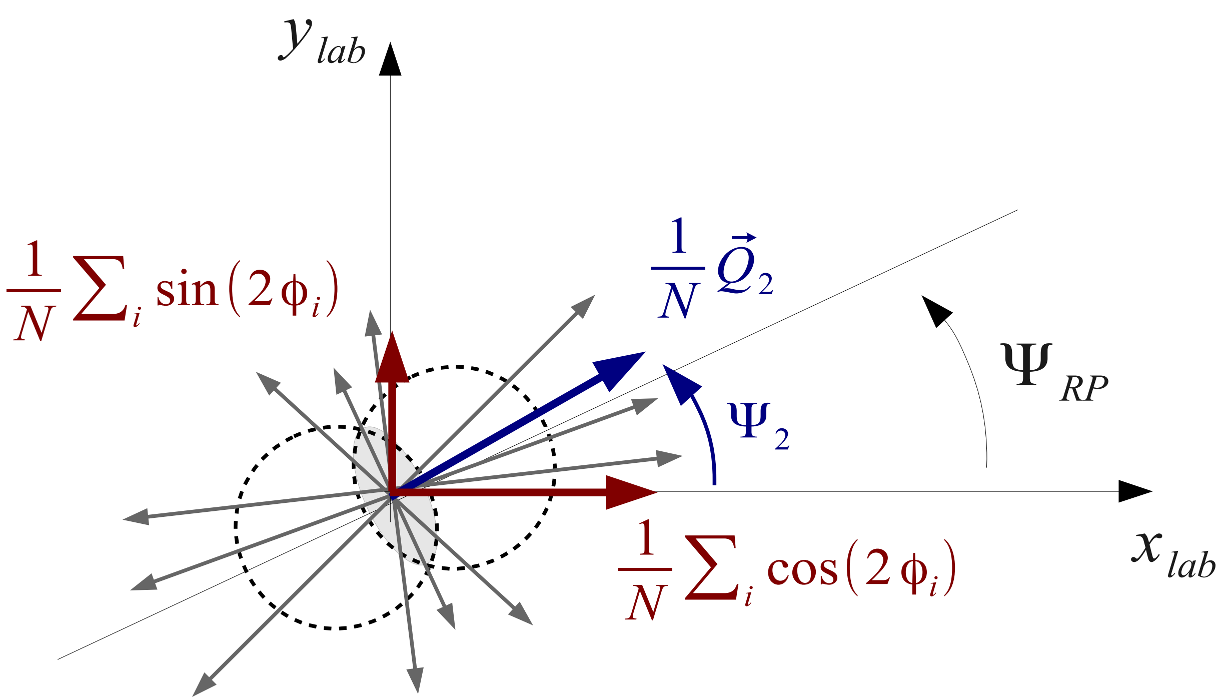

Vector sum of all particles direction:

$$Q_{n,x} = \sum_i w_i \cos(n\phi_i) \qquad Q_{n,y} = \sum_i w_i \sin(n\phi_i)$$

Experimental estimate of the reaction plane:

Event plane vector: $$\Psi_{n,EP} = \frac{1}{n}\tan^{-1}\left(\frac{Q_{n,y}}{Q_{n,x}}\right)$$

Measuring flow with the event plane vector

$$\frac{dN}{d(\phi-\Psi_{RP})} \sim 1 + 2\sum_{i=1} v_n(p_t,\eta) \cos[n(\phi-\Psi_{RP})]$$

Want to measure:

$$v_n = \langle \cos[n(\phi-\Psi_{RP})] \rangle$$

$\longrightarrow$

Measured:

$$v_n^{obs} = \langle \cos[n(\phi-\Psi_{n,EP})] \rangle$$

Measuring flow with the event plane vector

$$\frac{dN}{d(\phi-\Psi_{RP})} \sim 1 + 2\sum_{i=1} v_n(p_t,\eta)\cos[n(\phi-\Psi_{RP})]$$

Want to measure: Measured:

$$v_n = \langle\cos[n(\phi-\Psi_{RP})]\rangle \longrightarrow v_n^{obs} = \langle\cos[n(\phi-\Psi_{n,EP})]\rangle$$

Event plane vector and the reaction plane are correlated with finite resolution:

$$v_n = \frac{\langle\cos[n(\phi-\Psi_{n,EP})]\rangle}{\langle\cos[n(\Psi_{n,EP}-\Psi_{RP})]\rangle} = \frac{v_n^{obs}}{R_n}$$

Resolution can be measured from subevents:

$$R \sim \sqrt{\langle\cos[n(\Psi^a_{n,EP}-\Psi^b_{n,EP})]\rangle}$$

Anisotropic flow measurement and correlations

$$\frac{dN}{d(\phi_i - \Psi_{RP})} \sim 1 + 2 \sum_{n=1} v_n \cos[n(\phi_i - \Psi_{RP})]$$

$$v_n = \langle \cos[n(\phi_i - \Psi_{RP})] \rangle$$

- directly calculable only in theory when the reaction plane orientation is known

Anisotropic flow measurement and correlations

$$\frac{dN}{d(\phi_i - \Psi_{RP})} \sim 1 + 2 \sum_{n=1} v_n \cos[n(\phi_i - \Psi_{RP})]$$

$$v_n = \langle \cos[n(\phi_i - \Psi_{RP})] \rangle$$

- directly calculable only in theory when the reaction plane orientation is known

---

Event plane angle - experimental estimate of the reaction plane angle based on the measured azimuthal distribution of particles:

$$\Psi_{RP} \rightarrow \Psi_{EP} \left\{ \sum_{\phi_j} g(\phi_j) \right\}$$

$$v_n^{obs} = \langle \cos[n(\phi_i - \Psi_{EP})] \rangle \sim \langle \sum_{\phi_j \neq \phi_i} \cos n(\phi_i - \phi_j) \rangle$$

$$c_n\{2\} = \langle \cos n(\phi_i - \phi_j) \rangle$$

- two particle correlations

Measure anisotropic flow with azimuthal correlations

Non-flow correlations

Non-flow: correlations among the particles unrelated to the reaction plane

In case of two particle correlations: $\langle \cos[n(\phi_i - \phi_j)] \rangle = \langle v_n^2 \rangle + \delta_{2,n}$

Sources of non-flow correlations:

- Resonance decay
- Jet production
- In general - any cluster production

Non-flow correlations

Non-flow: correlations among the particles unrelated to the reaction plane

In case of two particle correlations: $\langle \cos[n(\phi_i - \phi_j)] \rangle = \langle v_n^2 \rangle + \delta_{2,n}$

Sources of non-flow correlations:

- Resonance decay
- Jet production
- In general - any cluster production

Example: 2-particle decay

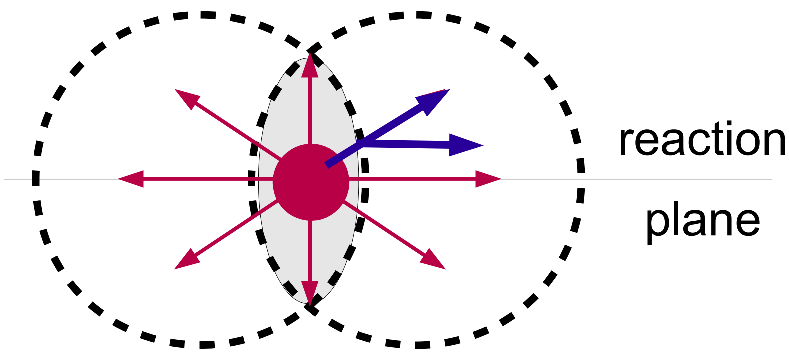

Collective flow:
correlations between particles through the common plane of symmetry

Probability to be correlated for one particle with another out of *M*-particles is *1/(M-1)*:

$$\delta_2 \sim \frac{1}{M-1}$$

To measure flow with 2-particle correlations:

$$v_n \gg 1/\sqrt{M}$$

$$M = 200 \rightarrow v_n \gg 0.07$$

For RHIC/LHC: $v_n \approx 0.04 - 0.07$

Suppressing non-flow with multi-particle correlations

Two particle correlations:

$$\delta_2 \sim \frac{1}{M}$$

Measurement requirement:

$$v_n \gg \frac{1}{M^{1/2}}$$

$$M = 200 \rightarrow v_n \gg 0.07$$

Four-particle correlations:

$$\delta_4 \sim \frac{1}{M^3}$$

$$v_n \gg \frac{1}{M^{3/4}}$$

$$M = 200 \rightarrow v_n \gg 0.019$$

k-particle correlations:

$$\delta_k \sim \frac{1}{M^{k-1}}$$

$$v_n \gg \frac{1}{M^{(k-1)/k}}$$

Large *k* ($k \rightarrow \infty$)

$$v_n \gg \frac{1}{M}$$

$$M = 200 \rightarrow v_n \gg 0.005$$

Multi-particle cumulants

Cumulant are used to study the genuine n-particle correlations

n-particle cumulant can be defined as a correlation function which is zero if there are no n-particle correlations in the system (it is insensitive to other, $k \neq n$, correlations)

Example:

2-particle correlations

$$\langle \cos[n(\phi_1 - \phi_2)] \rangle = \langle e^{in(\phi_1 - \phi_2)} \rangle$$

Note: imaginary part is zero (no sin terms)

2-particle cumulant:

$$c_n\{2\} = \langle e^{in(\phi_1 - \phi_2)} \rangle - \langle e^{in\phi_1} \rangle \langle e^{in\phi_2} \rangle$$

If there are no correlations in the particle distribution,

but $\langle e^{in\phi_{1,2}} \rangle \neq 0$ (for example non-uniform detector acceptance)

$$\langle \cos[n(\phi_1 - \phi_2)] \rangle \neq 0 \qquad c_n\{2\} = 0$$

Multi-particle cumulants and relation to flow

2-particle cumulant:

$$c_n\{2\} = \langle e^{in(\phi_1-\phi_2)}\rangle = v_n^2 + \delta_{2,n} \qquad \delta_2 \sim \frac{1}{M}$$

4-particle cumulant:

$$c_n\{4\} = \langle e^{in(\phi_1+\phi_2-\phi_3-\phi_4)}\rangle - 2\ \langle e^{in(\phi_1-\phi_2)}\rangle^2$$

$$c_n\{4\} = \left(v_n^4 + \delta_{4,n} + 4\mathrm{v}_n^2\delta_{2,n} + 2\,\delta_{2,n}^2\right) - 2\left(v_n^2 + \delta_{2,n}\right)^2$$

$$c_n\{4\} = \langle -v_n^4 + \delta_{4,n}\rangle \qquad \delta_4 \sim \frac{1}{M^3}$$

No contribution from 2-particle non-flow to the 4-particle cumulant

Multi-particle cumulants and relation to flow

2-particle cumulant:

$$c_n\{2\} = \langle e^{in(\phi_1-\phi_2)} \rangle = \langle v_n^2 + \delta_{2,n} \rangle$$

4-particle cumulant:

$$c_n\{4\} = \langle -v_n^4 + \delta_{4,n} \rangle$$

Connection of cumulants to the anisotropic flow

$$v_n\{2\}^2 = c_n\{2\} \qquad v_n\{4\}^2 = -c_n\{4\} \qquad v_n\{6\}^6 = \frac{1}{4} c_n\{6\}$$

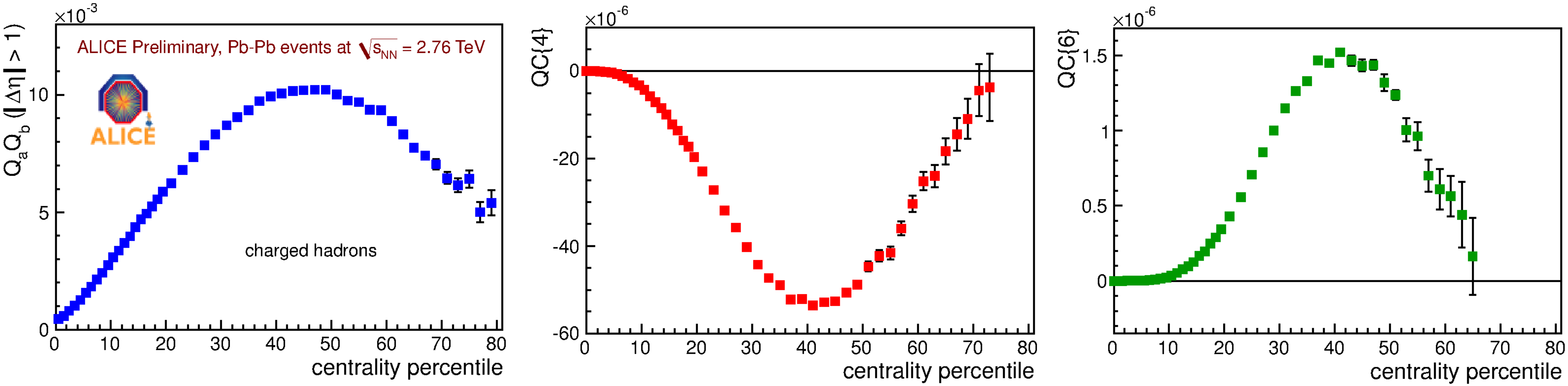

Characteristic pattern of the cumulants changing sign

Estimating flow with multi-particle cumulants

elliptic flow vs. centrality

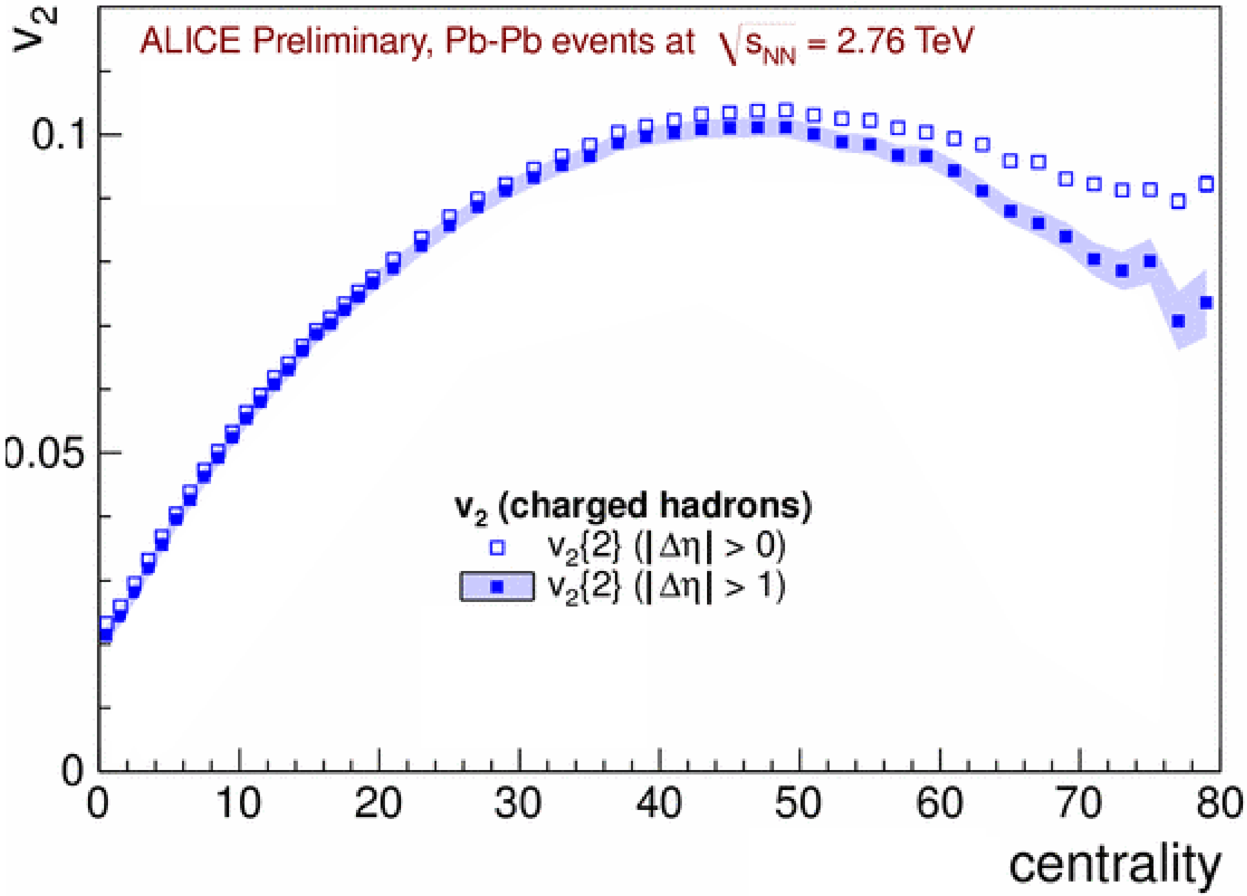

Rapidity separation between correlated particles suppress short-range non-flow:

$$v_2\{2\} > v_2\{2,|\Delta\eta|\}$$

Large non-flow in peripheral collisions

Estimating flow with multi-particle cumulants

elliptic flow vs. centrality

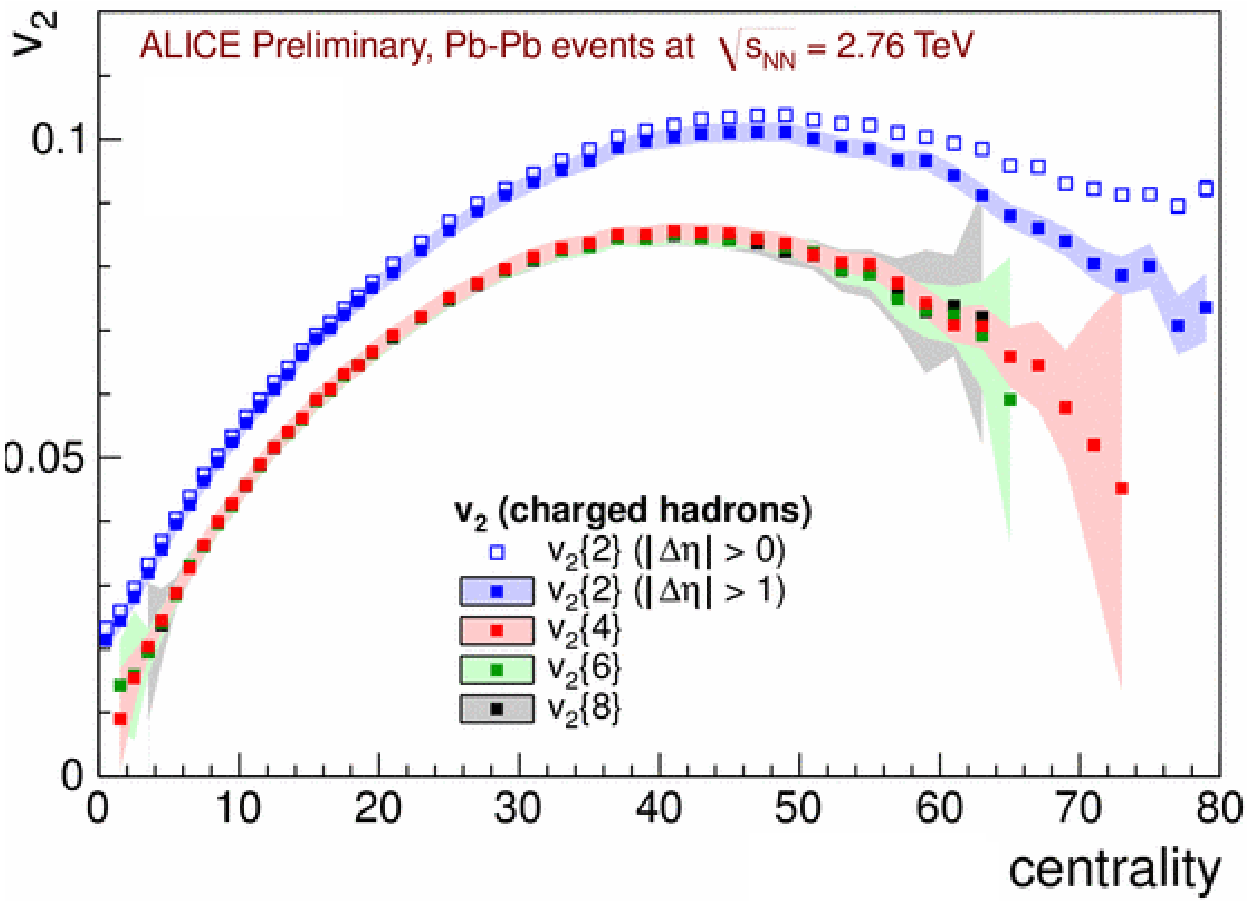

Rapidity separation between correlated particles suppress short-range non-flow:

$$v_2\{2\} \; > \; v_2\{2,|\Delta\eta|\}$$

Large non-flow in peripheral collisions

Note:

$v_2\{2\}$ and $v_2\{4\}$ differ not only because of non-flow, but also due to flow fluctuations (discussed later)

Multi-particle cumulants remove residual non-flow:

$$v_2\{4\} \; \approx \; v_2\{6\} \; \approx \; v_2\{8\}$$

Overview of methods to measure anisotropic flow

Based on 2-particle correlations:

$$v_n^{obs} = \langle \sum_{\phi \neq \phi_i} \cos n(\phi - \phi_i) \rangle \longrightarrow c_n\{2\} = \langle \cos n(\phi_i - \phi_j) \rangle$$

Event plane method

Scalar Product

$$v_n(p_T, y) = \frac{\sqrt{\langle M_a M_b \rangle}}{\langle M \rangle - 1} \frac{\langle Q_n u_{n,i}^*(p_T, y) \rangle}{\sqrt{\langle Q_n^a Q_n^{b\,*} \rangle}}$$

Overview of methods to measure anisotropic flow

Based on 2-particle correlations:

$$v_n^{obs} = \langle \sum_{\phi \neq \phi_i} \cos n(\phi - \phi_i) \rangle \longrightarrow c_n\{2\} = \langle \cos n(\phi_i - \phi_j) \rangle$$

Event plane method

Scalar Product

$$v_n(p_T, y) = \frac{\sqrt{\langle M_a M_b \rangle}}{\langle M \rangle - 1} \frac{\langle Q_n u^*_{n,i}(p_T, y) \rangle}{\sqrt{\langle Q_n^a Q_n^{b\,*} \rangle}}$$

Based on multi-particle cumulant:

GF: function which expanded in series gives multi-particle correlations as expansion coefficients

Cumulants from generating function (GF):

$$G_n(z) = \prod_{j=1}^{M} \left(1 + \frac{z^* e^{in\phi_j} + z e^{-in\phi_j}}{M}\right)$$

Q-cumulants (or direct cumulants)

$$\langle 4 \rangle = \frac{|Q_n|^4 + |Q_{2n}|^2 - 2 \cdot \mathfrak{Re}\left[Q_{2n} Q_n^* Q_n^*\right]}{M(M-1)(M-2)(M-3)} - 2\,\frac{2(M-2) \cdot |Q_n|^2 - M(M-3)}{M(M-1)(M-2)(M-3)}$$

$$\langle 2 \rangle = \frac{|Q_n|^2 - M}{M(M-1)}$$

$$v_n\{2\}^2 = c_n\{2\} \qquad v_n\{4\}^4 = -c_n\{4\} \qquad v_n\{6\}^6 = \frac{1}{4} c_n\{6\} \qquad v_n\{8\}^6 = -\frac{1}{33} c_n\{8\}$$

Overview of methods to measure anisotropic flow

Based on 2-particle correlations:

$$v_n^{obs} = \langle \sum_{\phi \neq \phi_i} \cos n(\phi - \phi_i) \rangle \rightarrow c_n\{2\} = \langle \cos n(\phi_i - \phi_j) \rangle$$

Event plane method

Scalar Product

$$v_n(p_T, y) = \frac{\sqrt{\langle M_a M_b \rangle}}{\langle M \rangle - 1} \frac{\langle Q_n u_{n,i}^*(p_T, y) \rangle}{\sqrt{\langle Q_n^a Q_n^{b\,*} \rangle}}$$

Based on multi-particle cumulant:

Cumulants from generating function (GF)

Q-cumulants (or direct cumulants)

GF: function which expanded in series

giv

exp

$$G_n(z) = \prod_{j=1}^{M} \left(1 + \frac{z^* e^{in\phi_j} + z e^{-in\phi_j}}{M}\right)$$

$$v_n\{2\}^2 = c_n\{2\} \qquad v_n\{4\}^4 = -c_n\{4\} \qquad v_n\{6\}^6 = \frac{1}{4} c_n\{6\} \qquad v_n\{8\}^6 = -\frac{1}{33} c_n\{8\}$$

Method based on the event flow vector:

Fitting Q-vector distribution

$$\frac{dN}{dq_n} = \frac{q_n}{\sigma_n^2} e^{-\frac{v_n^2 M + q_n^2}{2\sigma_n^2}} I_0\left(\frac{q_n v_n \sqrt{M}}{\sigma_n^2}\right) \qquad q_n \equiv \frac{Q_n}{\sqrt{M}}$$

Lee-Yang zeros

(first minimum of the generating function)

$$G_2^\theta(ir) = \left| \left\langle e^{irQ_2^\theta} \right\rangle_{\text{evts}} \right| \qquad V_n^\theta\{\text{LYZ}\} = \frac{j_{01}}{r_0^\theta}$$

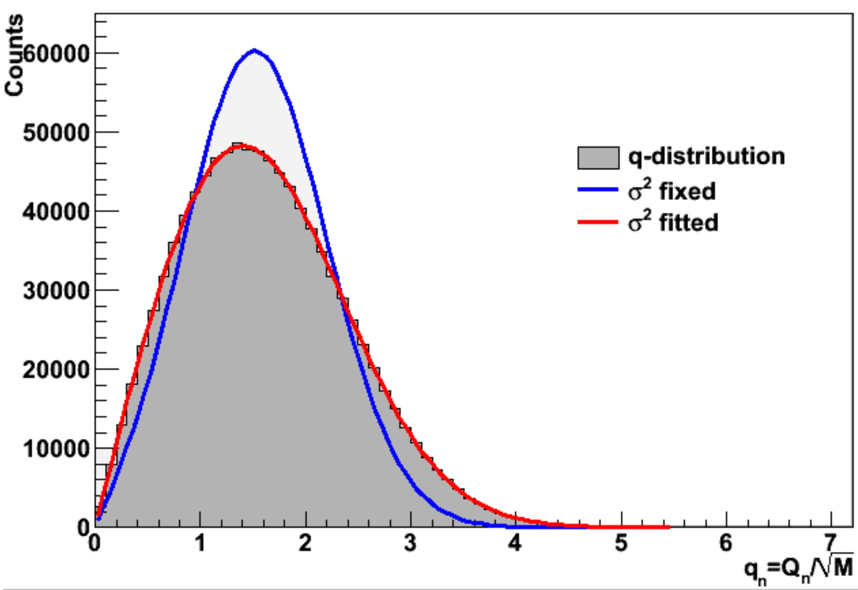

ALICE results from different techniques

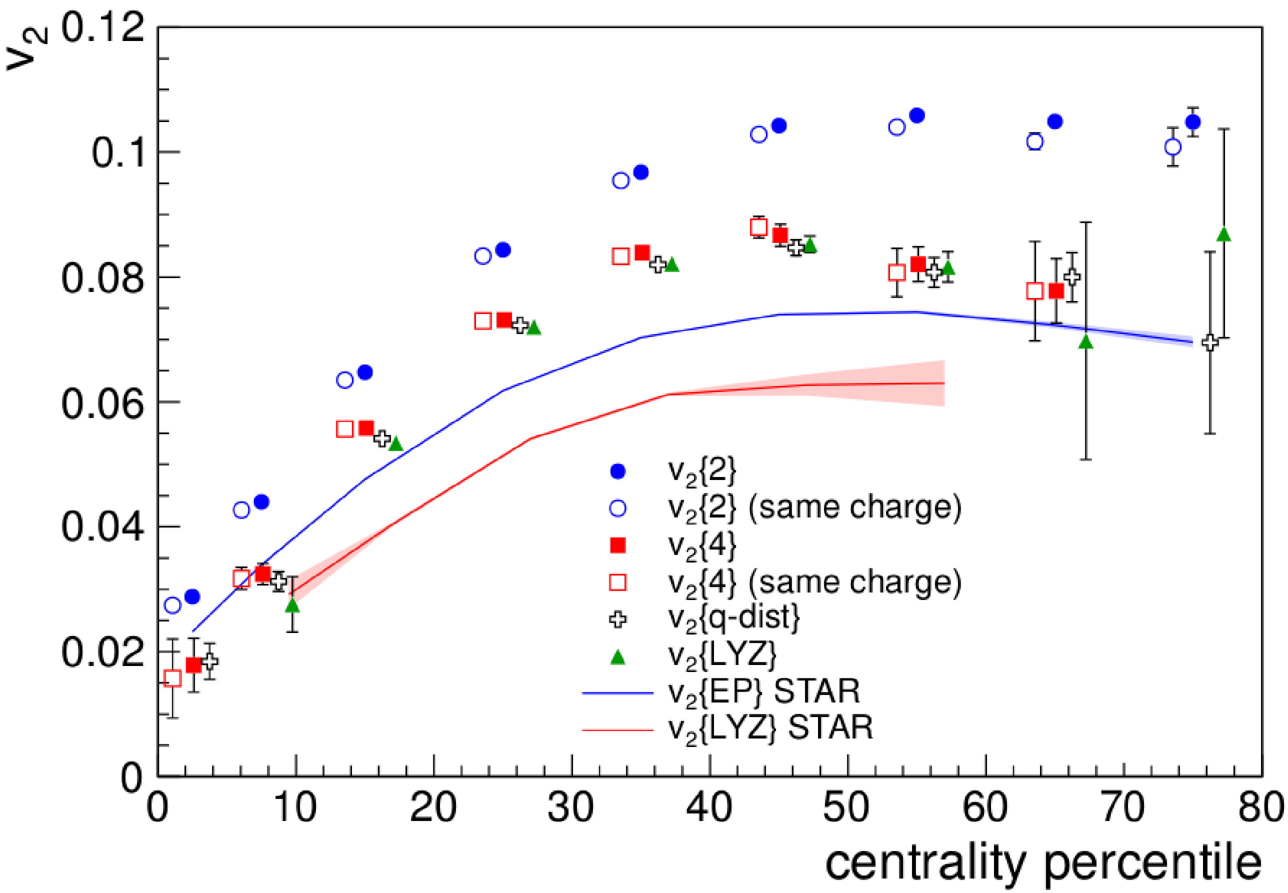

Results separate into two bands: from two and multi-particle correlations

In-plane elliptic flow:

the dominant flow component at the relativistic energies

$$\frac{dN}{d(\Delta\phi)} \sim 1 + 2\, v_2 \cos(2\,\Delta\phi)$$

Elliptic flow vs. collision energy

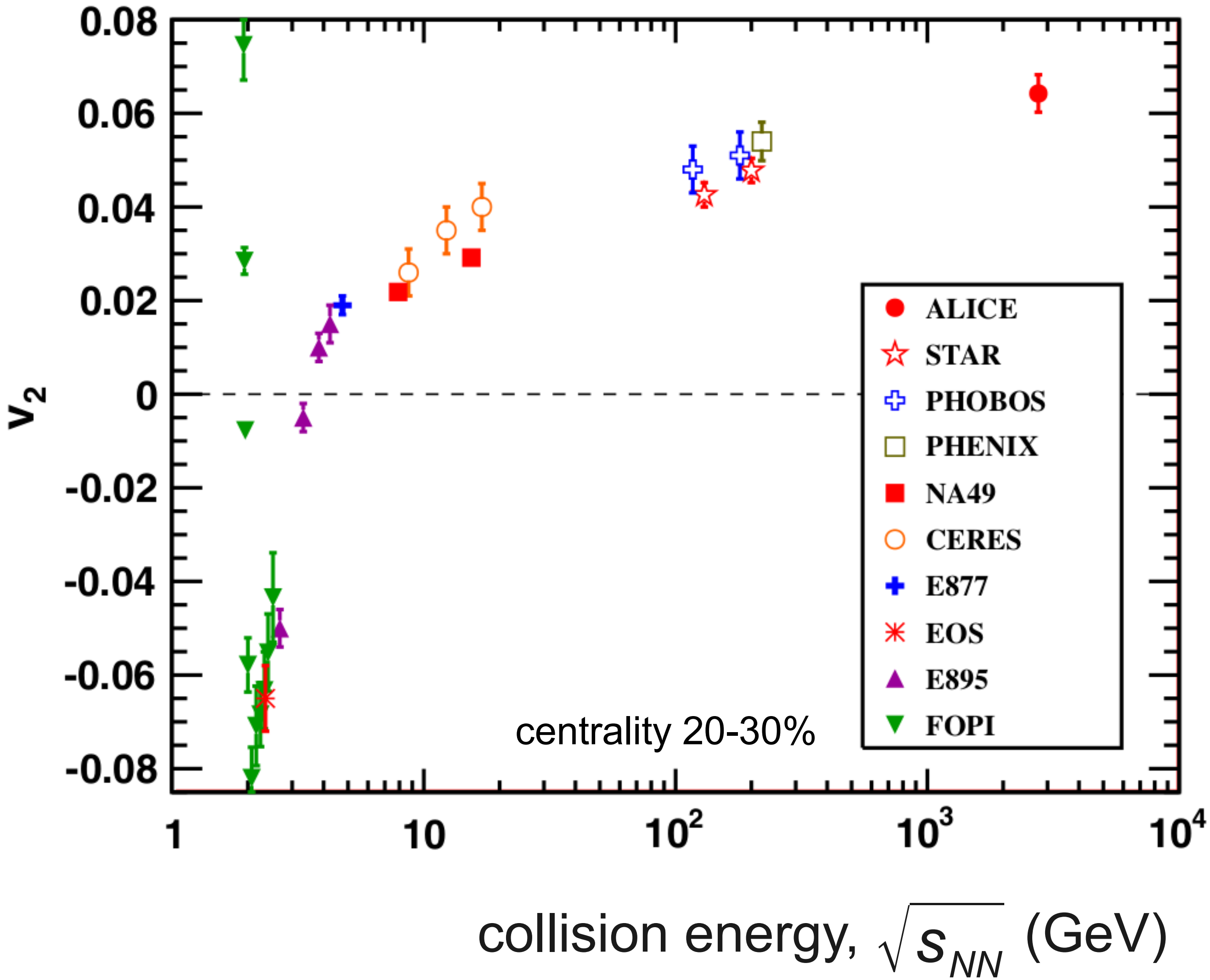

Experimental results covers about 4 decades of the collision energy

Data from GSI, AGS, SPS, RHIC, and LHC experiments

Elliptic flow: RHIC vs. LHC

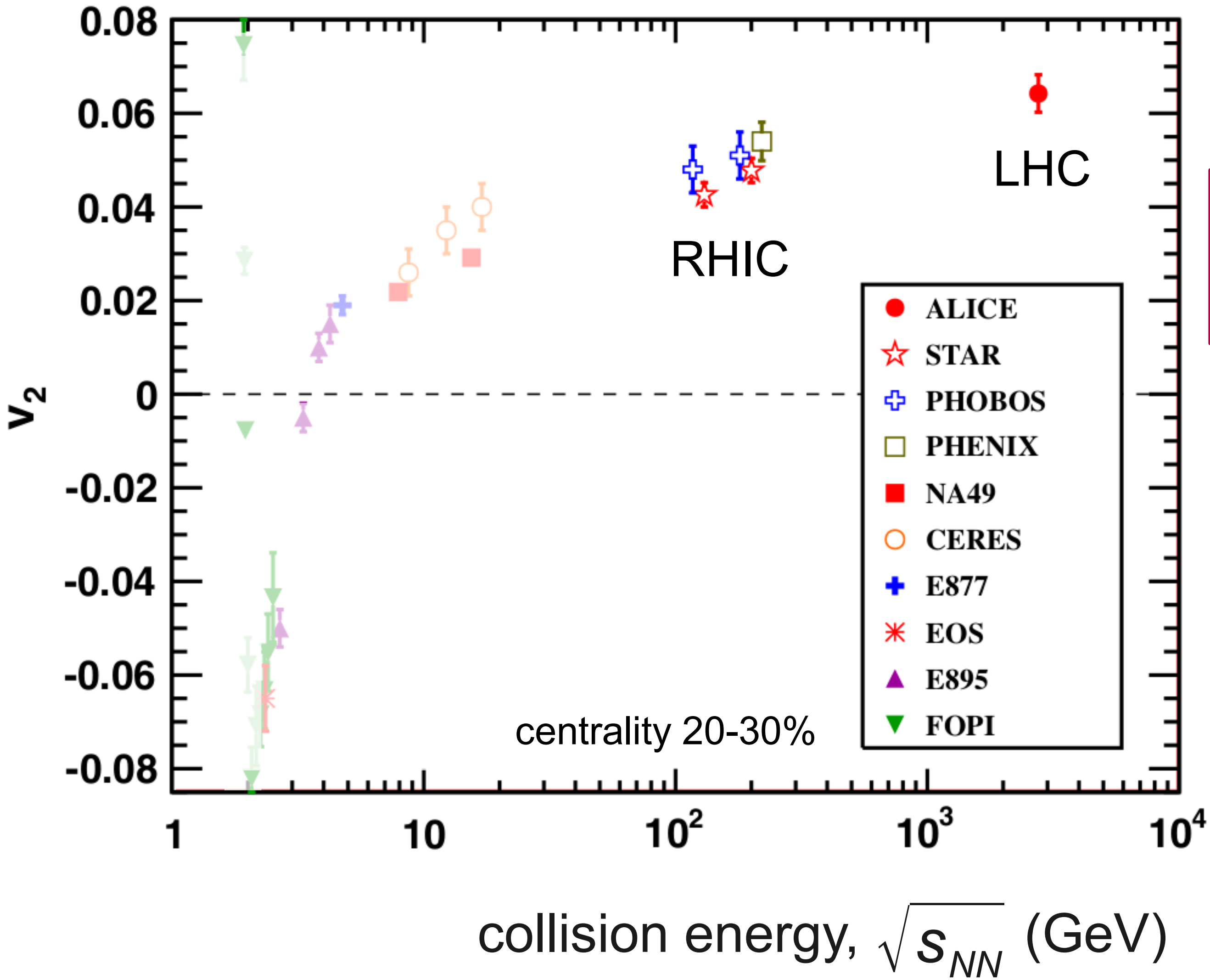

30% increase of v_2 from RHIC: stronger collectivity at LHC

But: measured v_2 vs. transverse momenta has similar shape and magnitude at RHIC and LHC

p_t differential elliptic flow vs. collision energy

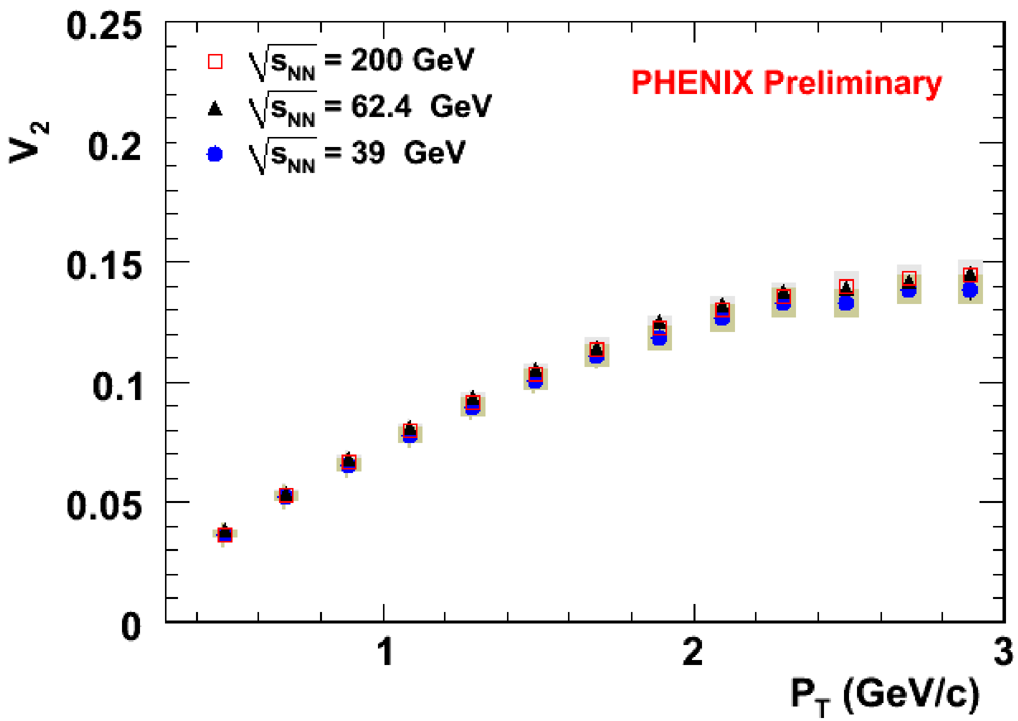

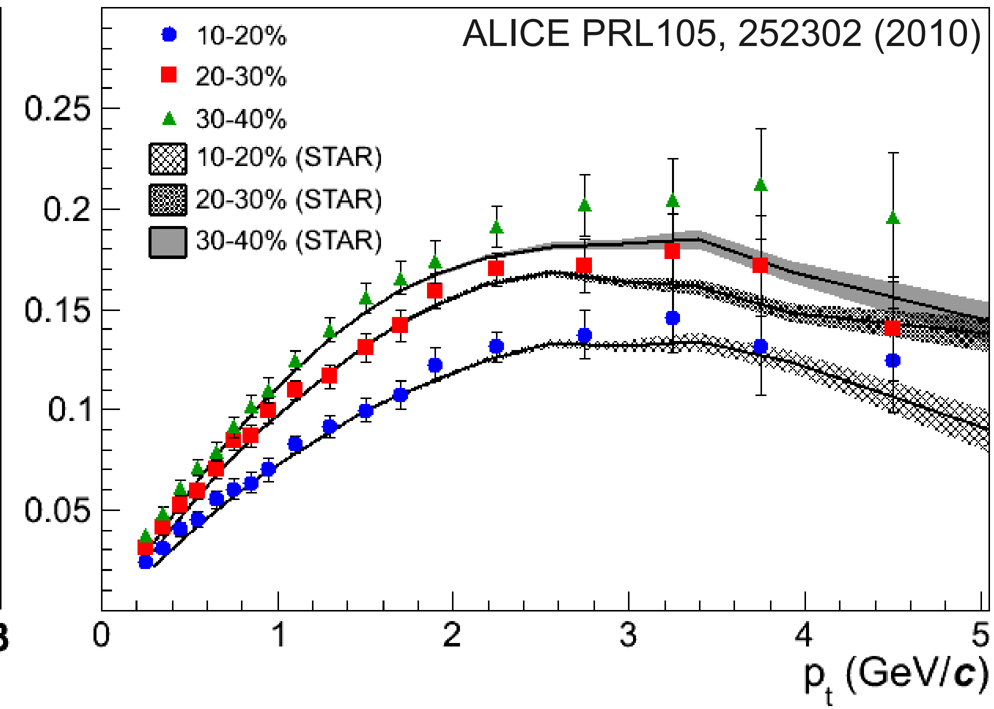

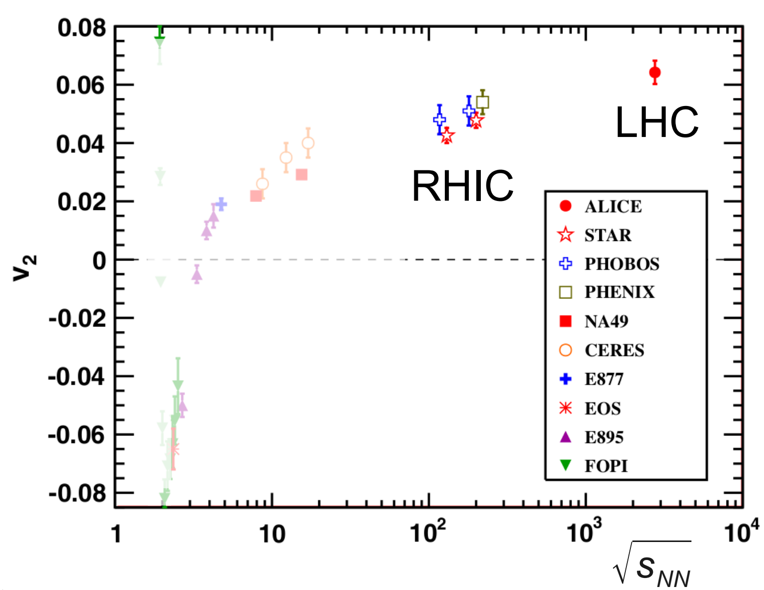

$v_2(p_t)$ has similar shape and magnitude:
increase of integral v_2 is driven
by stronger radial flow (boost to higher p_t)

Identified particle spectra: LHC vs. RHIC

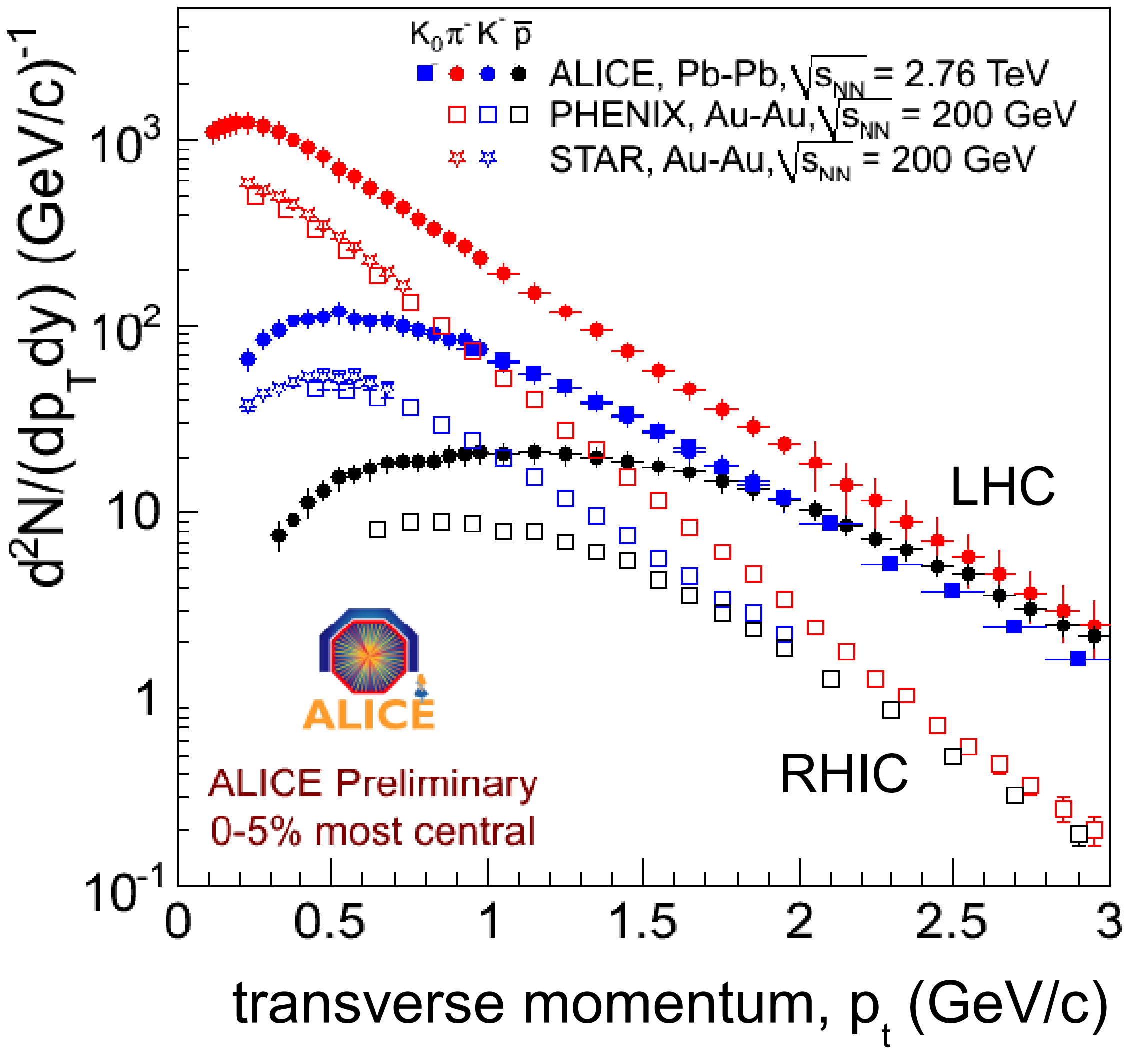

Spectra shapes changed significantly from RHIC to LHC

Radial expansion (flow):

Boost particles to higher p_t
(particles gain extra radial velocity)

From Blast wave spectra fits:
20% stronger radial flow at LHC
→ increase of integral v_2

Identified particle spectra: LHC vs. RHIC

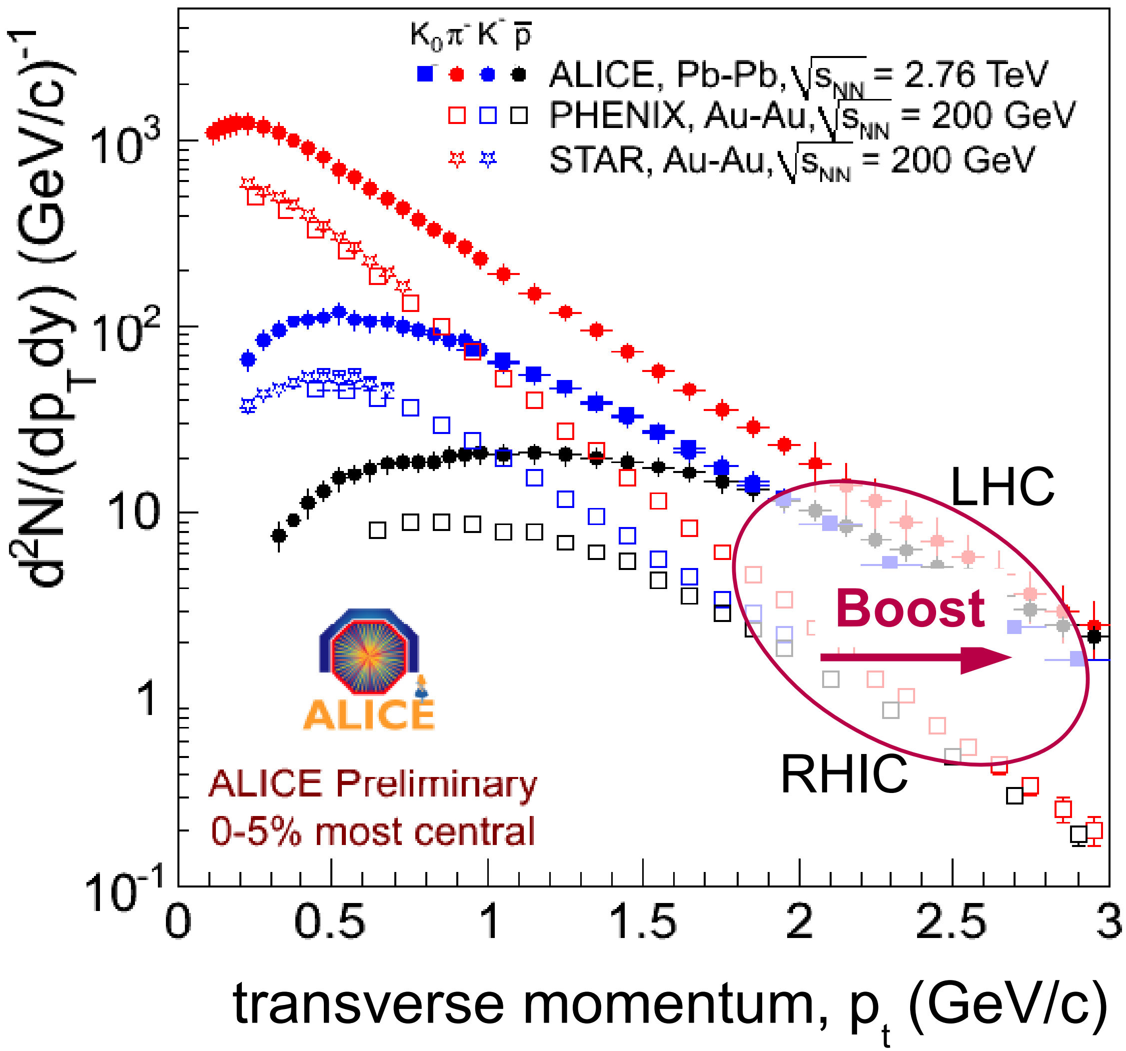

Spectra shapes changed significantly from RHIC to LHC

Radial expansion (flow):

Boost particles to higher p_t

(particles gain extra radial velocity)

From Blast wave spectra fits:
20% stronger radial flow at LHC
→ increase of integral v_2

Elliptic flow mass splitting

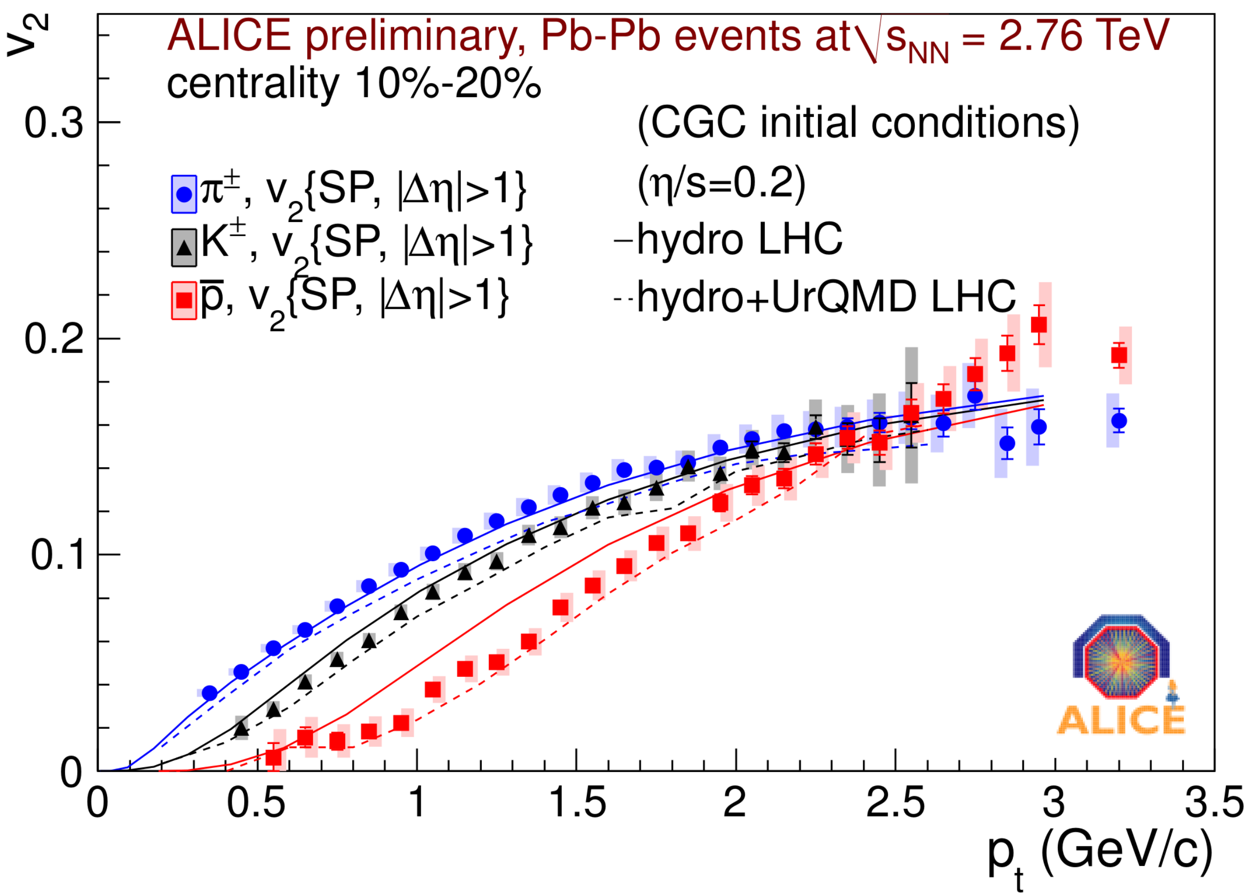

VISHNU: Heinz et. al, arxiv:1108.5323

Similar to spectra:
v_2 of heavier particles
is pushed to higher p_t

Viscous hydrodynamics
well describe flow of $\pi^{\pm}$ and $K^{\pm}$:
→ sensitivity to QGP viscosity

Including hadronic rescattering
with UrQMD model allows
better reproduce proton v_2:
→ sensitivity to the evolution

Coalesence and v_2 number of quarks scaling

Distribution of primordial particles
reflects the distribution of original particles:

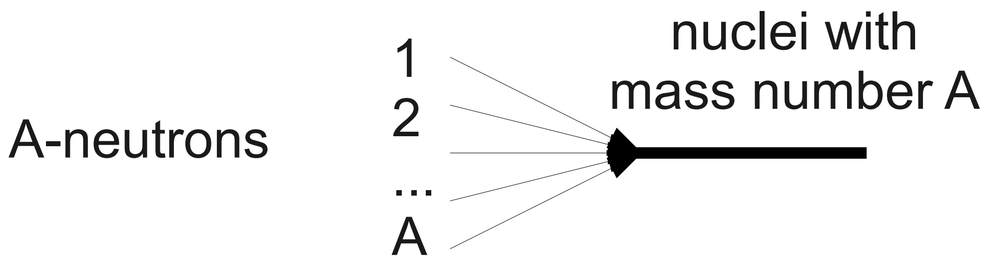

$$\frac{E_A d^3 n_A}{d^3 p_A} = B_A \left(\frac{E_p d^3 n_p}{d^3 p_p} \right)^A$$

$$\frac{dN}{d(\phi - \Psi_{RP})} \sim 1 + 2 \sum_{i=1} v_n(p_t, \eta) \cos[n(\phi - \Psi_{RP})]$$

If distribution is affected by flow,
it will be amplified by coalesence:

$$v_{n,A}(p_{T,A}) \approx A v_{n,p}(p_{T,A}/A)$$

Mesons:

$$\frac{d^3 n_M}{d^3 p_M} \propto [\frac{d^3 n_q}{d^3 p_q}(p_q \approx p_M/2)]^2$$

Baryons:

$$\frac{d^3 n_B}{d^3 p_B} \propto [\frac{d^3 n_q}{d^3 p_q}(p_q \approx p_B/3)]^3$$

Constituent number of quarks scaling

RHIC

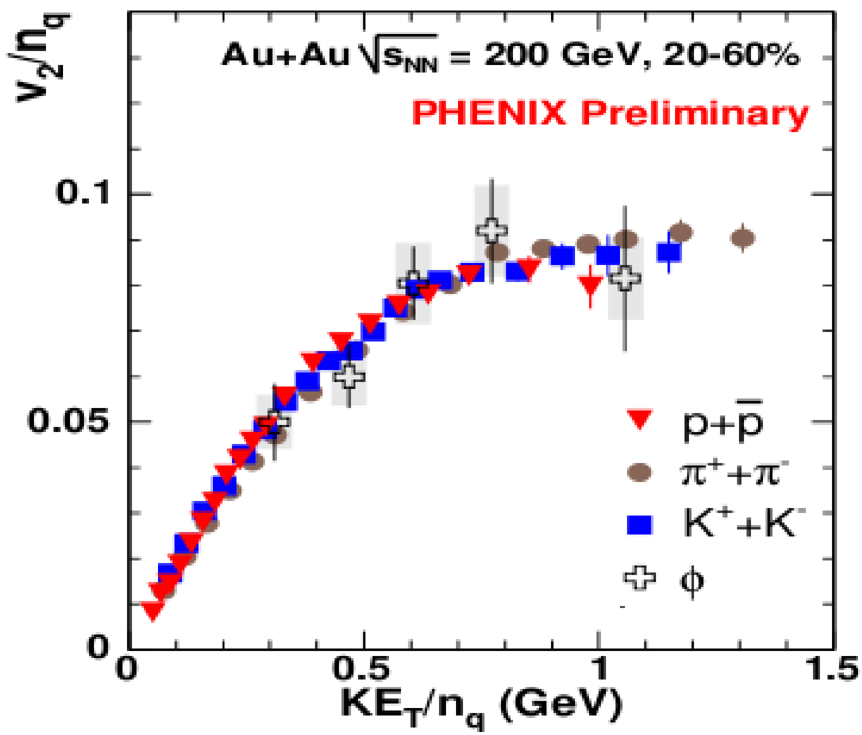

LHC

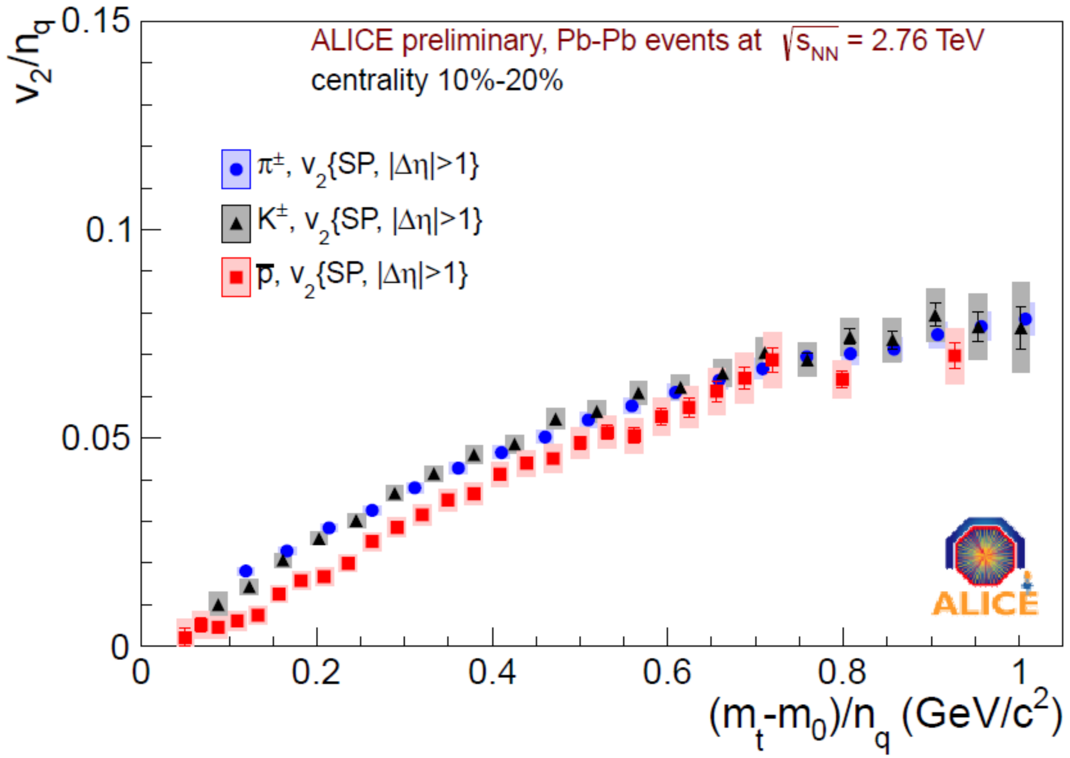

Observe approximate number of quark scaling:

Strong indication that system evolved through deconfined (QGP) phase

Flow fluctuations

Flow fluctuations

Transverse distribution of nucleons inside a nuclei
(e.g. can be simulated with Glauber Monte-Carlo)

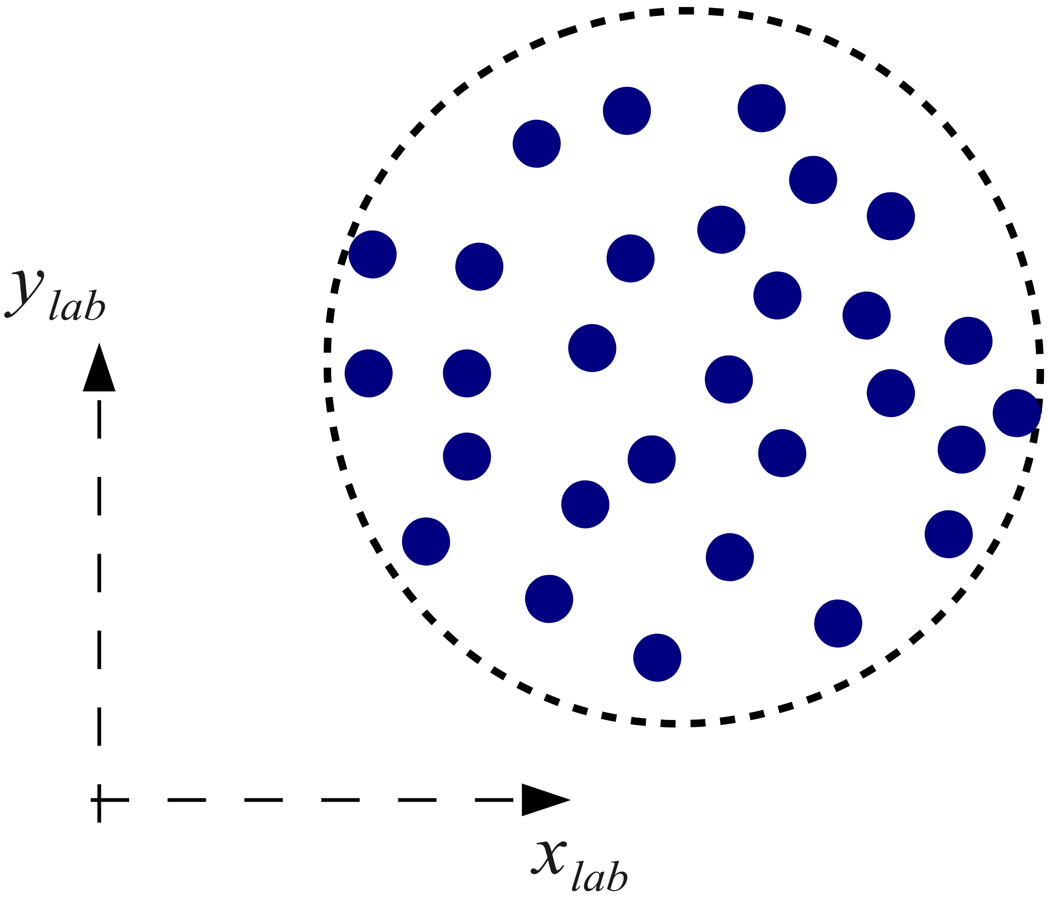

Flow fluctuations

A moment just before collision:
overlayed transverse distributions of nucleons inside each nuclei

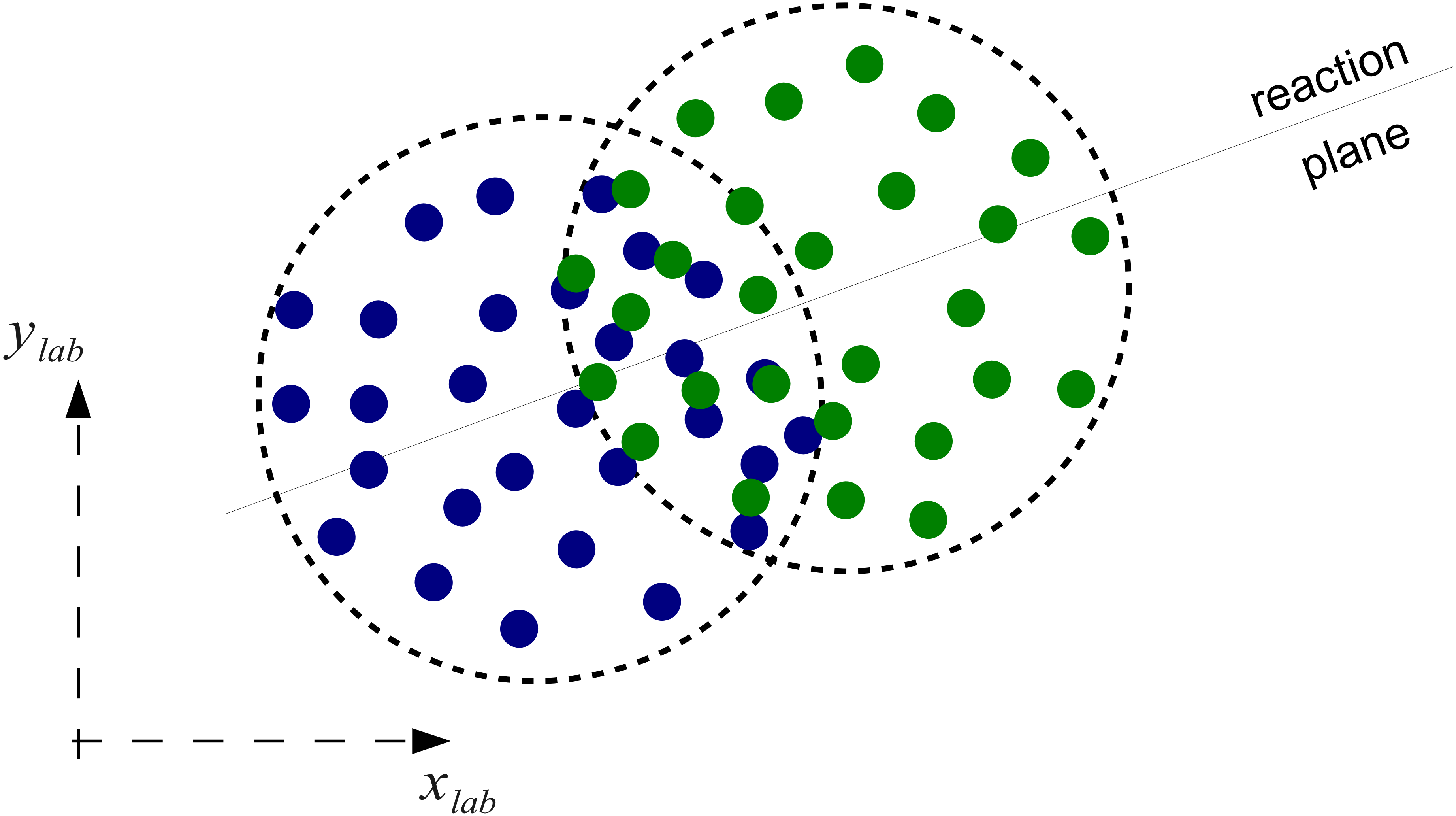

Flow fluctuations

Some of the nucleons (participants) interacted; others (spectators) passed by

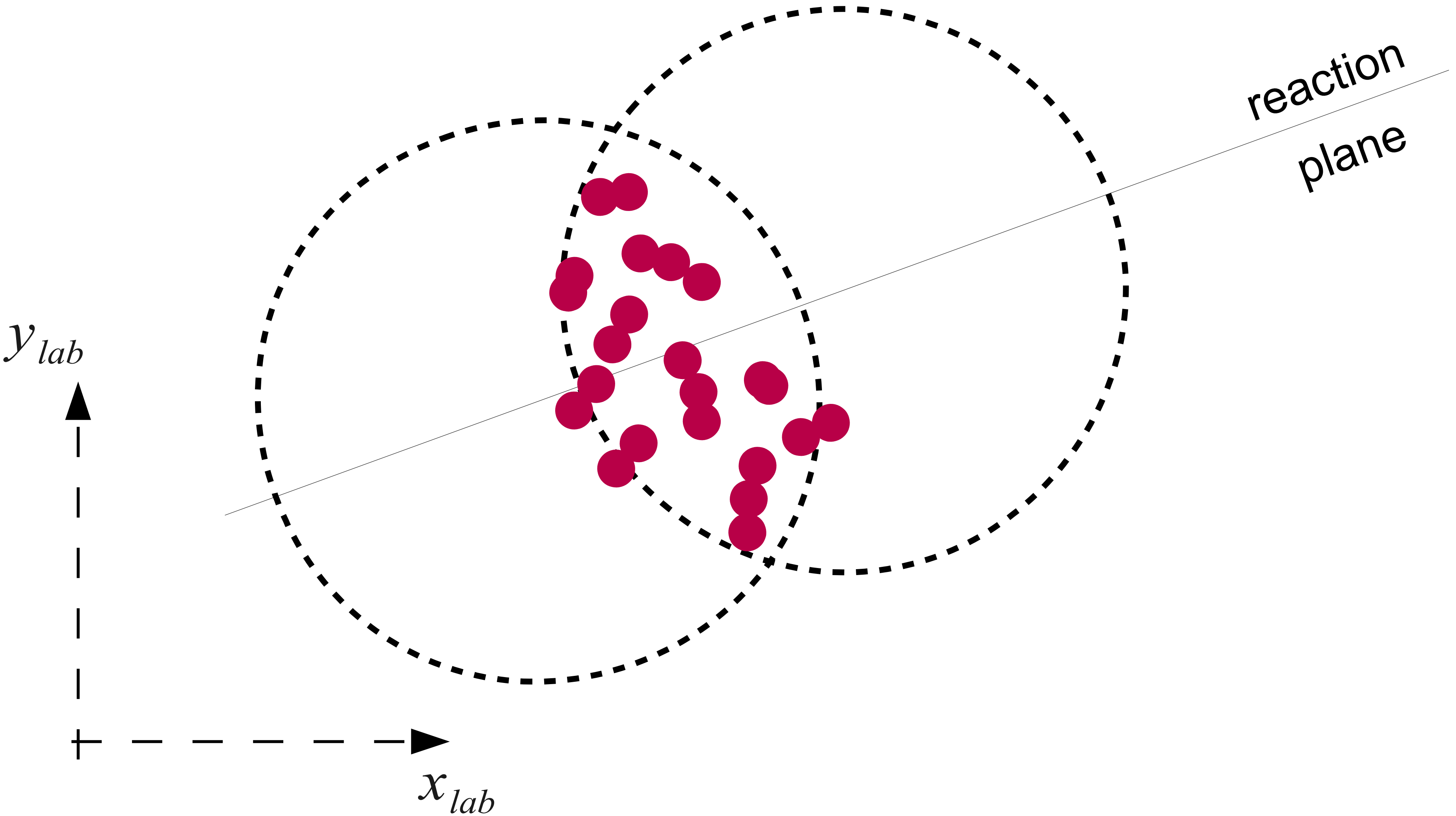

Flow fluctuations

Event-by-event flow fluctuations

Example:

same impact parameter
same reaction plane orientation
(same nucleons distributions,
Just rotated by some angle)

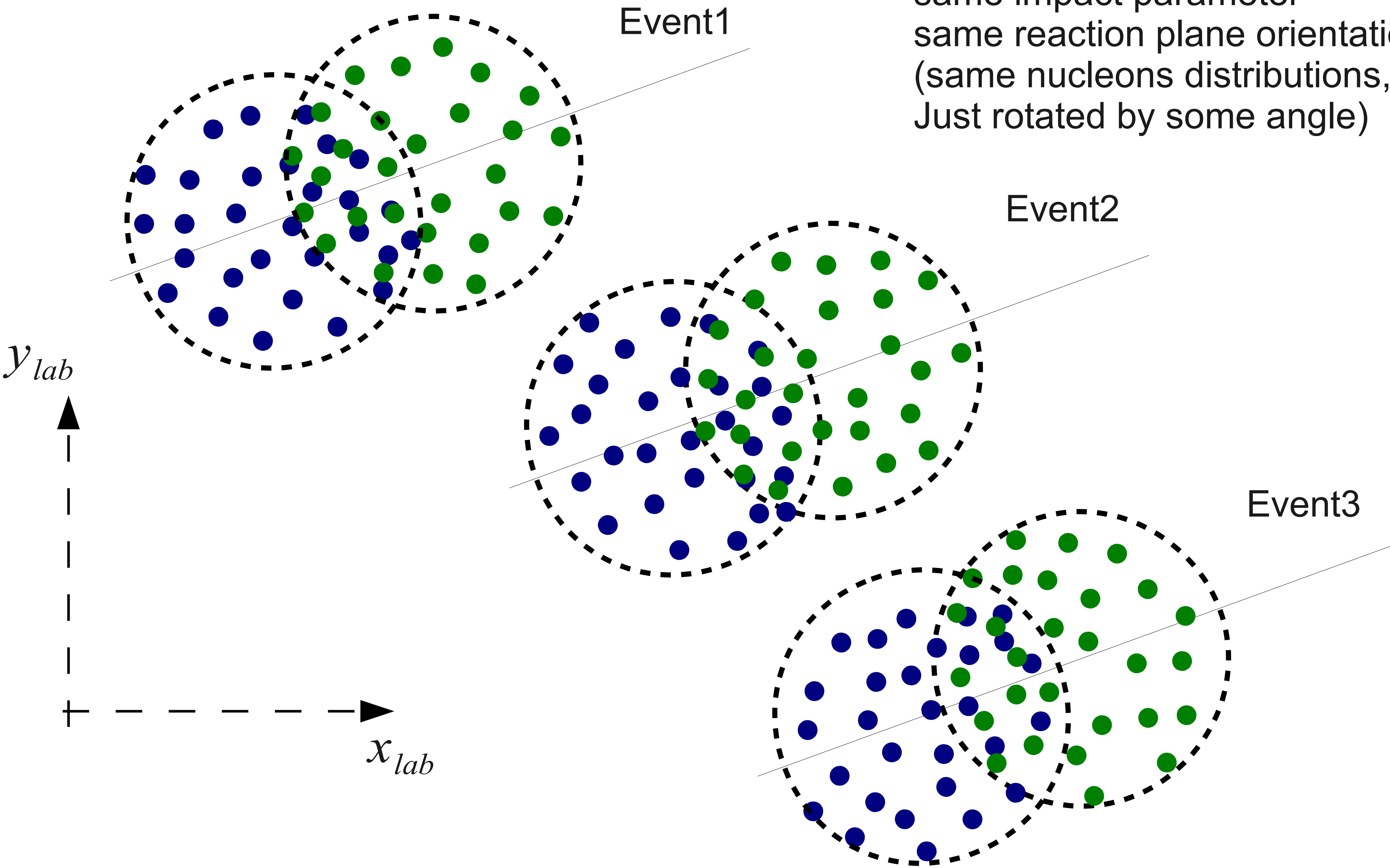

Flow fluctuations

Fluctuating spacial asymmetry result in the event by event fluctuations of anisotropic flow

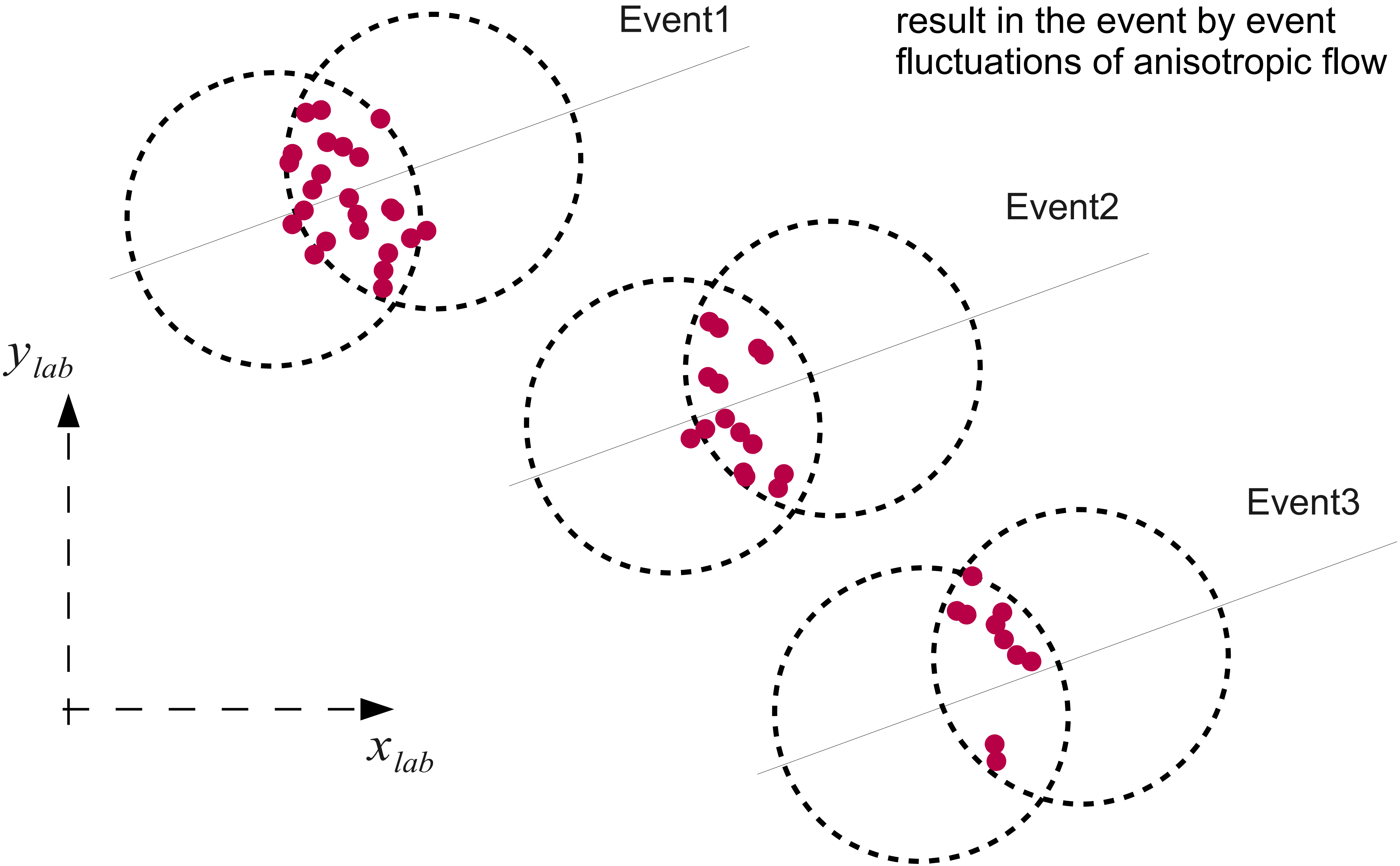

Flow fluctuations: participant eccentricity

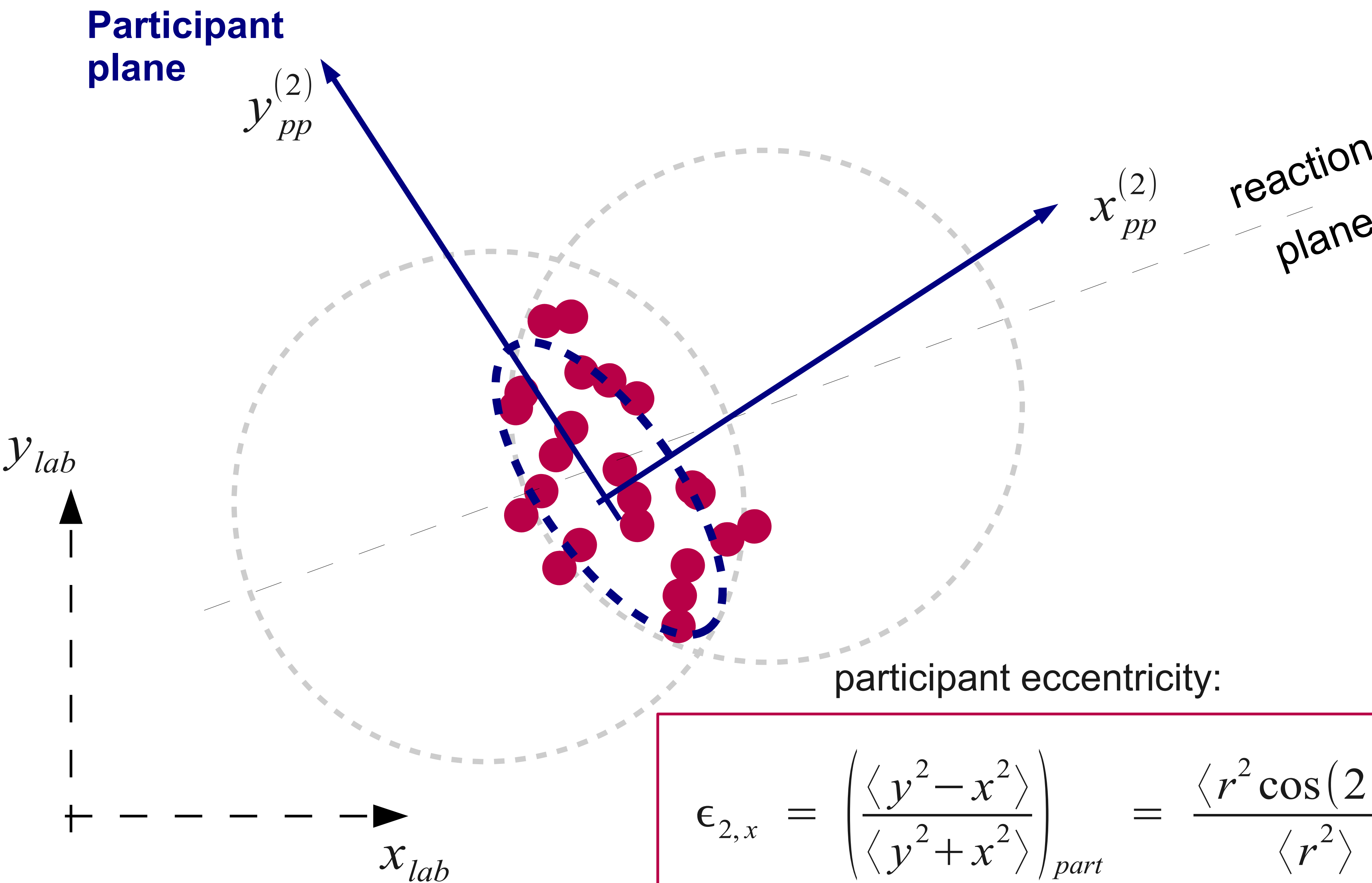

participant eccentricity:

$$\epsilon_{2,x} = \left(\frac{\langle y^2 - x^2 \rangle}{\langle y^2 + x^2 \rangle} \right)_{part} = \frac{\langle r^2 \cos(2\phi) \rangle}{\langle r^2 \rangle}$$

How fluctuations affect the measured flow?

2-particle azimuthal correlation:

$$c_n\{2\} = \langle \cos[2(\phi_i - \phi_j)] \rangle = \langle v_n^2 \rangle + \delta_{n,2}$$

$$\langle v_n^2 \rangle \neq \langle v_n \rangle^2$$

$$\langle v_n^2 \rangle = \langle v_n \rangle^2 + \sigma_n^2$$

$$\langle \cos[n(\phi_i - \phi_j)] \rangle = \langle v_n \rangle^2 + \sigma_n^2 + \delta_{n,2}$$

flow — fluctuations — non-flow

Elliptic flow fluctuations

2-particle correlations affected by 3 effects: $v_2\{2\} = \sqrt{\langle v_2 \rangle^2 + \sigma_2^2 + \delta_2}$

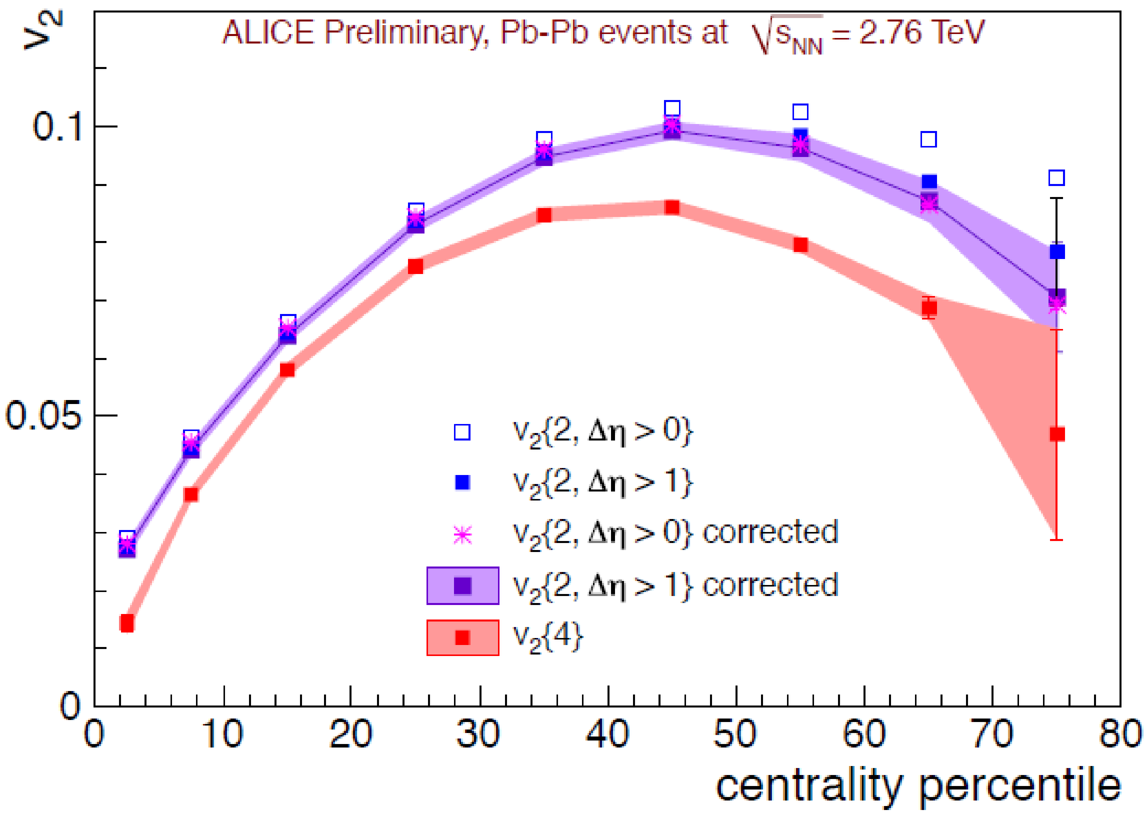

Residual non-flow subtracted based on HIJING Monte-Carlo:

$$v_2^{corr}\{2\} \approx \langle v_2 \rangle + \frac{\sigma_2^2}{2\langle v_2 \rangle}$$

Many-particle correlations free of non-flow:

$$v_2\{4\} \approx \langle v_2 \rangle - \frac{\sigma_2^2}{2\langle v_2 \rangle}$$

Fluctuations set the difference between $v_2^{corr}\{2\}$ and $v_2\{4\}$

Flow fluctuations are significant

Additional constraint on the initial condition

Estimating flow fluctuations from data

σ_2

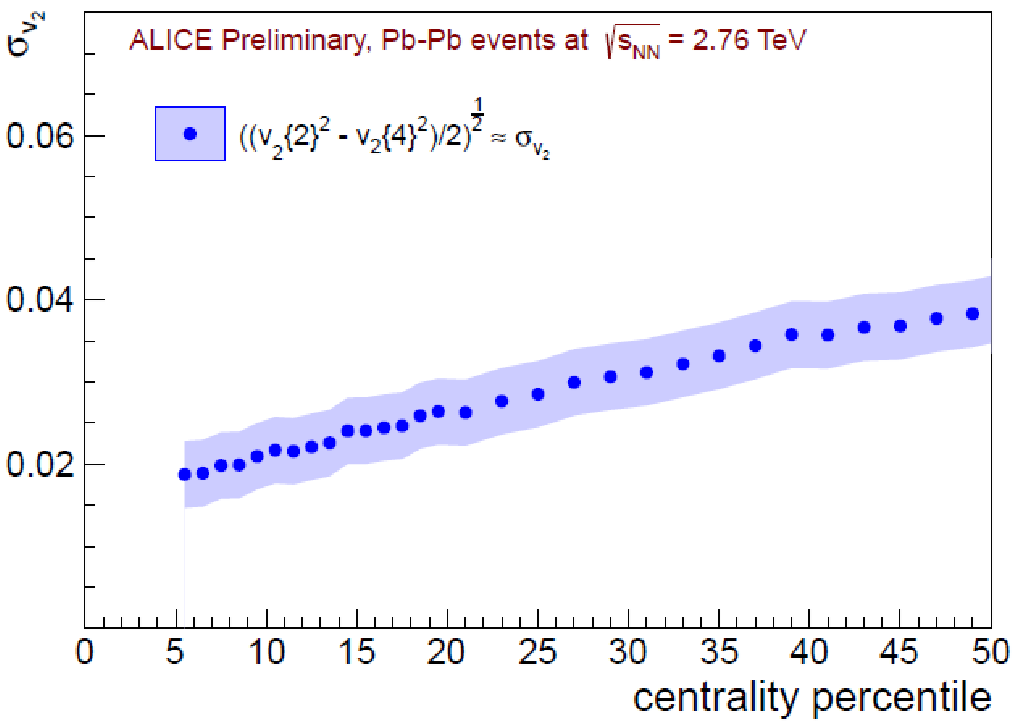

$\sigma_2 / \langle v_2 \rangle$

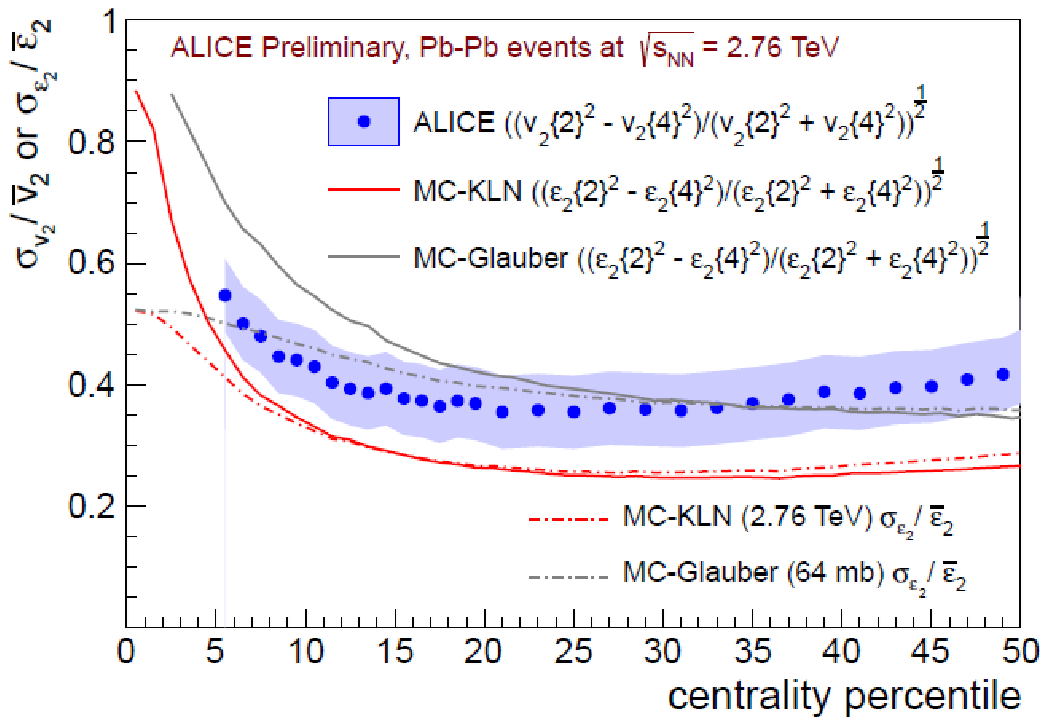

Gaussian fluctuations or $\sigma_n \ll \langle v_n \rangle$

$$\sigma_2 \approx \sqrt{\frac{v_2\{2\} - v_2\{4\}}{2}}$$

$$\langle v_2 \rangle = \sqrt{\frac{v_2\{2\} + v_2\{4\}}{2}}$$

Fluctuations can be significant

Helps to constrain initial condition

“Odd” harmonic flow and fluctuations

$$\frac{dN_\alpha}{d(\Delta\phi_\alpha)} \sim 1+2\sum_{i=1} v_{n,\alpha}\cos(n\Delta\phi_\alpha)$$

By symmetry of the collision, odd harmonic flow v_{2m+1} measured wrt. the reaction plane should vanish at mid-rapidity (or in any symmetric rapidity range):

$$v_{2m+1}^{odd}(-\eta) = -v_{2m+1}^{odd}(\eta)$$

Fluctuations does not obey the symmetry rule of the odd harmonic flow wrt. reaction plane. For example in case of directed flow:

$$v_1\{2\} = \sqrt{\langle v_1^2\rangle} = \sqrt{\langle v_1\rangle^2+\sigma_1^2} = \sigma_1 \neq 0$$

Conclusion: in the symmetric rapidity range all odd harmonics originates from flow fluctuations:

$v_{2m+1}^{even}(-\eta) = +v_{2m+1}^{even}(\eta)$ - rapidity “even” odd harmonic flow

Flow fluctuations: ellipticity

Participant plane
plane

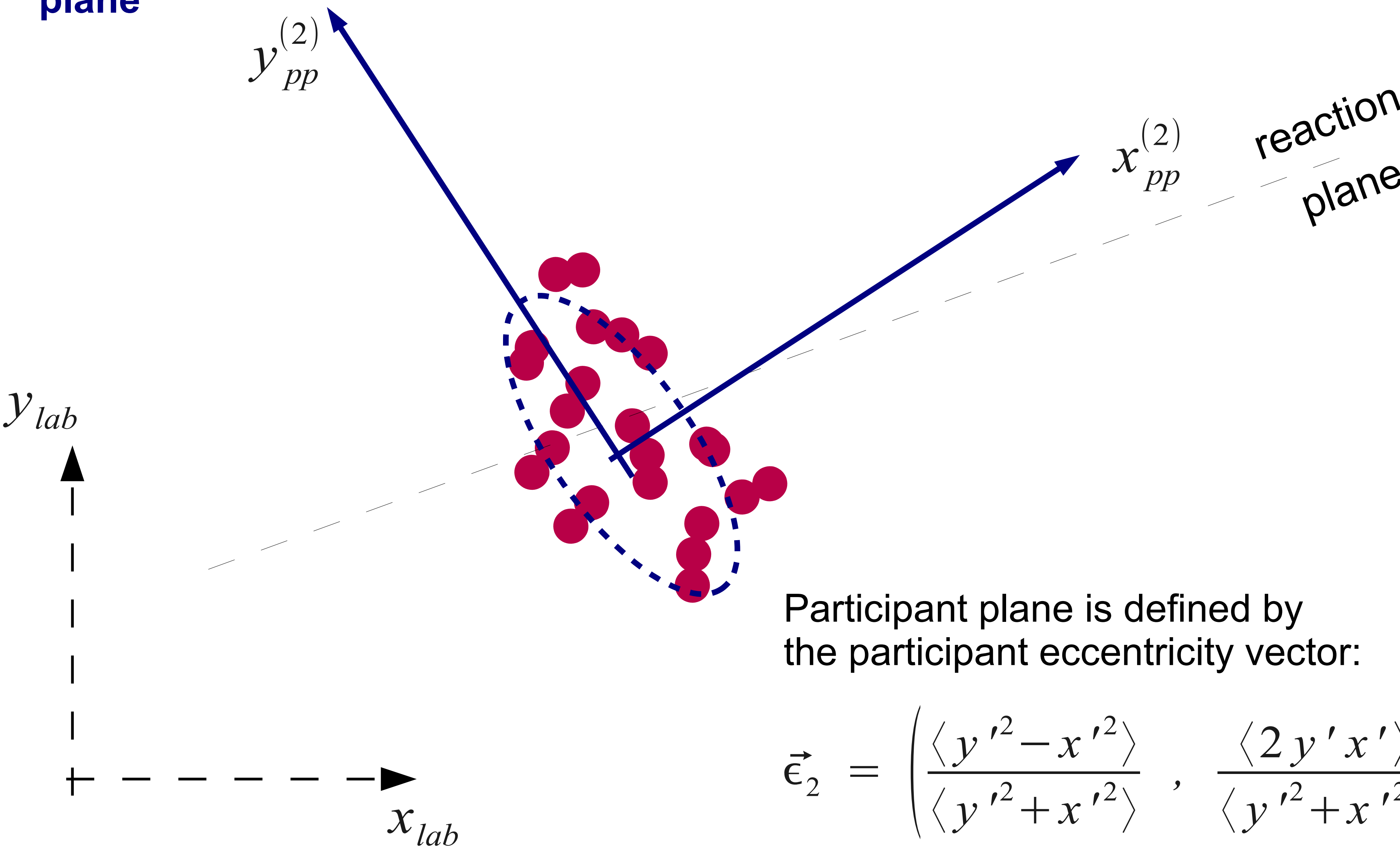

Participant plane is defined by
the participant eccentricity vector:

$$\vec{\epsilon}_2 = \left(\frac{\langle y'^2 - x'^2 \rangle}{\langle y'^2 + x'^2 \rangle} , \frac{\langle 2 y' x' \rangle}{\langle y'^2 + x'^2 \rangle} \right)_{part}$$

$$x' = x - \langle x \rangle \qquad y' = y - \langle y \rangle$$

Flow fluctuations: triangularity

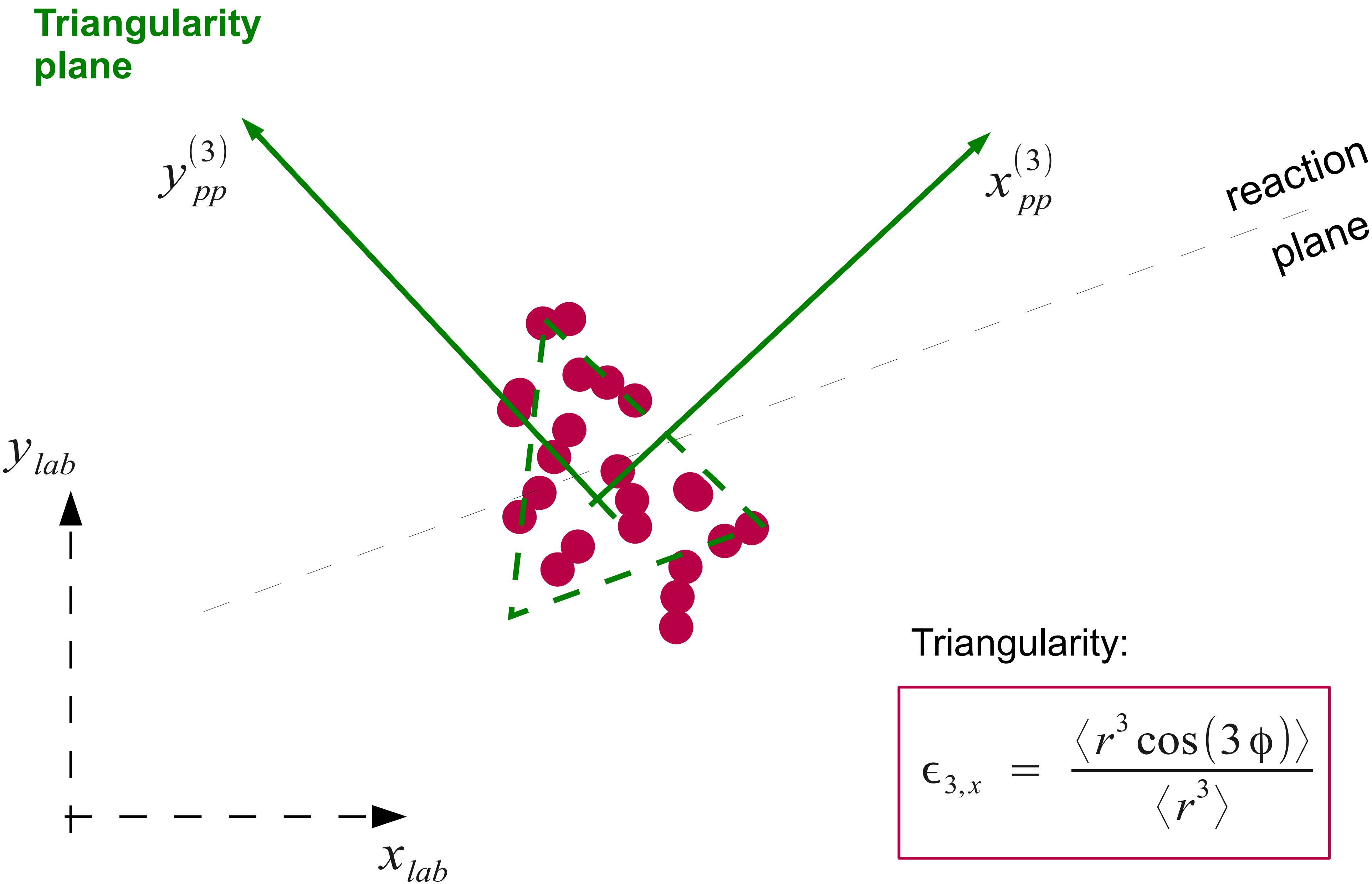

Triangularity:

$$\epsilon_{3,x} = \frac{\langle r^3 \cos(3\phi) \rangle}{\langle r^3 \rangle}$$

Triangular flow, v_3

Measured odd harmonic flow provides clean probe of fluctuations

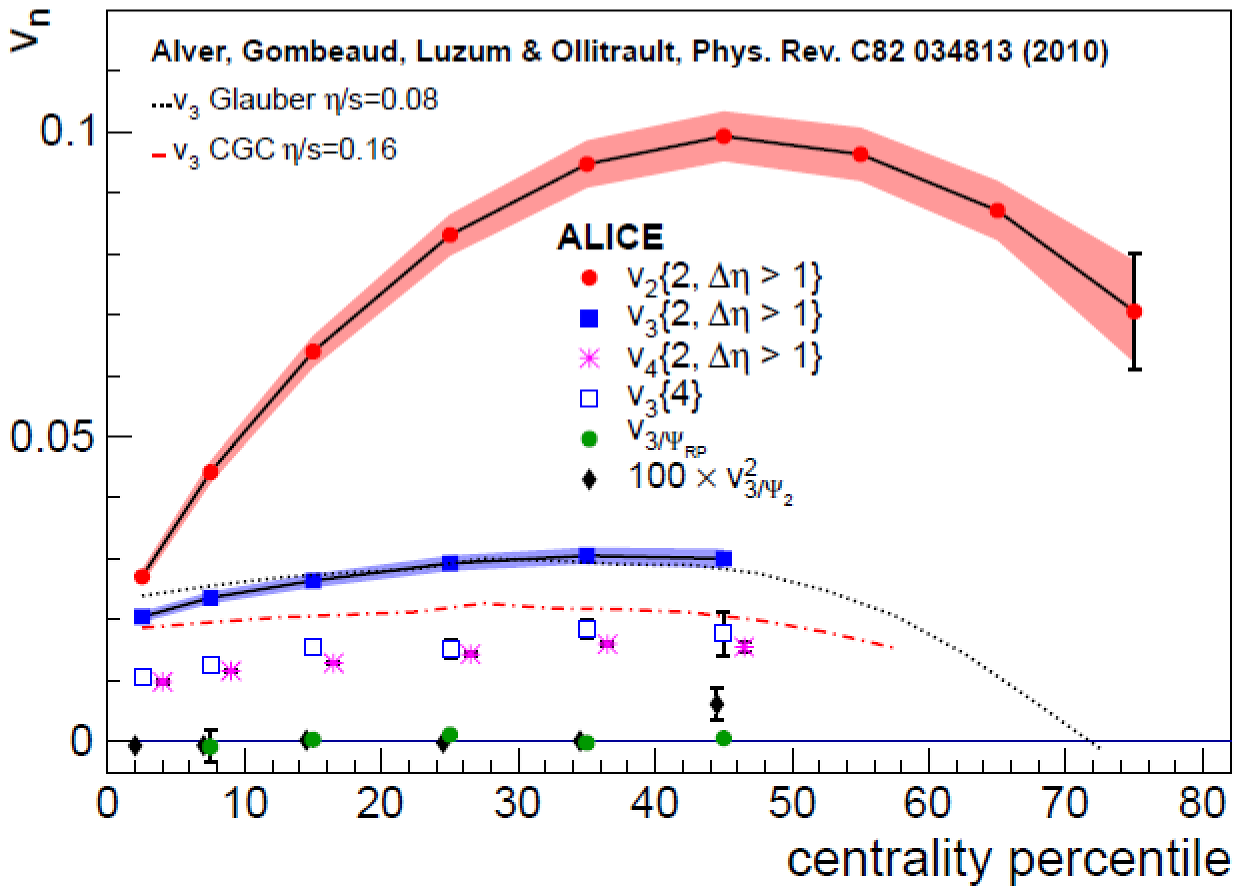

$$\langle v_3 \rangle = 0 \qquad \sigma_3 \neq 0$$

$\sigma_n \ll \langle v_n \rangle$ does not apply

Non-zero v_3 is observed

v_3 shows weak centrality dependence - collectivity
(non-flow correlations should drop as 1/multiplicity)

Triangular flow, v_3

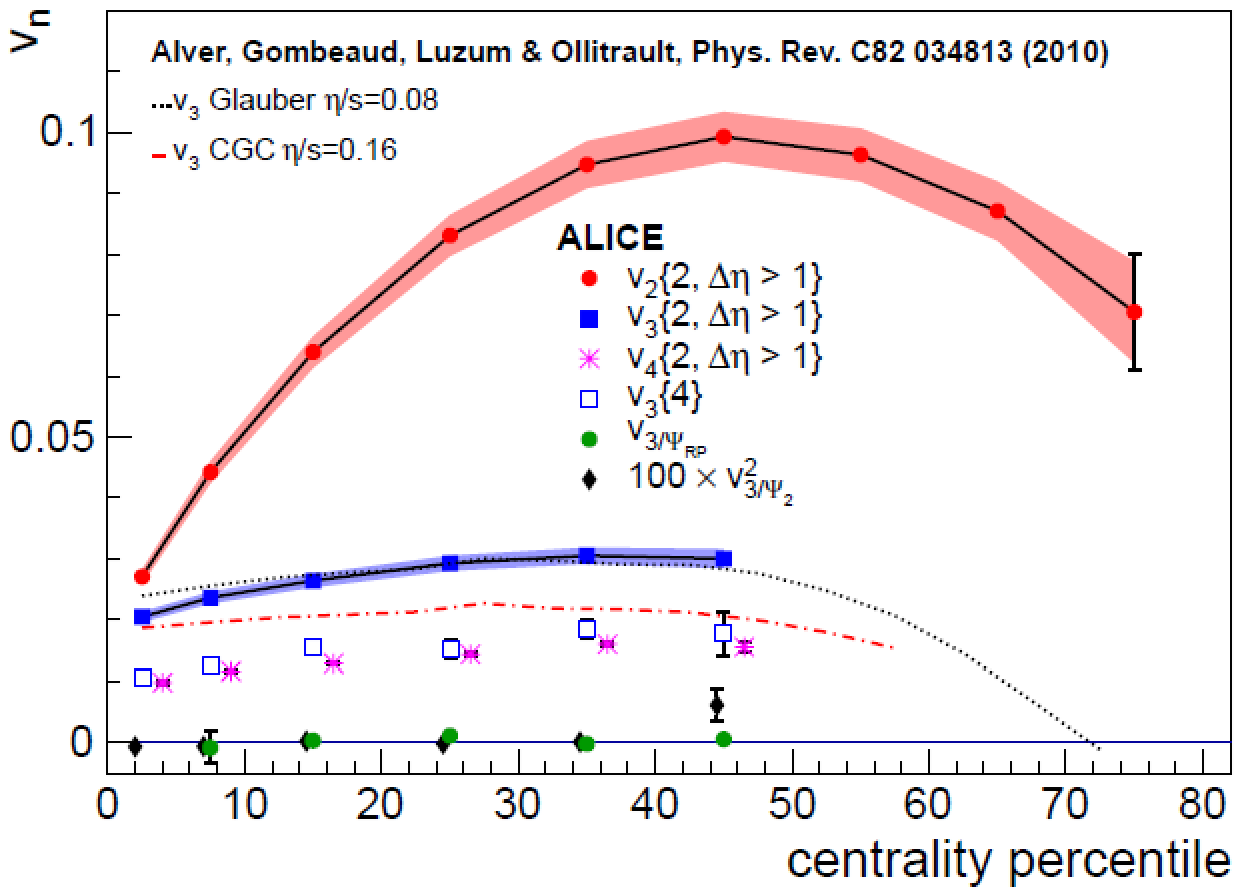

Cumulant results consistent with expectations for fluctuations:

$$\frac{v_3\{2\}}{v_3\{4\}} \approx 2$$

Uncorrelated to reaction plane zero v_3 with spectators:

$$v_3\{\Psi_{RP}\} \equiv v_3\{ZDC\} = 0$$

Mixed harmonics (3rd and 2nd):

$$v_3\{\Psi_2\} = 0$$

Weak centrality dependence

Strong evidence for the geometrical (due to spacial fluctuations) origin of v_3

Mass splitting: test of “hydrodynamic” origin of v_3

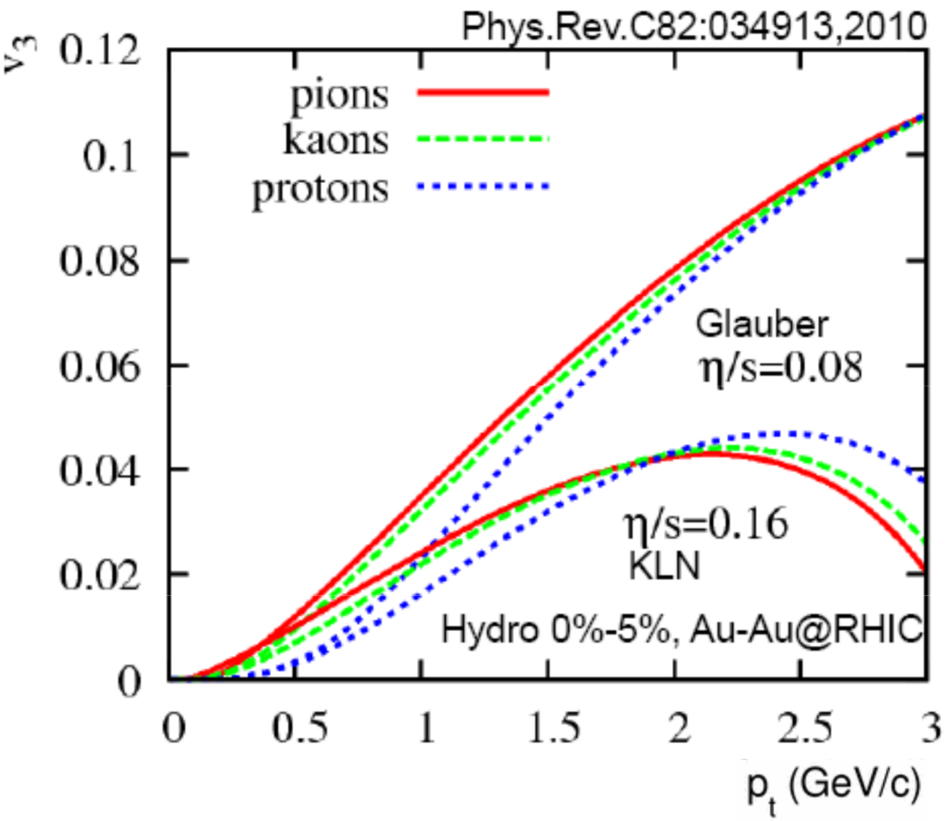

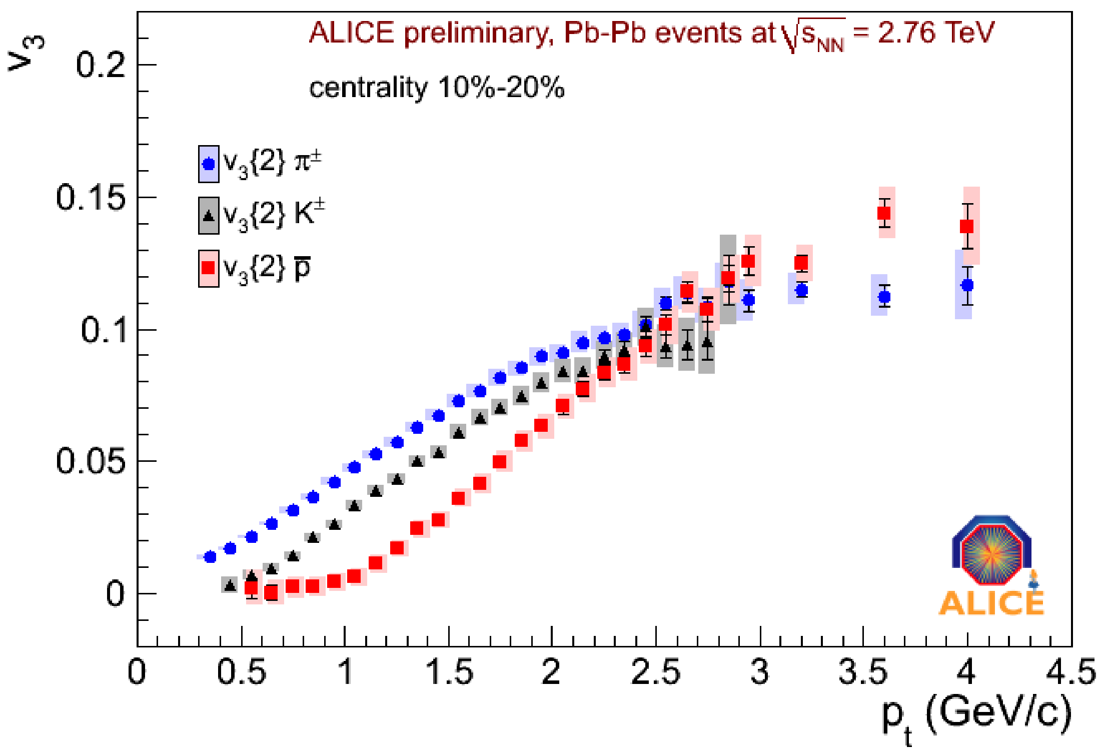

- Observed mass splitting for v_3 supports its hydrodynamic origin
- Additional strong constraint on viscosity and initial condition

Directed flow measured with spectators

$$\frac{dN}{d(\Delta\phi)} \sim 1 + 2\,\boldsymbol{v_1}\cos\Delta\phi$$

Sensitivity to spectator's directed flow with ZDC

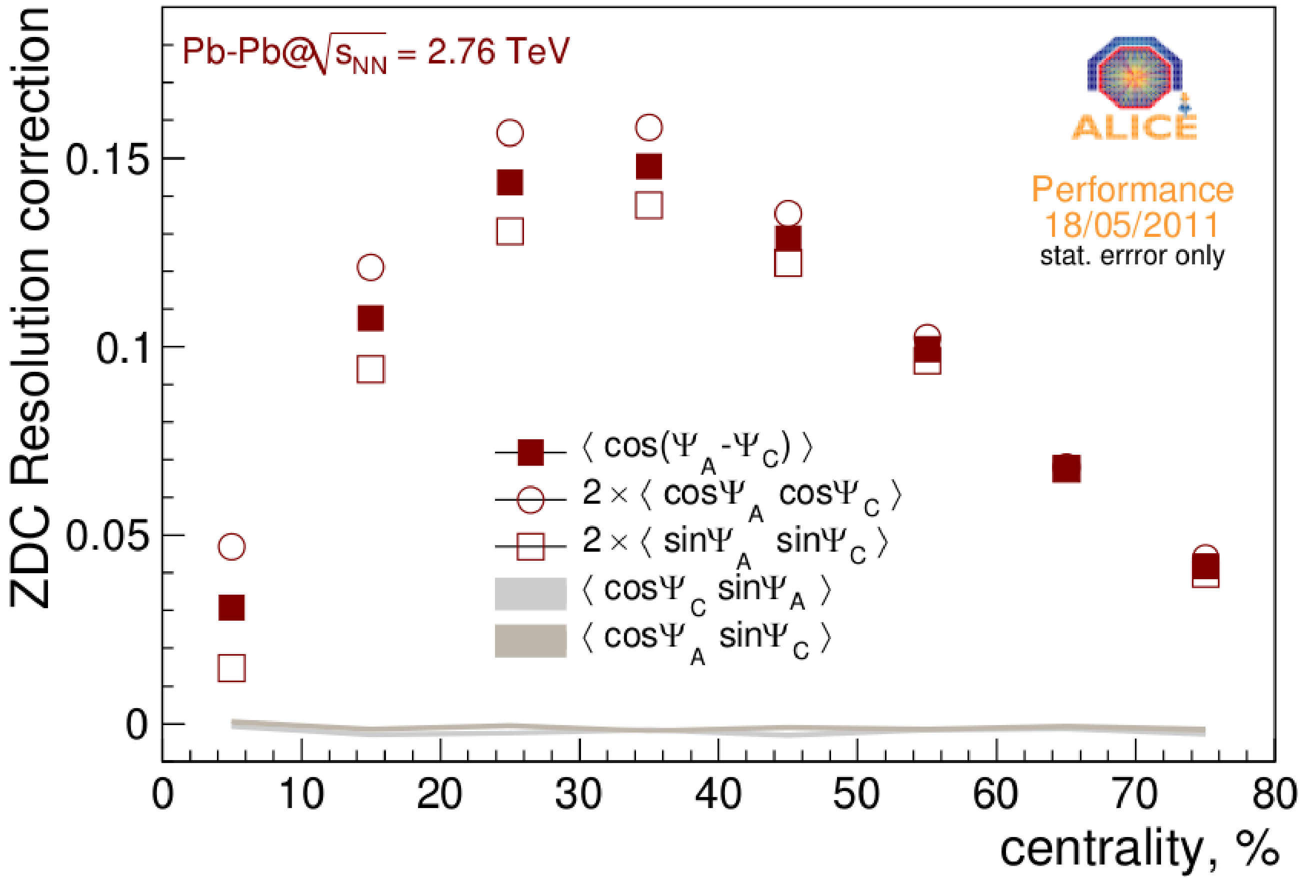

ZDC: 7.2 x 7.2 cm^2

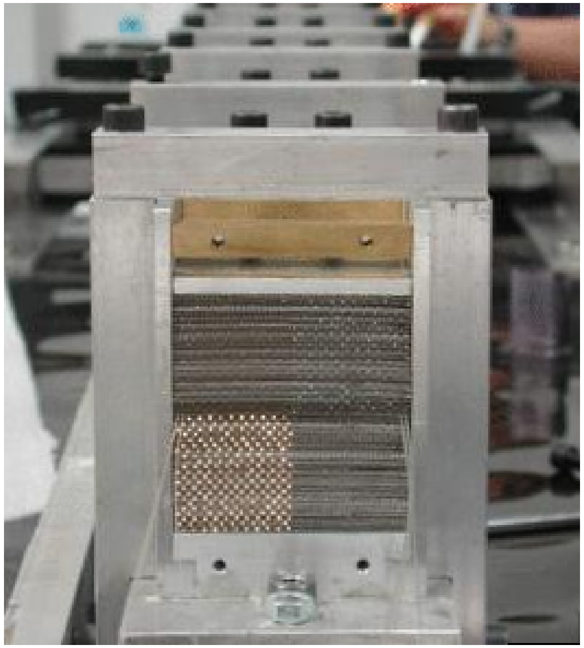

Observe correlation between spectators' deflection measured with neutron Zero Degree Calorimeters located 114meters on each side from the collision vertex:
sensitivity to the directed flow of spectator

Directed flow: η, p_t and centrality dependence

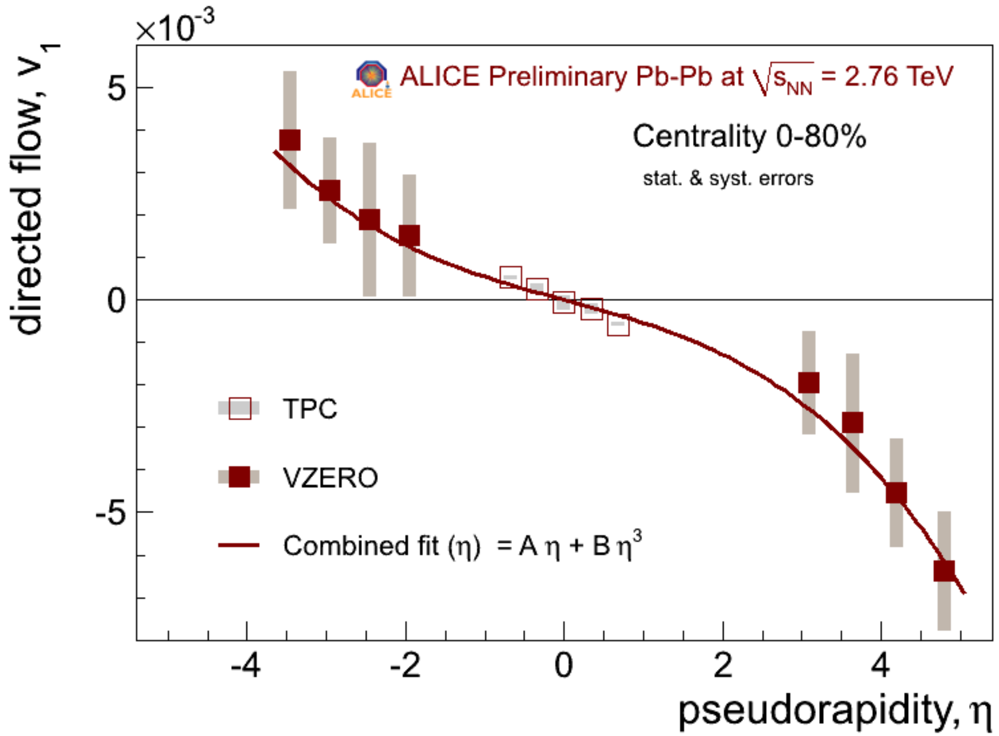

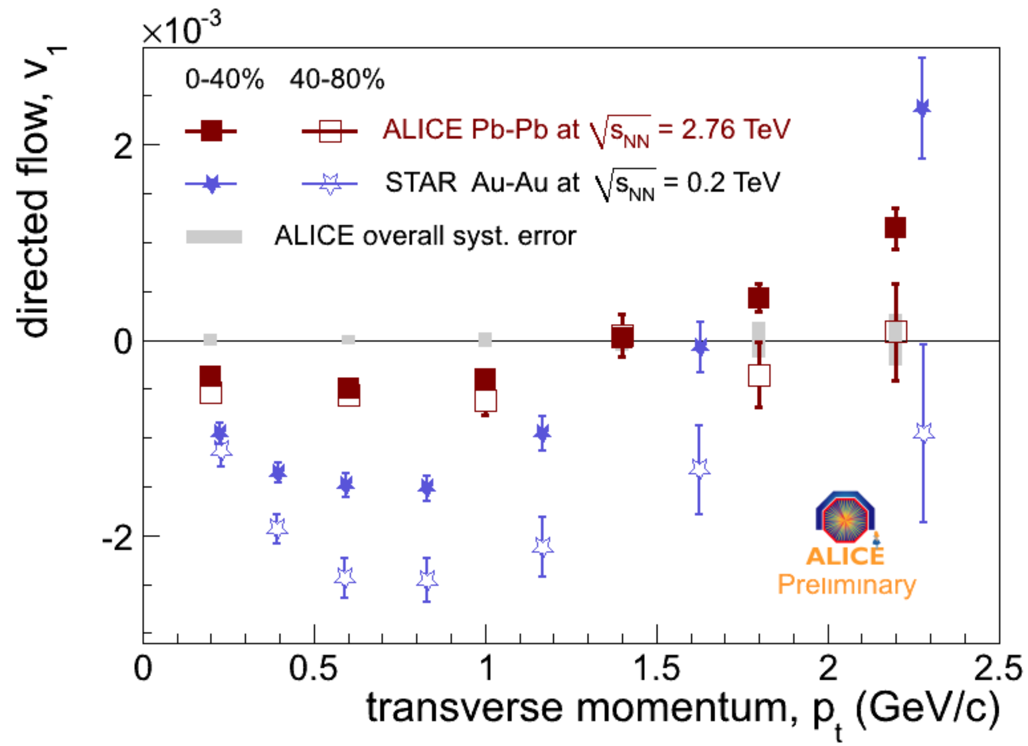

- Negative slope at midrapidity:
  - ✓ Same as at RHIC
  - ✓ In contrast to some of the theoretical predictions
- Zero crossing around p_T ~ 1.5 GeV

Directed flow: longitudinal scaling

STAR data: PRL 101, 252301 (2008)

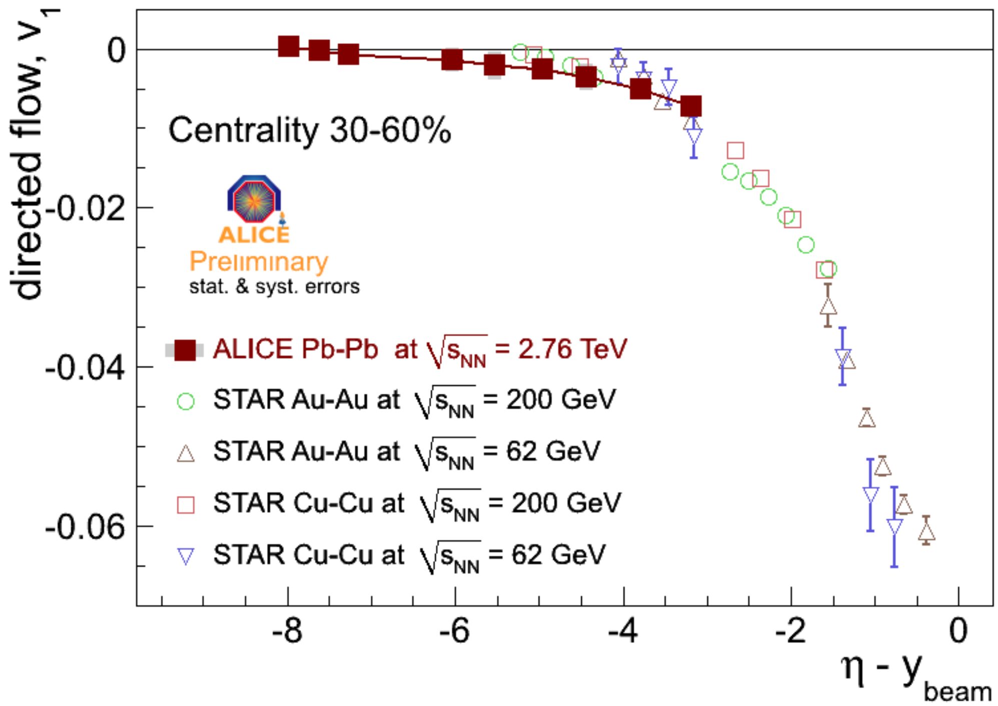

PHOBOS data: PRL97, 012301 (2006)

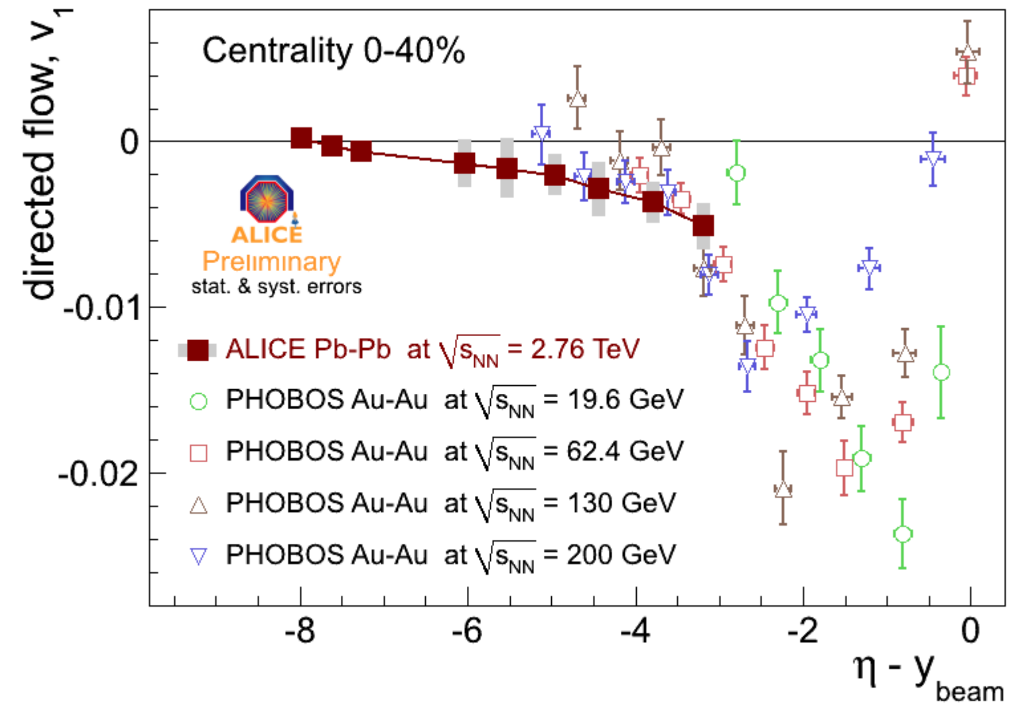

Universal trend when shifted to beam rapidity

Data follows the longitudinal scaling observed at RHIC

Two particle azimuthal correlation:

collective flow modulations
or ridge & mach cone?

?

$$C(\phi_1-\phi_2) \sim 1 + 2\sum_{i=1} v_{n,1} v_{n,2} \cos(n[\phi_1-\phi_2])$$

Two particle azimuthal correlations

$N_{same}^{AB}(\Delta\phi, \Delta\eta)$

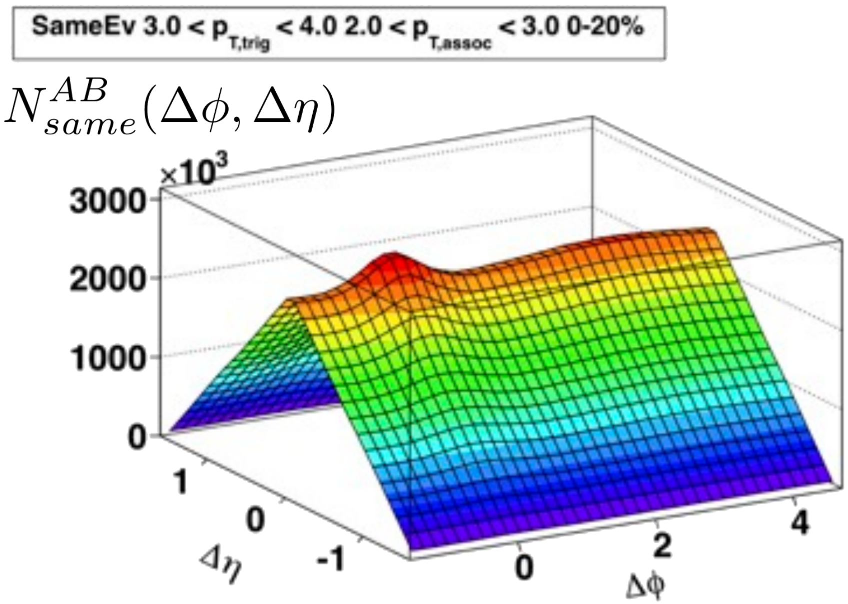

$N_{mixed}^{AB}(\Delta\phi, \Delta\eta)$

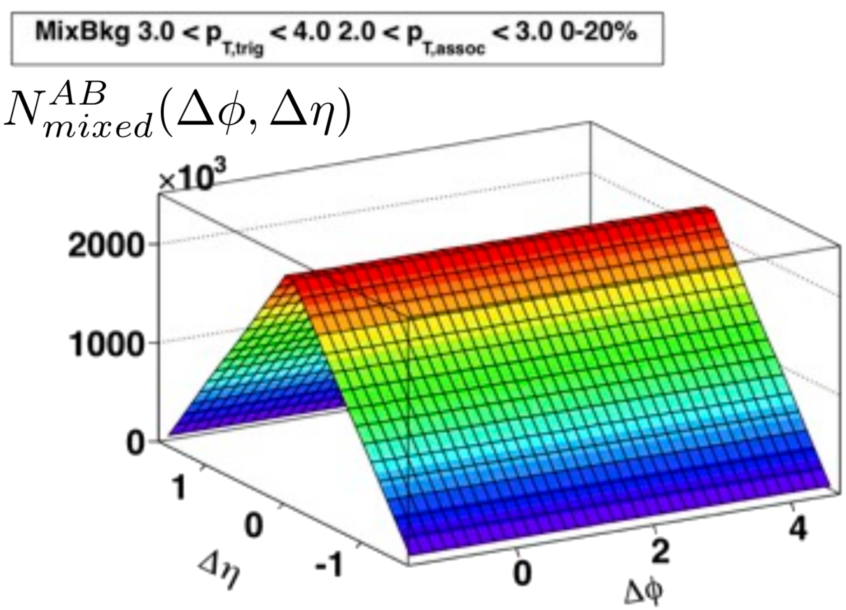

2D-correlations:

$$\Delta\phi = \phi_A - \phi_B \qquad \Delta\eta = \eta_A - \eta_B$$

Correlation function:

$$C(\Delta\phi) \equiv \frac{N_{mixed}^{AB}}{N_{same}^{AB}} \cdot \frac{dN_{same}^{AB}/d\Delta\phi}{dN_{mixed}^{AB}/d\Delta\phi}$$

Two particle azimuthal correlations

Correlations at small p_t (bulk particles)

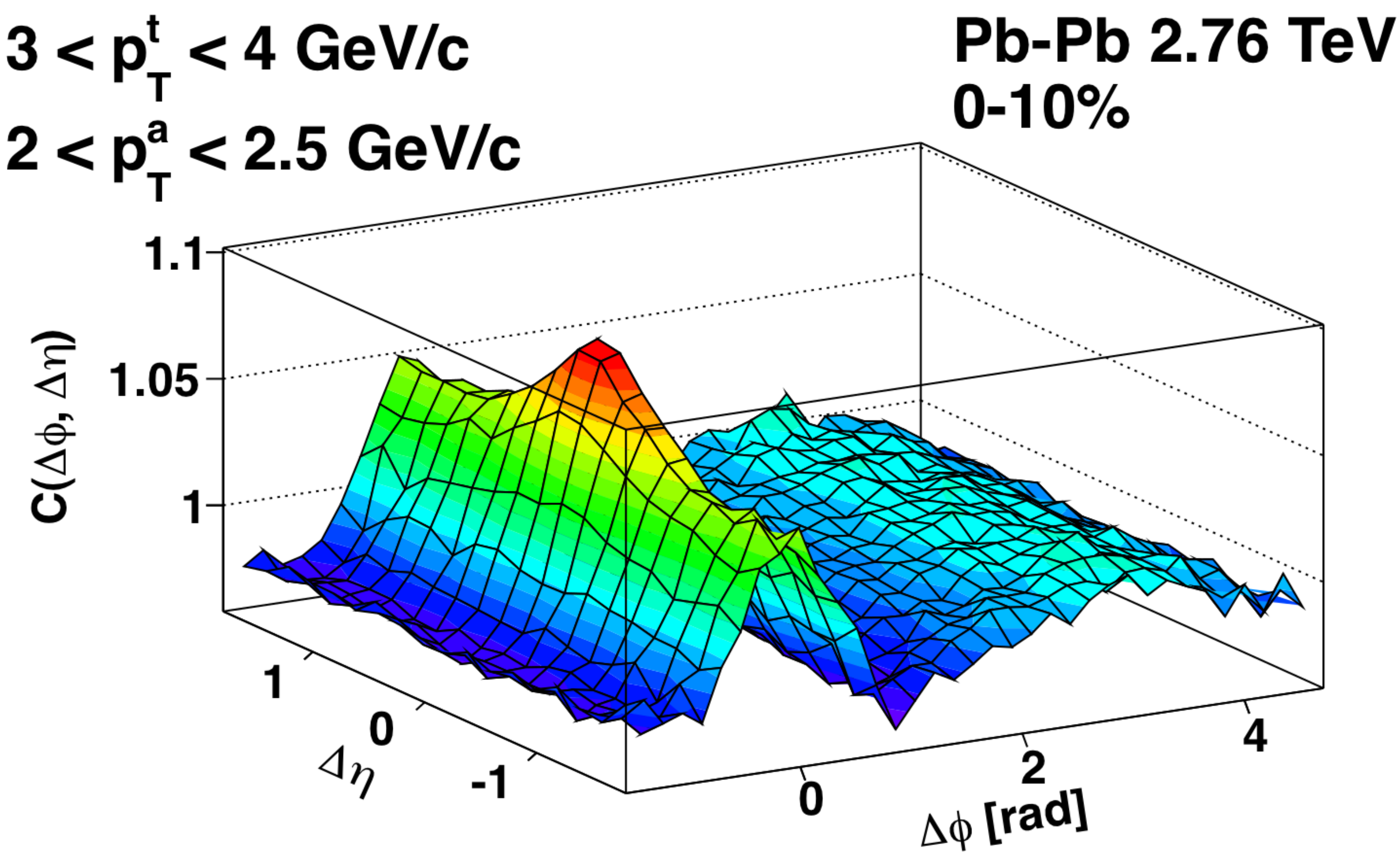

Non-trivial shape of the correlation function

Anatomy of the two particle correlations

Correlations at small p_t (bulk particles)

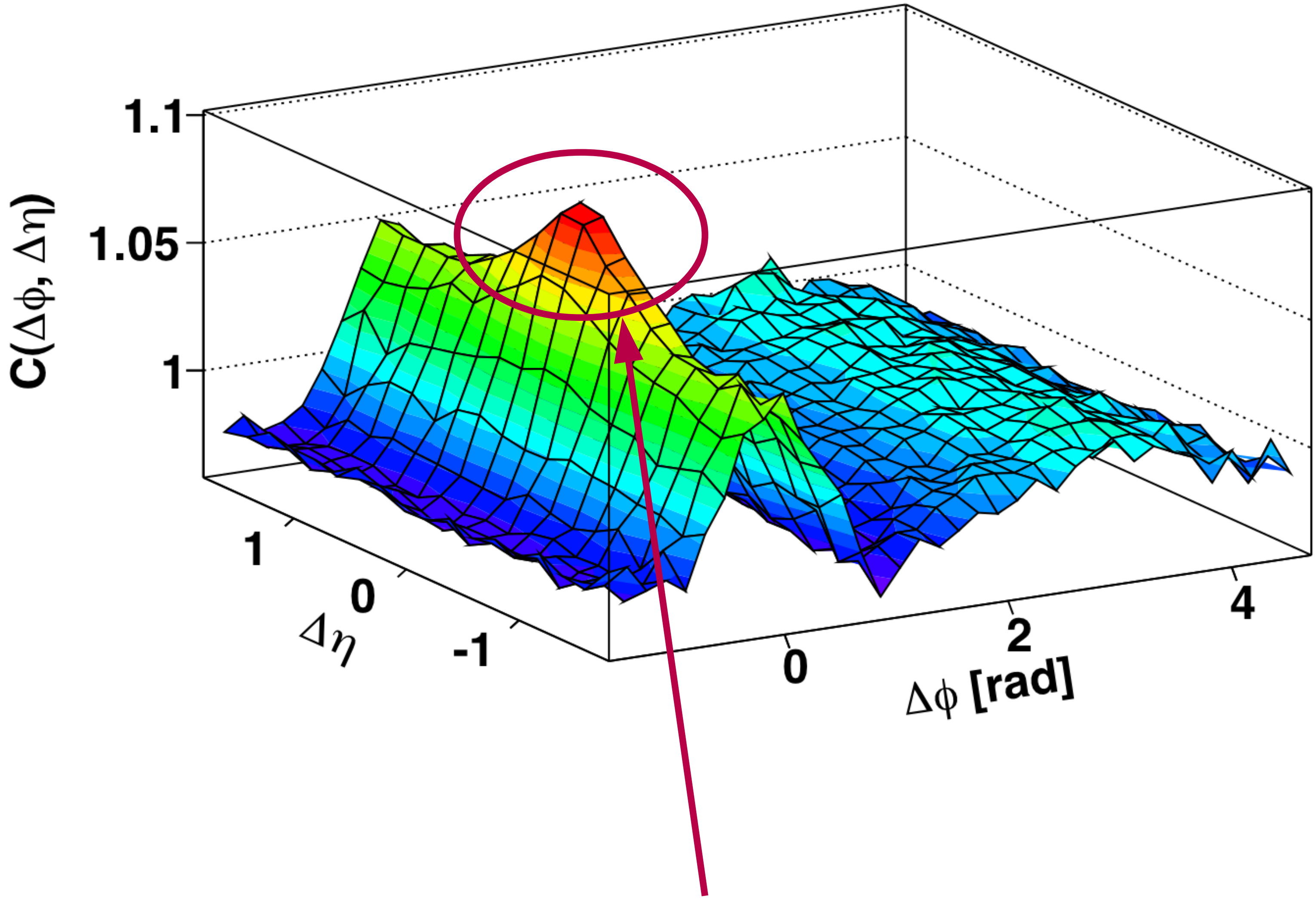

Same side “jet” peak

Anatomy of the two particle correlations

Correlations at small p_t (bulk particles)

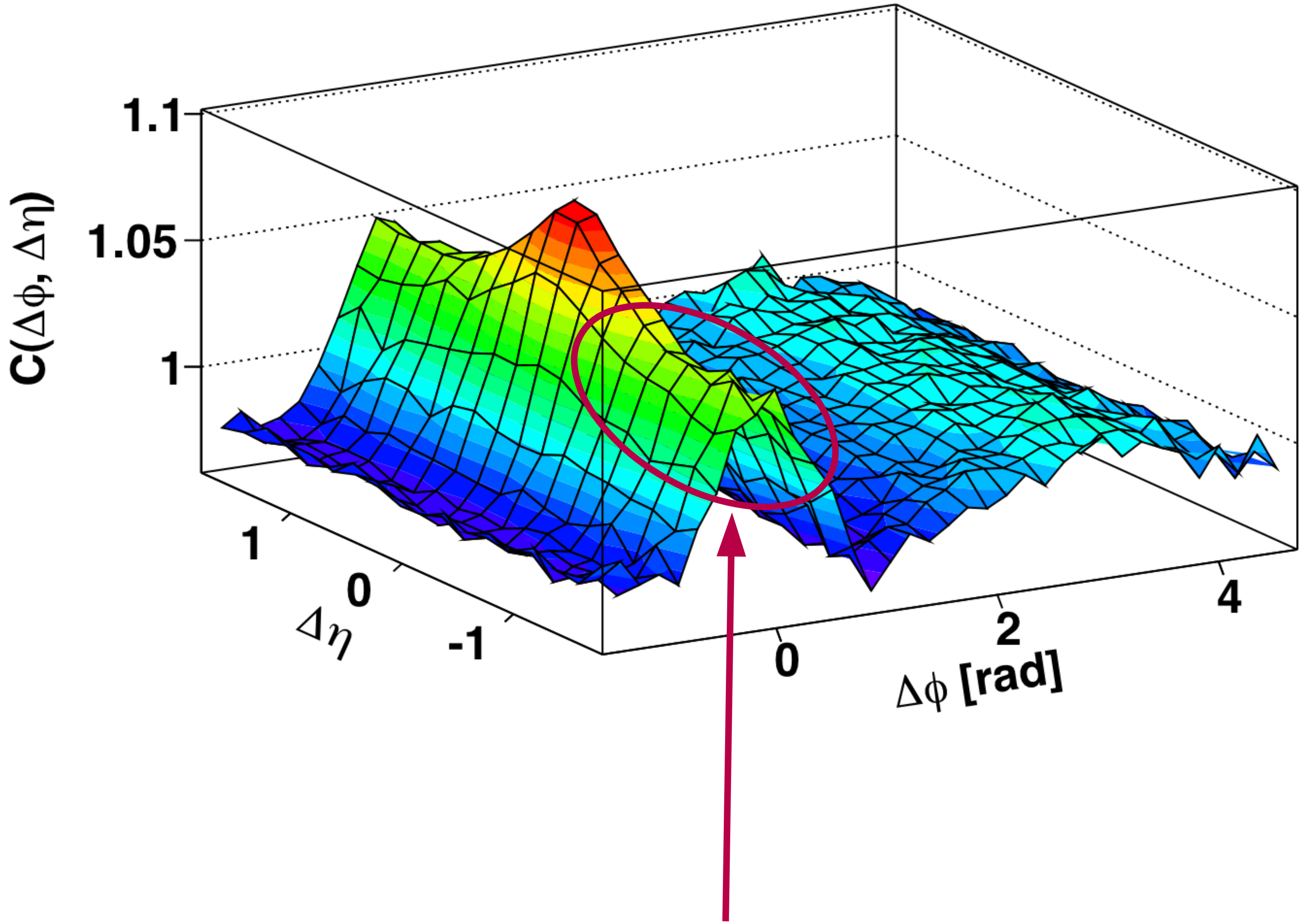

“ridge” (extended in rapidity)

Anatomy of the two particle correlations

Correlations at small p_t (bulk particles)

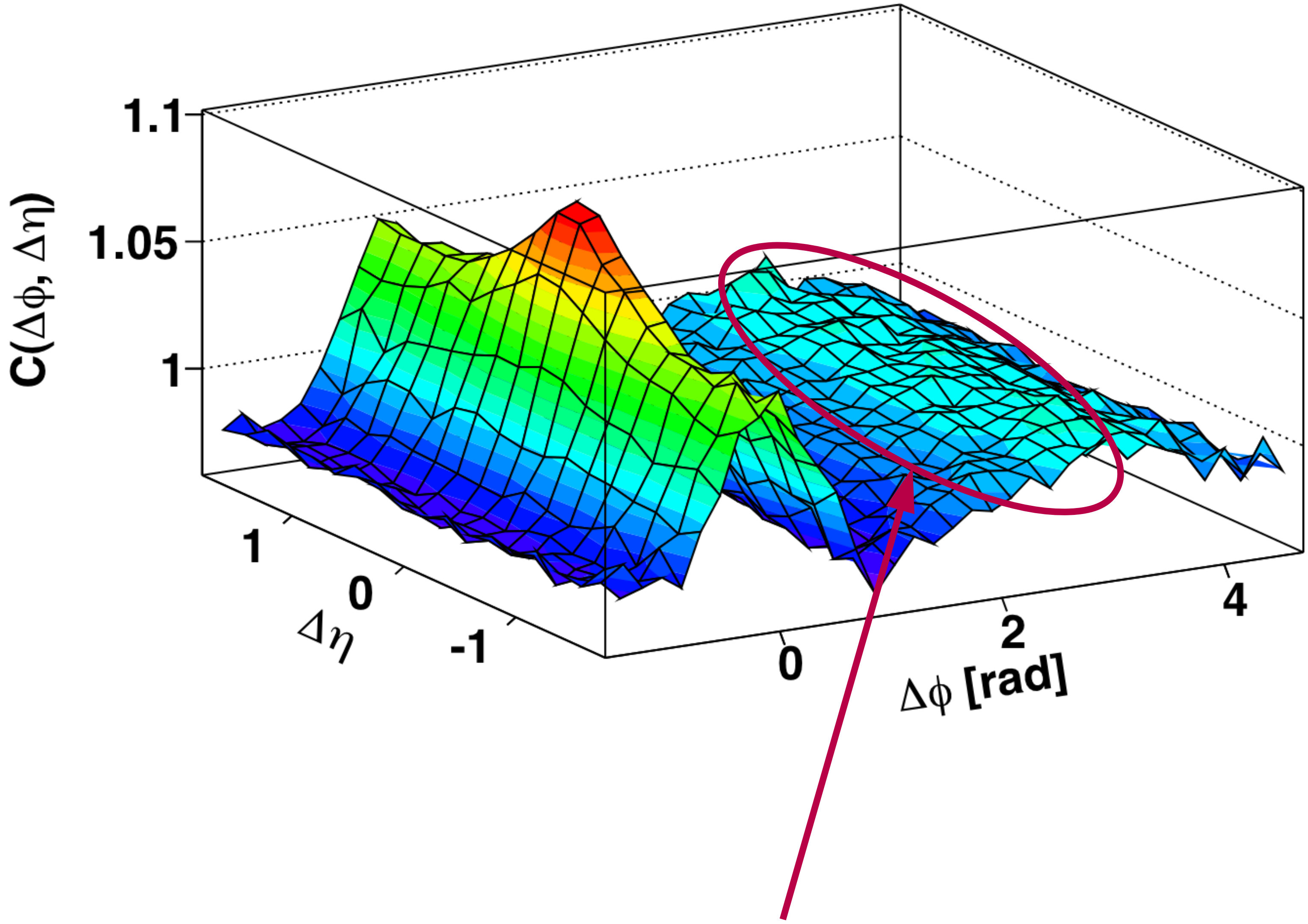

“Mach-cone” region
(double hump structure on the away side region)

Two particle azimuthal correlations: small and high p_t

Correlations at small p_t (bulk)

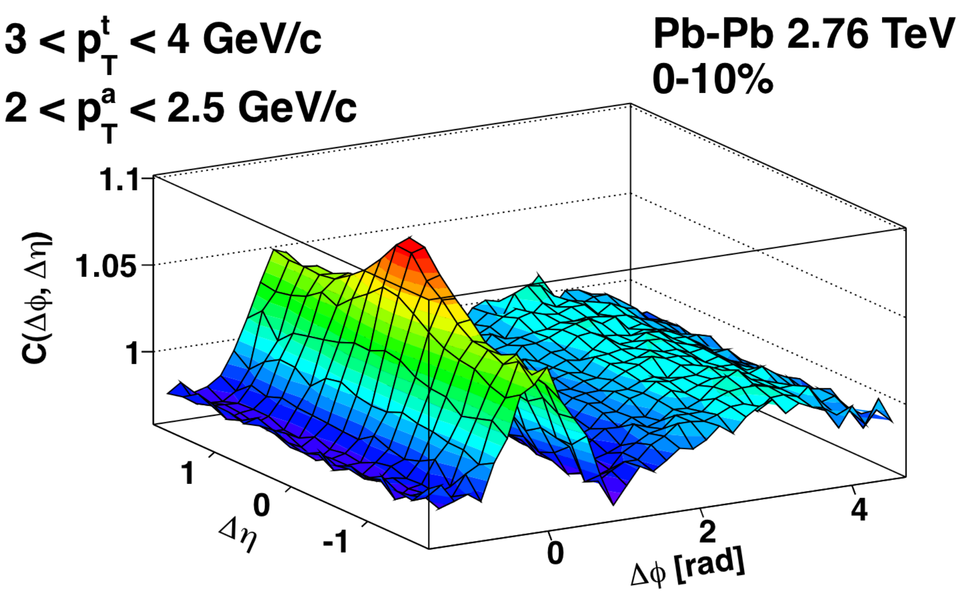

Correlations at high p_t (away side jet)

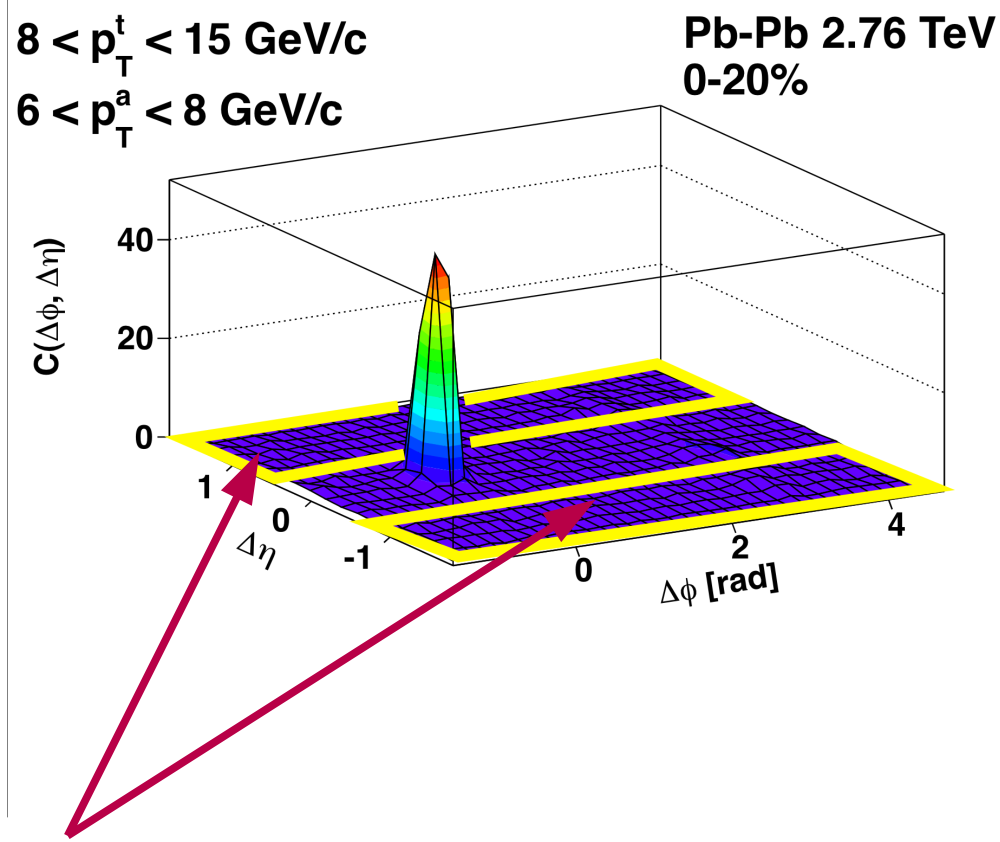

Lets study the azimuthal shape of the correlations outside of the jet peak in terms of collective modulations

Higher harmonics for very central collisions

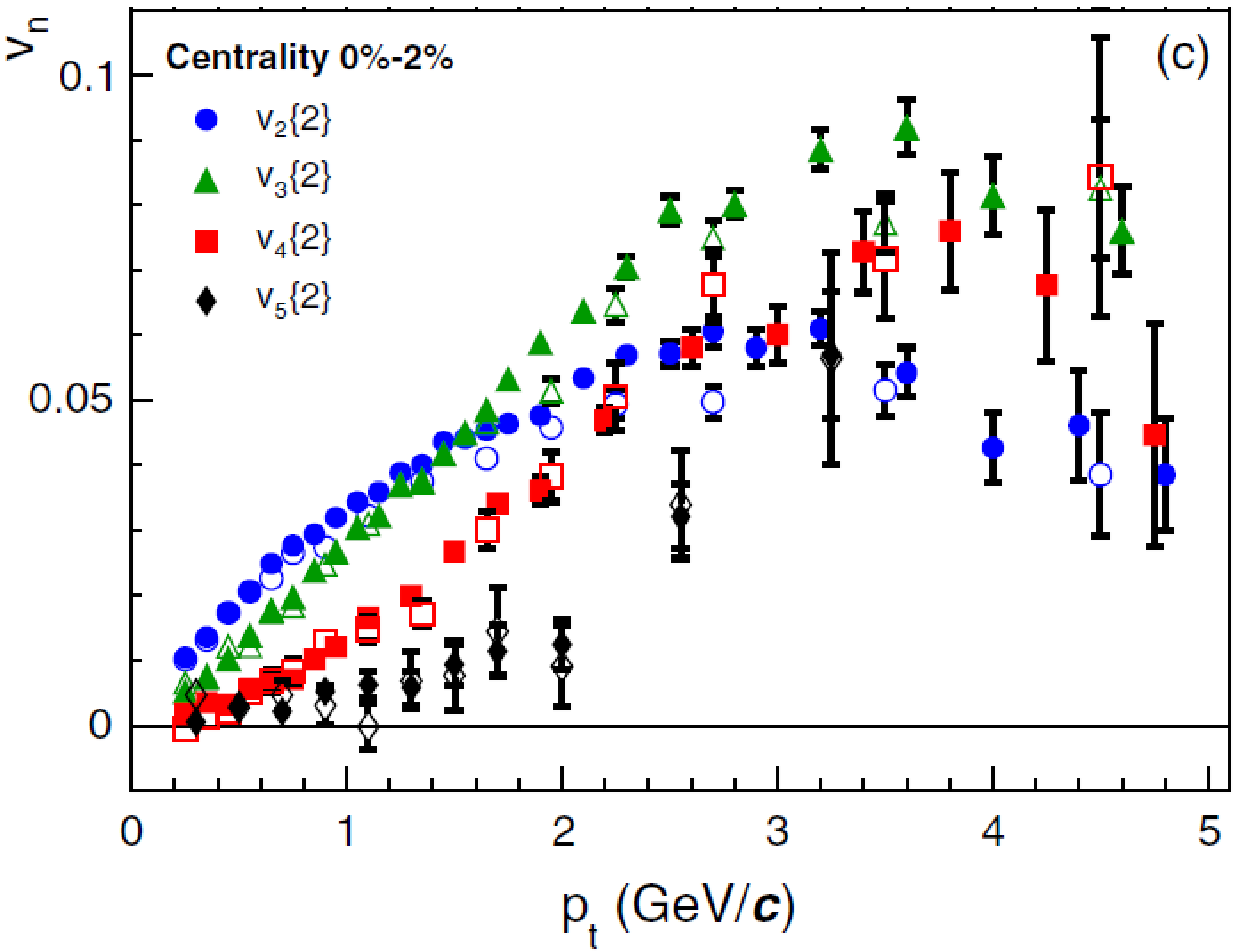

At p_t ~ 1.5 GeV v_3 become larger v_2

Two particle correlations and higher harmonic flow

Azimuthal correlations are studied with large rapidity gap: $0.8 < |\Delta\eta| < 1.8$

Correlations at small p_t (bulk)

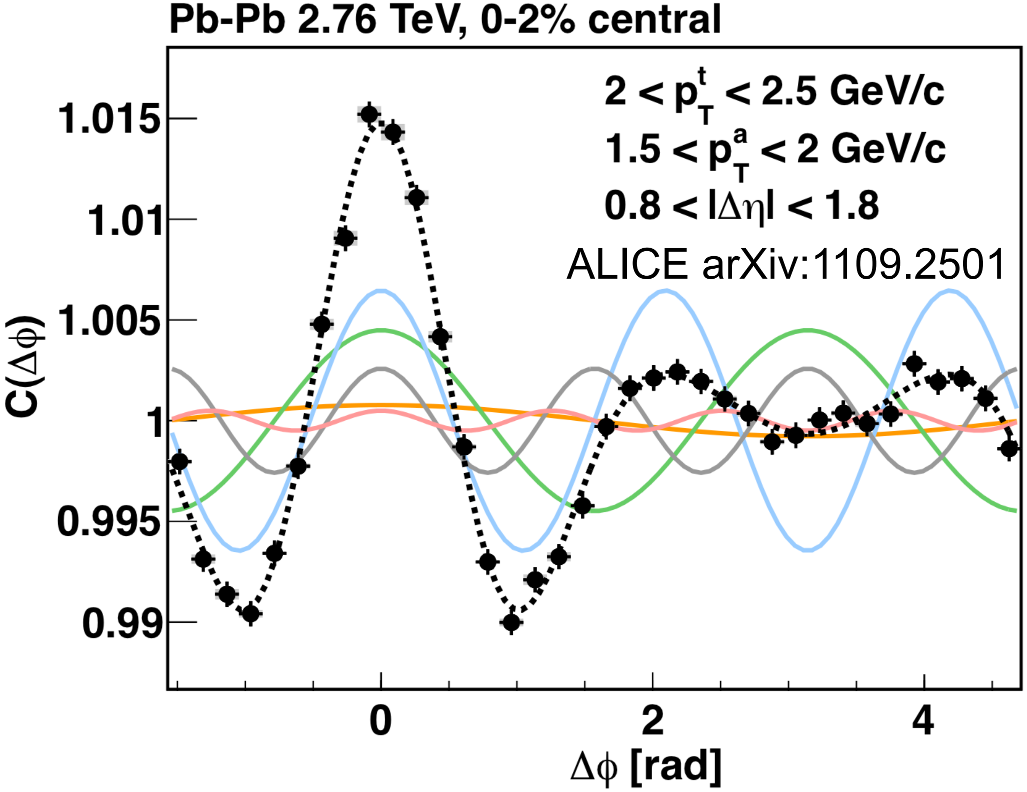

Correlations at high p_t (away side jet)

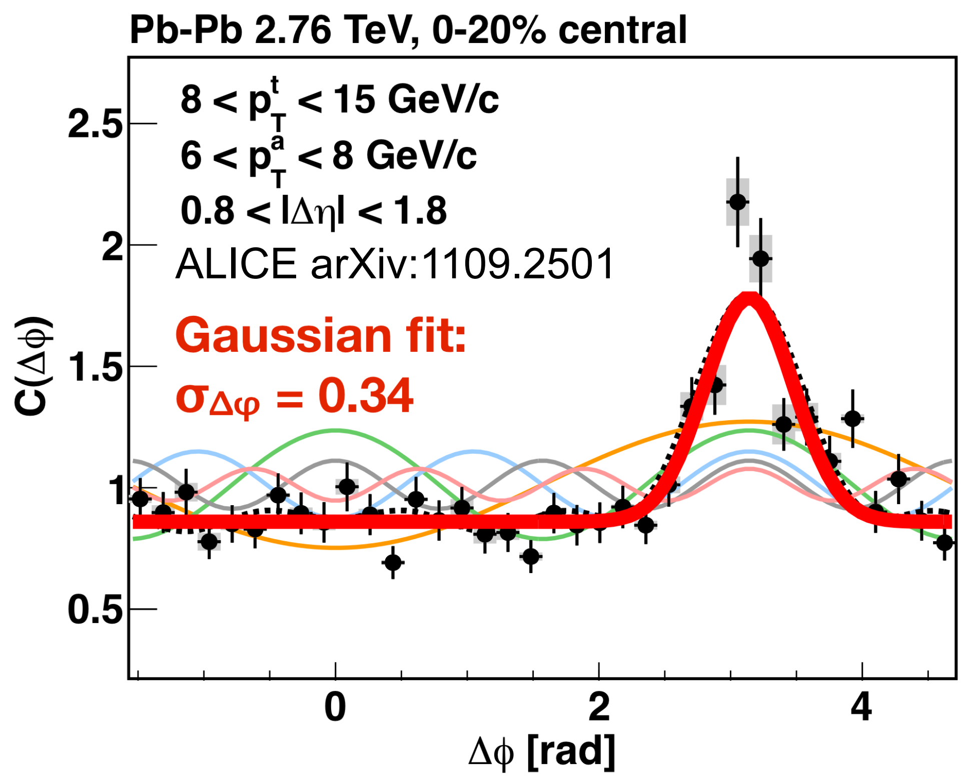

"ridge" and "mach-cone" like structures are naturally described by the collective flow effects

Power spectrum from two particle correlations

$$C(\phi_1 - \phi_2) \sim 1 + 2\sum_{i=1} V_n \cos(n[\phi_1 - \phi_2])$$

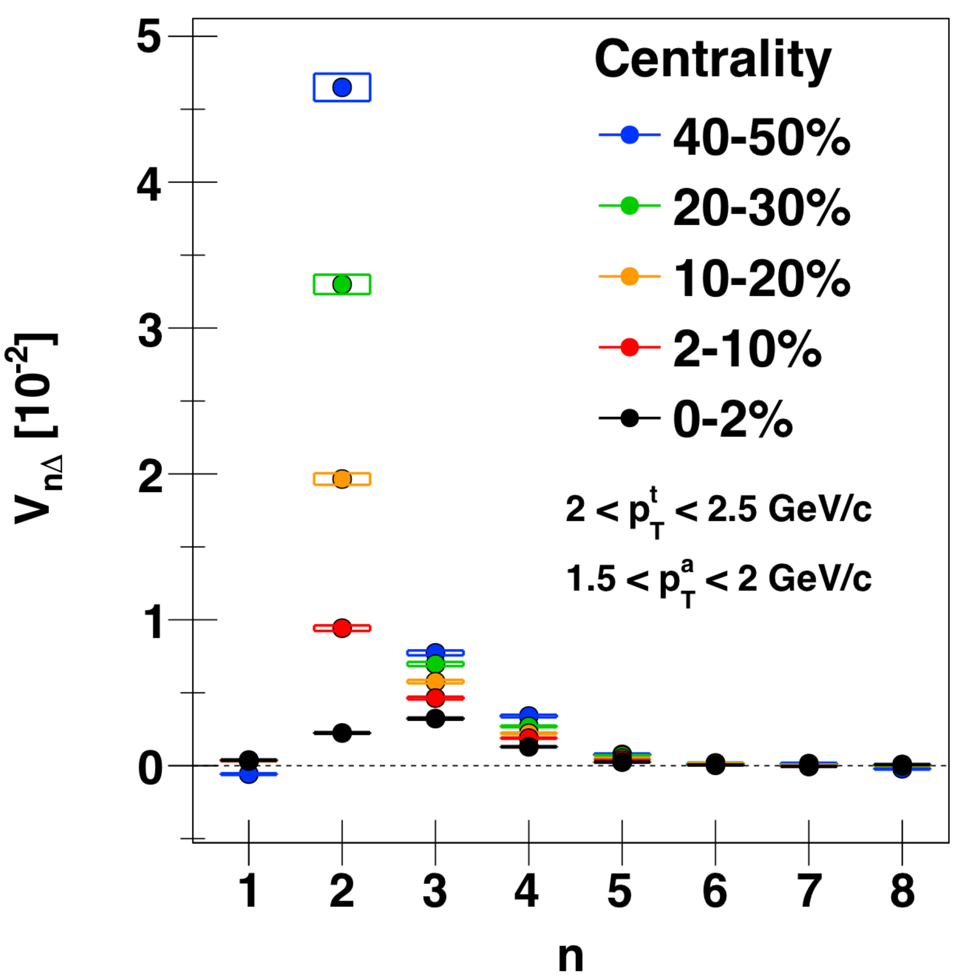

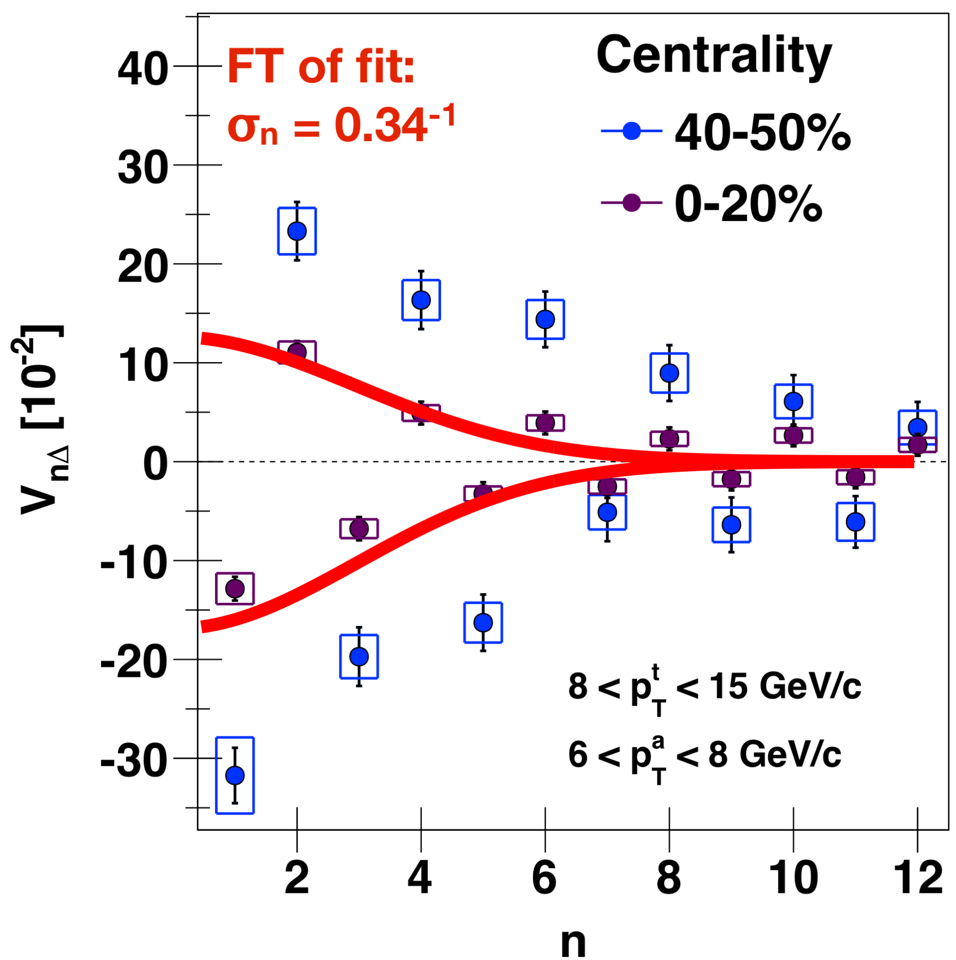

Anisotropic flow: summary

- Anisotropic transverse flow is an important experimental observable to study the evolution of a heavy-ion collision and understand the properties of the quark-gluon plasma (QGP).

- It provides constraints on:
  - ✓ Equation of state of the created matter
  - ✓ Transport properties (i.e. viscosity) of the QGP matter
  - ✓ Shape of the initial conditions in a heavy-ion collision

- Helps to understand the origin of the correlations between produced particle

- Path length dependence of the parton energy loss (flow at high transverse momenta)

Backup

Elliptic flow at high p_t

Elliptic flow, v_2

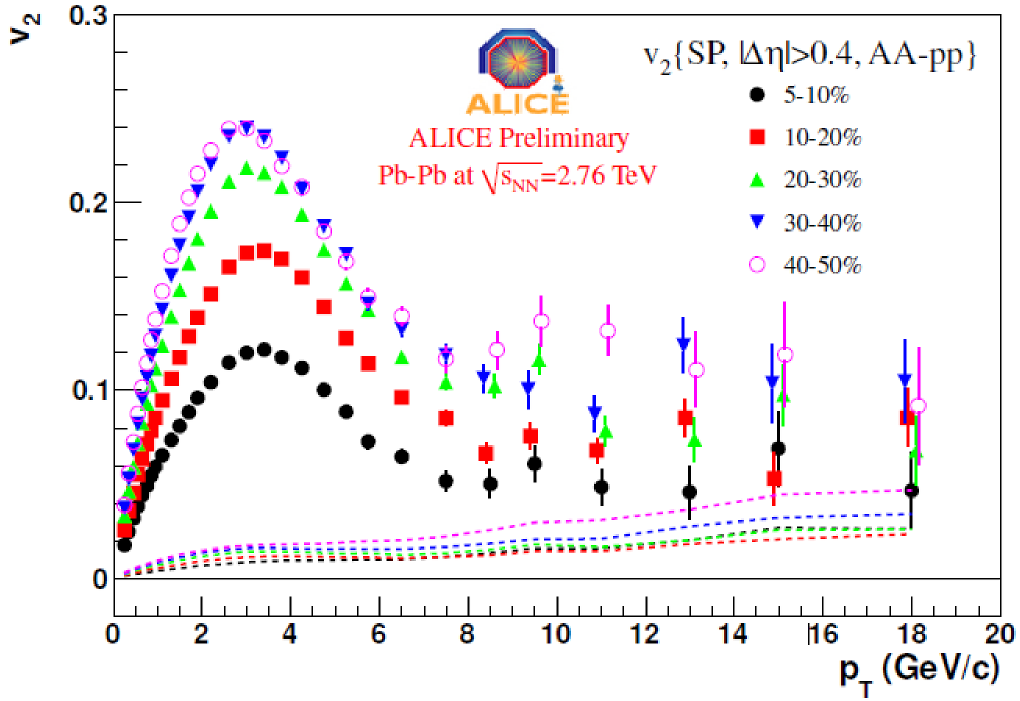

Nuclear modification factor, R_{AA}

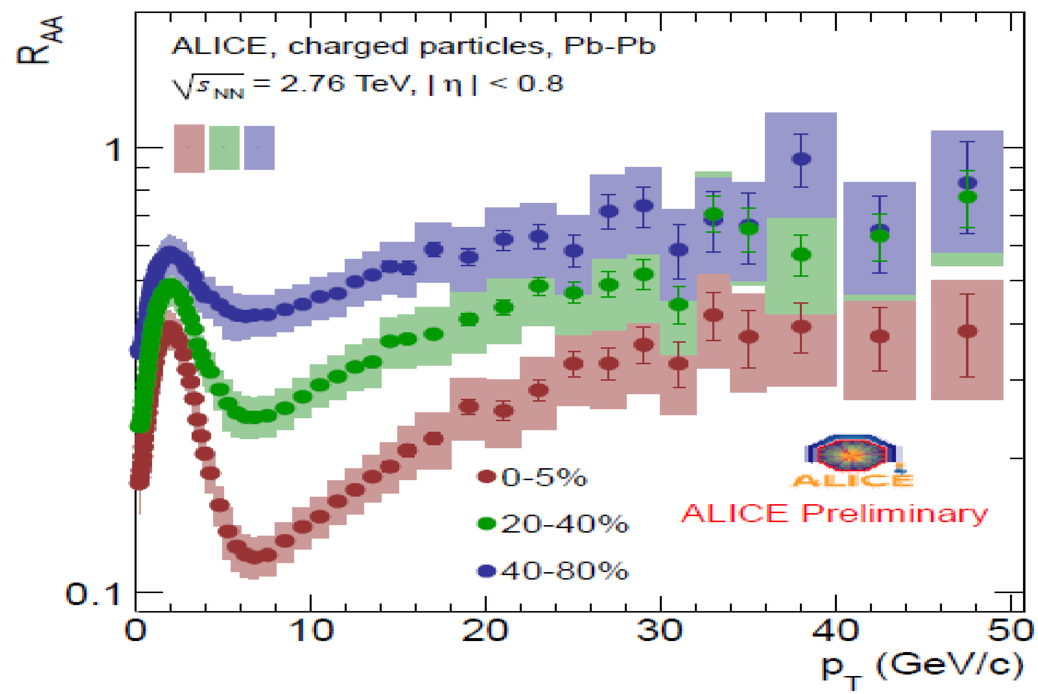

- Non-zero elliptic flow at large transverse momenta p_t > 8 GeV
- Centrality dependence is consistent with suppression measure via nuclear modification factor R_{AA}

Identified particle v_2 at high p_t

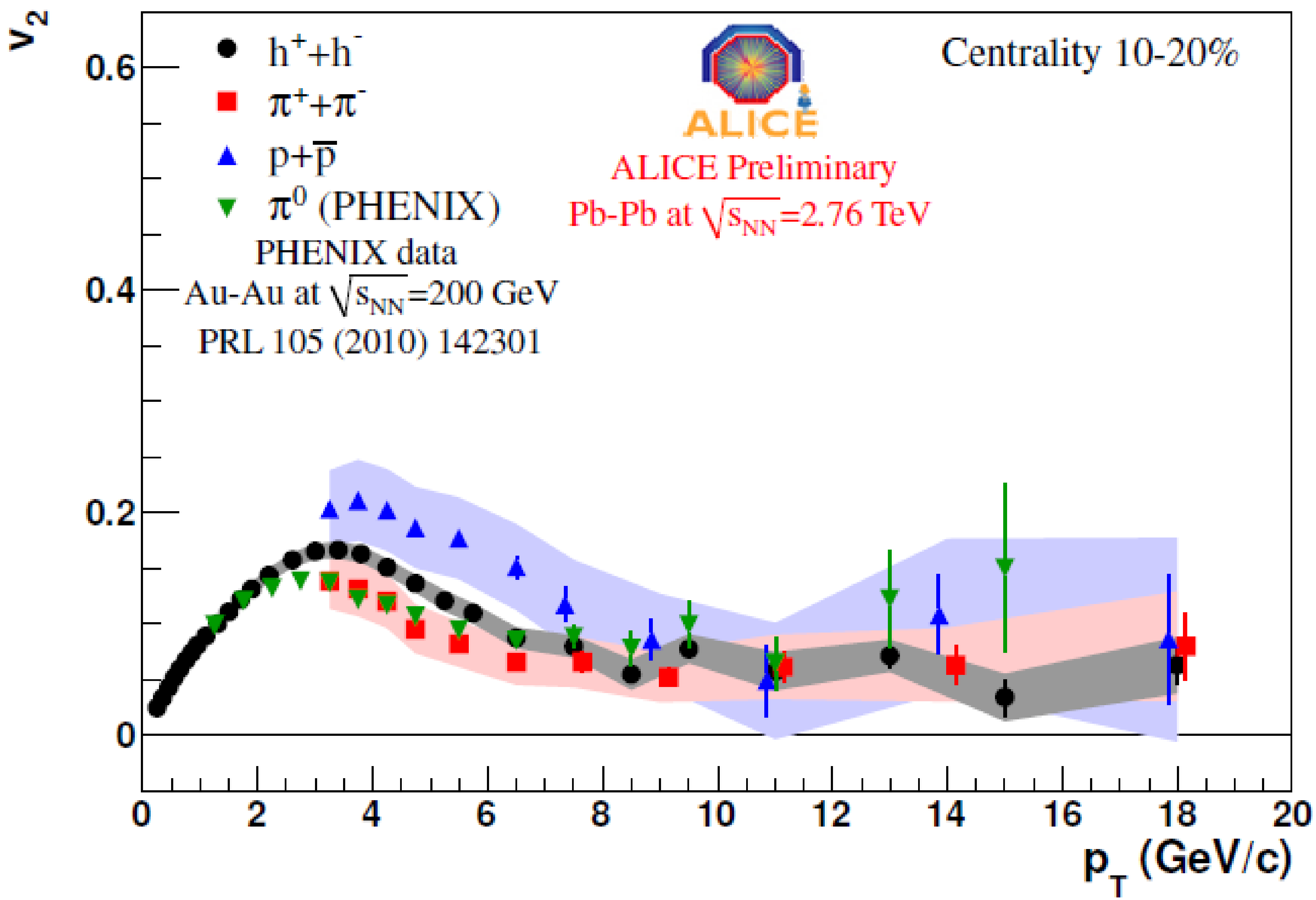

Bulk:
descrbed by hydro

Coalesence:
breaks at p_t ~ 8GeV

High $p_{t:}$
jet quenching

Direct photon v_2

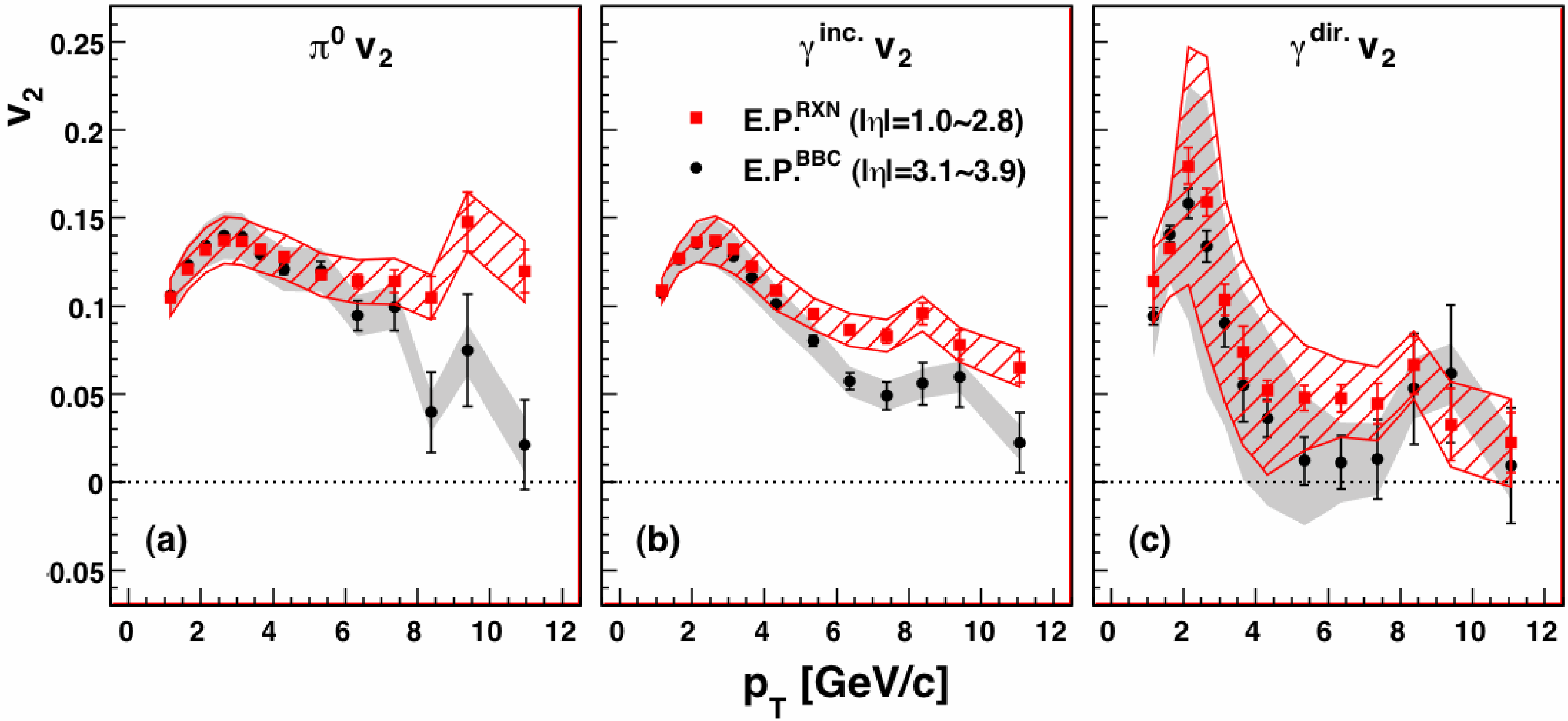

Chatterjee, Srivastava
PRC79, 021901 (2009)

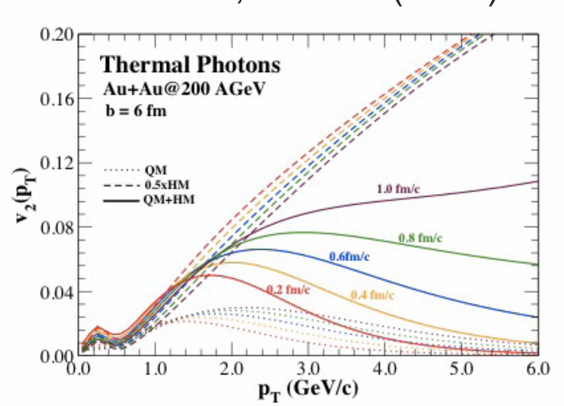

significant difference between π^0 and $\gamma^{inc.}$ v_2 above 5GeV/c

surprisingly large $\gamma^{dir.}$ v_2 is seen, similar to hadron v_2 at low p_T

$\gamma^{dir.}$ v_2 is small at high p_T, consistent with prompt photon

v_2 of heavy quarks (charm from $D^0 \rightarrow K+\pi$)

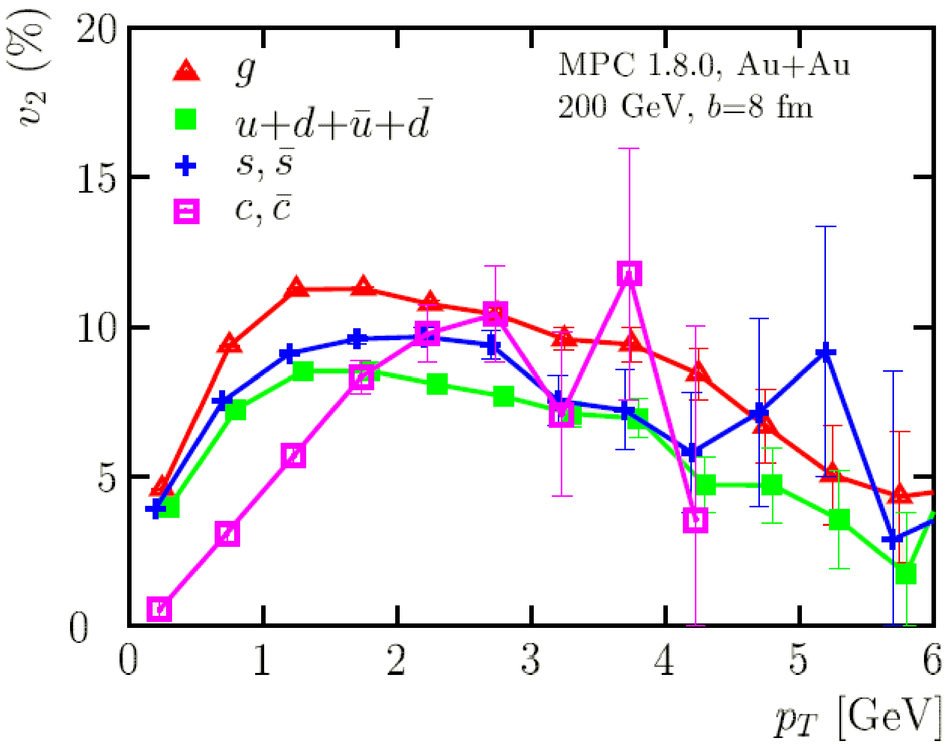

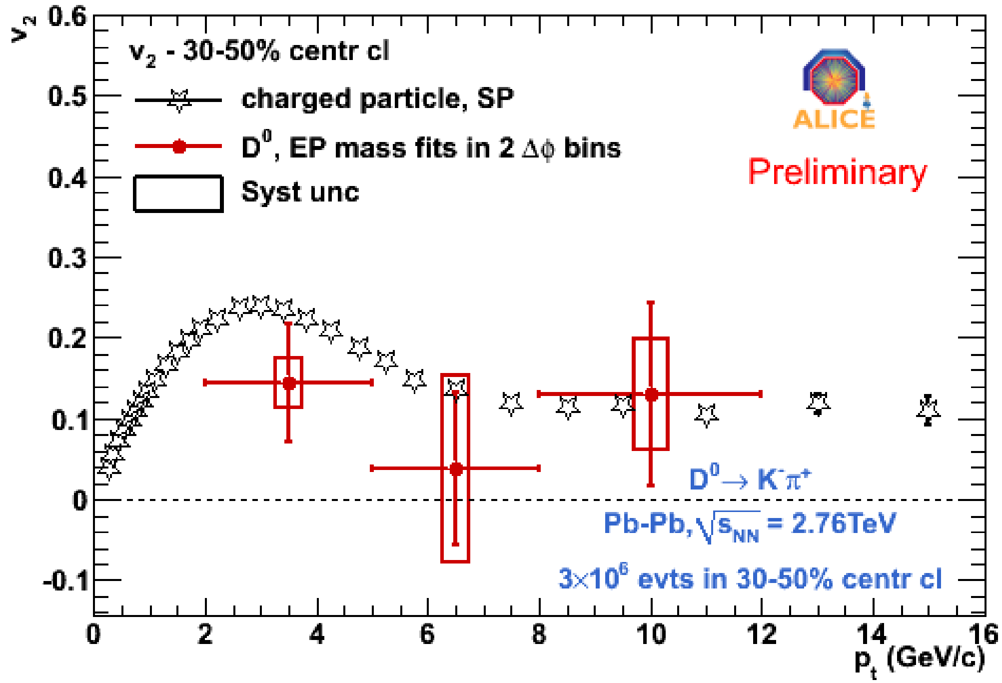

- Charm quark v_2 predicted to be smaller than flow of light quarks at small transverse momentum
- No particle type dependence at high p_t

Within large statistical errors, the flow of D^0 is consistent with that of charged particles